Nonnormality and Its Influence on the Stability and Behavior of Ecological Food Webs

By

KAELA S. VOGEL

DISSERTATION

Submitted in partial satisfaction of the requirements for the degree of

DOCTOR OF PHILOSOPHY

in

Applied Mathematics

in the

OFFICE OF GRADUATE STUDIES

of the

UNIVERSITY OF CALIFORNIA

DAVIS

Approved:

Alan Hastings, Chair

Louis Botsford

Robert Guy

Committee in Charge

2021

To my partner, David. I could not have done this without your support.

To Linda and Wade, you have become family to me.

To my siblings Jessa and Bryan, who keep me sane.

To my parents, who have sacrificed so much to raise me.

To my Intel(R) Xeon(R) CPU E3-1505M v5 @ 2.80GHz, for not melting during my optimization runs and defying Murphy's Law to survive to submitting my dissertation.

Contents

Abstract vi

Acknowledgments viii

Chapter 1. Introduction 1

Chapter 2. An introduction to pseudospectra 4

2.1. A motivating example: Eigenvalues fail to describe solution behavior 5

2.2. Introduction to pseudospectra 9

2.3. Distance to instability 13

2.4. Computation of Pseudospectra 14

2.5. Understanding transient dynamics 16

2.6. Pseudospectra in context 21

Chapter 3. Generalized Lotka-Volterra equations and their simulation 24

3.1. The generalized Lotka-Volterra equations 24

3.2. Simulation and parameter set generation 26

3.3. Results of the parameter set generation 27

Chapter 4. A study on pulse perturbations and the transient behavior of nonnormal systems 30

4.1. A preface 30

4.2. Introduction 30

4.3. Methods 33

4.4. Results 37

4.5. Discussion/Conclusions 41

Chapter 5. Food web structure, nonnormality, and reactivity 47

5.1. Introduction 48

5.2. Methods 50
5.3. Results 58
5.4. Discussion 71
Chapter 6. A mechanistic understanding of transient dynamics due to nonnormality 79
Appendix A. Code for generating pseudospectra 82
Appendix B. Parameter set generation for the generalized Lotka-Volterra equations 85
B.1. Code for data generation 85
B.2. Average values for the Jacobian matrix and stable equilibrium for each module 86
Appendix C. Code for iteratively finding the numerical abscissa for removal perturbations 90
Appendix D. Code for finding the real distance to instability 94
Bibliography 100

Nonnormality and its influence on the stability and behavior of ecological food webs

Abstract

The historic approach to food web research in theoretical ecology is frequently computational with the focus on figuring out what sort food web attributes (e.g. topological structure, network weights, etc.) confer stability to food webs. Much of the theory derived from the computational approach for food web research relies on the linear stability of systems of ordinary differential equations; where the stability of the resulting Jacobian matrices that encapsulate all the species interaction structure and weights is used to determine whether we expect to see a community of that type (or not). This approach almost always depends on using the eigenvalues of the matrix to judge stability, which say something about the eventual asymptotic decay of a perturbation to that system. Asymptotic metrics, such as the rightmost eigenvalue, are a sub-optimal metric for stability to use for several reasons. First, natural systems are in a constant state of experiencing disturbances. Second, the non-equilibrium dynamics during the transient phase of a system after a disturbance can be strikingly different from the asymptotic dynamics and may take a surprisingly long time to decay. Third, field observations frequently happen on much shorter timescales than the system dynamics, contributing to a mismatch between empirical observations and theoretical predictions.

This research aims to understand how food web structure and the network weights influence the transient finite-time behavior of food webs using a mixture of the old computation methods with new techniques yet to be fully explored in ecology. I use the generalized Lotka-Volterra equations to parameterize eight common food web module structures and create a large data set of feasible systems based on random draws of the of original parameters (on the order of thousands to millions depending on the structure). Since the old methods focus on linearizations of nonlinear systems, I will focus on one source of odd transient dynamics that afflicts linear systems: Nonnormality of the Jacobian matrix leading to sensitivity to perturbations of its entries and transient amplification of perturbations to the equilibrium. One powerful technique used for nonnormal systems is pseudospectra, which uses the norm of the resolvent to understand the finite-time dynamical behavior of nonnormal systems. I will introduce nonnormality, pseudospectra and its relationship to old methods in ecology to recognize systems with transient growth in Chapter 2, such as reactivity and the Kreiss constant.

One weakness of both of using pseudospectra and the numerical abscissa (otherwise known as reactivity in ecological literature) is that the worst case behavior predicted by these metrics is dependent on the particular structure of the perturbation. To explore how perturbation structure may contribute transient growth in natural systems, I look at two common types of equilibrium perturbations. Resource pulse perturbations, where just the basal species is perturbed, and removal pulse perturbations where I put the additional condition on the vector sign structure that all entries must be negative. I found that resource pulse perturbations are unlikely to be amplified, but simultaneous removal of both the top predator and its prey is far more likely to cause transient amplification in model food webs than what one would predict given the probability of randomly drawing a vector with all negative entries.

I hypothesize that sensitivity to perturbations is common is due to unavoidable asymmetry in the predator prey interactions due to assimilation efficiency or predator-prey body size ratios. I test this by comparing a metric of nonnormality, Henrici's departure from normality to the ratio between predator and prey interactions (coupling symmetry), and find that there is a cutoff coupling symmetry to determine whether a system is forced to become reactive and this is strongly dependent on the number of trophic levels in the module. Reactivity is strongly linearly correlated with nonnormality for our simulated food webs, and this seems to be due in part to the most nonnormal systems also having eigenvalues near zero. Finally, to understand how long transient in response to perturbations of the equilibrium may relate to sensitivity to changes in the underlying model parameters, I also calculate a pseudospectral metric, real distance to instability, for a subset of our data. We find that the eigenvalue may also be an unreliable metric for how close a system is to mathematical instability as well as how a system responds to equilibrium perturbations.

Acknowledgments

Thank you to my advisor, Alan Hastings, for inspiring and guiding me to do actual applied mathematics on biological questions rather than incidentally applied mathematics. I am forever grateful for your expertise, patience, and kindness, it was a long and winding road to get here. Thanks to all the folks at the population biology tea (in particular Sebastian Schreiber and Marissa Baskett on my qualifying committee) for your career advice and the wonderful conversation over the years.

I somehow managed to fall backwards into research that required a lot of computing outside of my expertise. Thank you to Gabe Gellner for getting me into the Julia programming language and providing the first implementation of the Lanczos iteration algorithm for computation of pseudospectra. Your and Kevin McCann's ideas on food web theory have been very influential to this dissertation. I am also lucky to happen upon two optimization guys in my time as a graduate student. A whole chapter of this dissertation was inspired by an off the cuff conversation with Will Wright at a math department tea, was whiteboarded later with him in the kitchen at party, and the end result a day later was the modified gradient ascent algorithm for the Rayleigh quotient on a restricted domain used in Chapter 4. Social events with fellow math nerds are important. I must also thank the mysterious Jeff, introduced to be my a friend, who has been a great source for all my random little optimization implementation questions that happened in the setup for the real distance to instability computation. You are the best internet stranger a person could ask for.

Graduate school happened to taken place during an extremely difficult period of my life and I have had to learn to accept the kindness of others. Thank you to Joseph Corliss and Jacob Johnson for being my note takers when I could not write, as well as being friends, you and the rest of the first year homework group made staying up far to late too finish analysis homework bearable. Thank you to the wonderful office staff, past and present, who are the true glue that keeps the department together: Tina Denena, Sarah Driver, and Victoria Whistler. You made dealing with all the bureaucratic parts of graduate school painless and were wonderful to work with when Jenny Brown and I found ourselves setting up the SDC TA system.

To all my students who took time out of their day to thank me at the end of the quarter. You maybe don't know it, but it means so much to your instructors to know we made a positive difference in your life.

Thank you to David Weber, Dmitry Shemetov, Emily Quinn Finney, Calina Copos, Jordan Snyder, Robert Bassett, David Lavoie, Kirill Paramonov, and Shawn Witte. You've kept me sane during different parts of my PhD. Thanks to Patricio D. Cruz y Celis Peniche, from May to August 2020 we were an isolated nation of two. I could not have asked for a better person to survive the world burning down with, you have introduced me to new ideas and sharpened my critical thinking skills. I highly recommend rooming with a evolutionary cultural anthropologist when you schedule your crumpling of society.

This research was funded in part by the NSF Graduate Research Fellowship.

CHAPTER 1

Introduction

The following dissertation is quite timely, pseudospectra likely originated as an obscure idea introduced in an unpublished thesis in the year 1967 [**94**], but since then has probably been reinvented at least five times in slightly different forms ([**92**], Chapter 6) where it was eventually popularized in 1992 with Trefethen's numerous examples of nonnormal matrices and their behavior [**90**]. Since then it became important to the field of fluid dynamics [**27**, **93**] and robust stability and optimal control, which developed many of the algorithms used here [**15**, **16**]. Now pseudospectral theory has made it to network theory, in the process of completing this dissertation the field has already started to see publications on nonnormality in real networks of all sorts [**6**], in networks with Lotka-Volterra type dynamics specifically [**18**], in linear time-delayed periodic systems [**13**], and in human population dynamics [**73**].

We save the detailed introduction for nonnormal behavior for the next chapter, but the primary problem is that any system whose dynamics can described by a nonnormal matrix (or more generally by a bounded linear operator) may show dynamics that defy the behavior predicted by eigenvalues, such as eigenvalue sensitivity to changes in the operator and transient amplification of perturbations one would expect asymptotic decay from. The latter is critical to the study of ecological communities since historically much of the ecological research has been built on looking at eigenvalues, which represent the stable, asymptotic behavior of the models. Given that ecological systems are constantly perturbed by both biotic and abiotic factors, it is highly unlikely any system reaches asymptotic dynamics, and the transient dynamics on the way to the equilibrium might be quite different than the asymptotic dynamics [**41**]. There is frequently a mismatch between the time scale the data was collected and the time scale assumed by the model; much of the research in ecology has been conducted under the assumption that the assemblage of species we observe in field experiments are at some sort of equilibrium that corresponds to the local asymptotic stability of a model system. However, field data is frequently collected on short timescales (relative to the timescale of the system

dynamics) and it is therefore critically important to understand the range of possible nonequilibrium dynamics, especially when the data is used for management decisions [**32**, **96**].

In the following chapter we aim to provide an intuitive introduction to how long transients after a perturbation can arise in linear systems as well as introduce the idea of pseudospectra. We cover the history of tools in ecology to deal with nonnormal dynamics and as well as relate it back to pseudospectra, and introduce some new ideas on thinking how ecological systems may have (or manage to avoid) parameter sensitivity and long transients in response to perturbations. In Chapter 3 we take the computational approach widely used for answering questions about stability and introduce the model ecological networks parameterized by the generalized Lotka-Volterra equations which we will use Chapter 4 and 5.

One of the weaknesses of using the pseudospectral approach is that it tells you what sort of transient dynamics are possible and gives lower bounds on the worst case behavior, but it does not give information on the structure of the perturbations that results in that behavior. In short, not all perturbations of the equilibrium will result in transient growth, this behavior is directionally dependent, i.e. dependent on the particular structure of the perturbation. Chapter 4 uses optimization of the initial growth after a perturbation on a restricted domain to investigate transient amplification to perturbations that strictly add or remove species. This sort of perturbation is important for managing multi-species reserves and fisheries or studying some common types of resource pulse perturbations like extreme flooding (ENSO bringing moisture to normally arid palaces [**82**]), cicada emergence [**97**], fruit and seed masting [**52**, **75**]), or spatial accumulation and release (eg. storms bringing seaweed to terrestrial locations [**86**]). We identify a new subclass of system, food webs which show transient amplification to removal perturbations, and show that the type of perturbations that lead to this behavior are conserved across different network module structures.

In the penultimate chapter, our efforts in Chapter 2 to categorize the possible stability and transient behaviors of small ecological food webs comes to fruition. We find that well-known metric for transient amplification (reactivity/numerical abscissa [**68**]) correlates strongly and linearly with a metric of nonnormality (Henrici's departure from normality, [**45**, **92**]), but our model ecological networks seem to cluster in a particular region of nonnormality and reactivity. We introduce the

first example of using the real distance to instability to theoretical ecology, a metric that relates loss of stability to changes in the entries of the Jacobian matrix and show it is possible for 1) Systems which do not show transient amplification of perturbations can still be more sensitive than expected to eigenvalues becoming positive if the underlying system parameters are changed and 2) It is possible to find systems with the same eigenvalues and real distance to instability that show distinctly different transient behavior. Our results also suggest that interaction asymmetry between predators and prey due to body size ratio, assimilation efficiency or metabolics **[12, 31, 103]** may introduce an unavoidable source of nonnormality while also interacting with stability and tendency to amplify perturbations in a complicated way.

The history of tools used to understand transient dynamics and ecological stability is inextricably tied to the history of computing. Yodzis' 1988 paper mentions taking weeks of VAX 11/780 CPU cycles to construct 100 plausible community matrices and compute the inverse **[101]**. Trefethen's 2005 book Spectra and Pseudospectra records a time of 25 minutes to run inverse Lanczos iteration to compute the pseudospectra of a 400×400 matrix on 100×100 grid (**[92]**, Chapter 39): performing the exact same algorithm under the same conditions now takes 19.7 seconds on a mediocre processor purchased on a graduate student budget. And it is not just the available raw computing power and cheap memory, advances in the available open source computing languages mean implementing algorithms to take advantage of parallelization and GPU computing can now practically be done in pseudocode. Gone are the days where debugging frakencode C calls in matlab and python was the only way to use a high-level language that runs in a reasonable time frame, languages like Julia have dramatically cut down the mental overhead that goes into setting up the models in the first place. Even though ecologists have been aware transient amplification of perturbations since 1997 **[68]**, it likely would have been impossible to do the same sort of large scale numerical experiments with pseudospectra-derived metrics that we can do today.

CHAPTER 2

An introduction to pseudospectra

The goal of this dissertation is to understand the stability and transient dynamics of ecological networks of various sizes and structures and many of the tools we will be using are largely based on either the idea of, or direct application of pseudospectra. This chapter is a brief introduction to the problems nonnormality may cause and how pseudospectra may give us a better understanding the behavior of nonnormal systems.

From an ecologists perspective, there are many interesting models that involve the time evolution of a system of ordinary differential equations (ODEs), that is, we have a system

$$\frac{\mathrm{d}\mathbf{x}}{\mathrm{d}t} = \mathbf{A}\mathbf{x}, \ \mathbf{x}(0) = \mathbf{x}_0 \tag{2.1}$$

where $\mathbf{A}$ is an invertible matrix that either represents the coefficients of a linear ODE or the coefficients of a linearized system about an equilibrium. Equation 2.1 has a unique solution as long as $\mathbf{A}$ is nonsingular

TABLE 2.1. Symbols used in this chapter

$\mathbf{A}$	Generic $n \times n$ matrix
$\mathbf{\Lambda}$	$n \times n$ matrix with the eigenvalues of $\mathbf{A}$ on the diagonal
$\mathbf{V}$	$n \times n$ matrix with the eigenvectors of $\mathbf{A}$ as the columns
$\Lambda(.)$	The set of eigenvalues
$\lambda_i(.)$	generic eigenvalue
$\Lambda_\varepsilon(.)$	The set of ε-pseudospectra
$\Lambda_\varepsilon^{\mathbb{R}}(.)$	The set of real-structured ε-pseudospectra
$\omega(.)$	The numerical abscissa or reactivity of a matrix
$\alpha(.)$	The spectral abscissa, $\alpha(\mathbf{A}) = \max_i \mathfrak{Re}(\lambda_i(\mathbf{A}))$
$\alpha_\varepsilon(.)$	The ε-pseudospectral abscissa
$\mathcal{K}(.)$	The Kriess constant of a matrix
$\kappa(.)$	The condition number of a matrix
$\mathrm{dep}_F(.)$	Henrici's departure from normality of a matrix
$\sigma(.)$	The set of singular values of a matrix

$$\mathbf{x}(t) = \mathrm{e}^{t\mathbf{A}}\mathbf{x}_0.$$

We can rewrite the general solution in eigenvalue-eigenvector form for an $n-$dimensional system. Let $\mathbf{V}$ be the matrix whose columns are the eigenvectors of $\mathbf{A}$ and $\mathbf{\Lambda}$ be the diagonal matrix of eigenvalues of $\mathbf{A}$, the diagonalization and subsequent eigenvalue-eigenvector form of the solution is

$$\mathbf{x}(t) = (\mathbf{V}\mathrm{e}^{t\mathbf{\Lambda}}\mathbf{V}^{-1})\mathbf{x}(0) = \mathbf{V}\mathrm{e}^{t\mathbf{\Lambda}}(\mathbf{V}^{-1}\mathbf{x}(0)) = c_1\lambda_1\mathbf{v}_1 + c_2\lambda_2\mathbf{v}_2 + \ldots + c_n\lambda_n\mathbf{v}_n$$

where

$$[c_1, c_2, \ldots, c_n]^T = \mathbf{V}^{-1}\mathbf{x}(0), \tag{2.2}$$

and $\lambda_i, \mathbf{v}_i$ are the eigenvalues and eigenvectors of $\mathbf{A}$, respectively. The point here to make is that to write out a solution to the ODE in Eq. 2.1 with initial conditions, we have to transform the initial condition vector into the eigenvector basis of $\mathbf{A}$. Unless $\mathbf{V}$ is an orthogonal basis, we have to solve a linear equation to get those coefficients. Quite a lot can happen to the initial condition $\mathbf{x}(0)$ during this operation, the next section covers this in depth.

2.1. A motivating example: Eigenvalues fail to describe solution behavior

Let's say we have three linear systems of ODEs

$$\begin{aligned} \dot{x}_1 &= -x_1 + 0x_2 \qquad \dot{x}_1 = -x_1 + 2x_2 \qquad \dot{x}_1 = -x_1 + 9x_2 \\ \dot{x}_2 &= 0x_1 - 2x_2 \qquad \dot{x}_2 = 0x_1 - 2x_2 \qquad \dot{x}_2 = 0x_1 - 2x_2 \end{aligned}$$

If we put theses into matrix-vector form ($\dot{\mathbf{x}} = \mathbf{A}\mathbf{x}$), the three "$\mathbf{A}$" matrices that represent the 2-D dynamical systems are

$$\mathbf{A}_1 = \begin{bmatrix} -1 & 0 \\ 0 & -2 \end{bmatrix} \qquad \mathbf{A}_2 = \begin{bmatrix} -1 & 2 \\ 0 & -2 \end{bmatrix} \qquad \mathbf{A}_3 = \begin{bmatrix} -1 & 9 \\ 0 & -2 \end{bmatrix}. \tag{2.3}$$

Because all of the matrices are upper-triangular form, we can easily see they all have the same eigenvalues (and therefore the same $t \to \infty$ behavior) and can be written in the form

$$\mathbf{x}(t) = \mathrm{e}^{t\mathbf{A}}\mathbf{x}(0) = (\mathbf{V}\mathrm{e}^{t\mathbf{\Lambda}}\mathbf{V}^{-1})\mathbf{x}(0), \qquad \mathbf{\Lambda} = \begin{vmatrix} -1 & 0 \\ 0 & -2 \end{vmatrix},$$

the only difference being in what the matrix of eigenvectors, $\mathbf{V}$ is for each system. This may seem like an innocuous difference, but the devil is in the details. If we look at the matrix 2-norm of $\mathrm{e}^{t\mathbf{A}}$ as a function of t

$$f(t) = \max_{|x|_2=1} |\,\mathrm{e}^{t\mathbf{A}}|_2$$

for our three systems in Fig. 2.1 they have wildly different behavior in finite time. *Note: We will be using* $|.|_2$ *around a matrix to refer to the induced* l^2*-norm of that matrix as defined above. When we want to refer to the Frobenius (Hilbert-Schmidt) norm of a matrix we will use* $|.|_F$. The key to the very different behaviors is in what happens with the initial conditions in Eq. 2.2. The culprit in this case are the eigenvectors. The matrix $\mathbf{A}$ may have a complete set of eigenvectors, but there is no requirement that they are orthogonal. As we can see in Figure 2.2, while this selection of systems all have the same eigenvalues their eigenvectors are quite different. Comparing the $\mathbf{V}^{-1}$ for our three systems below, we can see that for the third system any initial condition vector with an entry in the second index is going to be positively mauled by the eigenbasis transformation.

$$\mathbf{V}_1^{-1} = \begin{vmatrix} -1 & 0 \\ 0 & -1 \end{vmatrix} \qquad \mathbf{V}_2^{-1} = \begin{vmatrix} 1 & -0.667 \\ 0 & -1.20 \end{vmatrix} \qquad \mathbf{V}_3^{-1} = \begin{vmatrix} 0 & 9.06 \\ 1 & 9.0 \end{vmatrix}.$$

For our third system there will always be at least one direction vector, regardless of starting magnitude, that will be amplified by shoving it through $\mathrm{e}^{t\mathbf{A}}$ and this means that $\mathrm{e}^{t\mathbf{A}}$ can initially show positive growth away from the equilibrium despite having all negative eigenvalues. As demonstrated by our third system, one of the tell-tale signs for systems that might show transient growth in this manner are large entries in $\mathbf{V}^{-1}$, or if we assume that $|\,\mathbf{V}|$ is around 1, an equivalent condition is that the condition number $\kappa(\mathbf{V})$ for $\mathbf{V}$ is large

$$\kappa(\mathbf{V}) = |\,\mathbf{V}|\,|\,\mathbf{V}^{-1}| \gg 1. \tag{2.4}$$

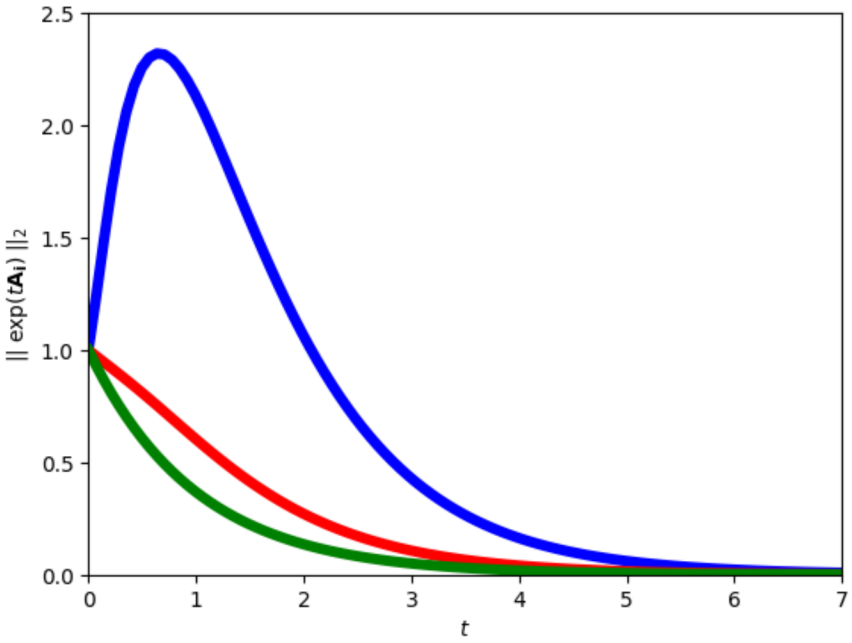

FIGURE 2.1. The behavior of $|\,e^{t\mathbf{A}}|_{\,2}$ for our matrices $\mathbf{A}_1$, $\mathbf{A}_2$, and $\mathbf{A}_3$ with time.

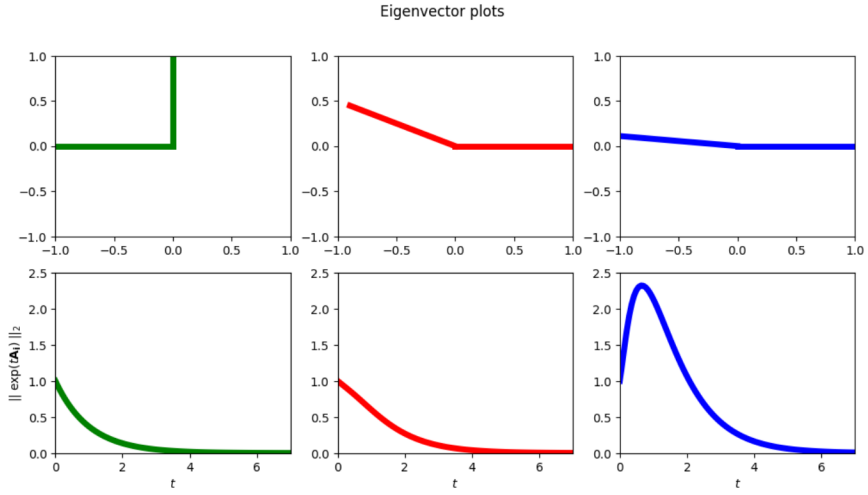

FIGURE 2.2. Top: Visualizations of the eigenvectors for $\mathbf{A}_1$ (green), $\mathbf{A}_2$ (red), and $\mathbf{A}_3$ (blue). Bottom: The corresponding plots of $|\,e^{t\mathbf{A}}|_{\,2}$.

This phenomena is due to the fact that the eigenbasis of $\mathbf{A}$ was not orthogonal, which is equivalent to saying $\mathbf{A}$ is nonnormal. A matrix $\mathbf{A}$ is said to be *nonnormal* if does not commute with its adjoint ($\mathbf{A}\mathbf{A}^* \neq \mathbf{A}^*\mathbf{A}$). Now there are many equivalent conditions for normality, a list of seventy can be found in **[49]** and nineteen more in **[28]**: nonnormal operators get comparatively less attention in the

literature. Normal matrices and orthogonal bases are mathematically nice to deal with; it is little wonder so much time has been devoted to their study, but normality is a strong condition that many matrices or bounded linear operators arising from applications will not meet. The matrices belonging to the rather exclusive club of normality are the diagonal, symmetric, Hermitian, skew-symmetric, skew-Hermitian, orthogonal, unitary, and circulant matrices. Other than the circulant matrices, normal matrices have a high degree of symmetry and are therefore easy to recognize.

2.1.1. A scalar metric of nonnormality. Since we will be studying nonnormal systems exclusively, is useful to have a metric of nonnormality. One that we will make use of is Henrici's departure from nonnormality **[45]**. This is certainly not the only option, others are reviewed here **[92]**. If a nonnormal matrix is a matrix that is not unitarily diagonalizable, an easy metric would be to do a unitarily diagonalize it and measure how "off" it is. A Schur decomposition of $\mathbf{A}$ is given by

$$\mathbf{A} = \mathbf{U}(\mathbf{\Lambda} + \mathbf{R})\mathbf{U}^*,$$

where $\mathbf{U}$ is a unitary matrix, $\mathbf{\Lambda}$ is a diagonal matrix, and $\mathbf{R}$ is strictly upper-triangular. One may be used to seeing the factorization $\mathbf{UTU}^*$, $\mathbf{T}$ is upper triangle, when "Schur" is mentioned, we use the sum $\mathbf{\Lambda} + \mathbf{R}$ for a few reasons: 1) To stress the fact that the Schur factorization is an eigenvalue-revealing factorization and $\mathbf{\Lambda}$ is the diagonal matrix of the eigenvalues of $\mathbf{A}$ and 2) Taking some norm of $\mathbf{R}$ is a natural way of quantifying the nonnormality of a matrix. We have made a conscientious decision to use "A Schur factorization" because Schur factorizations are not unique. Henrici gets around this by taking the minimum value of the norm of $\mathbf{R}$ over all possible Schur decompositions **[45]**, we will get around the problem of non-uniqueness by using the unitarily equivalence property of the Frobenius norm so that $|\,\mathbf{A}|_F^2 = |\,\mathbf{\Lambda} + \mathbf{R}|_F^2 = |\,\mathbf{\Lambda}|_F^2 + |\,\mathbf{R}|_F^2$ (this is true because $\mathbf{\Lambda}$ and $\mathbf{R}$ do not share any nonzero entry locations). Therefore we define Henrici's departure from nonnormality as

$$\mathrm{dep}_F(\mathbf{A}) = |\,\mathbf{R}|_F^2 = \sqrt{|\,\mathbf{A}|_F^2 - |\,\mathbf{\Lambda}|_F^2} = \left(\sum_{j=1}^{N} \sigma_j^2 - \sum_{j=1}^{N} \lambda_j{}^2 \right)$$

where $\{\Lambda_j\}$ and $\{\lambda_j\}$ are the singular and eigenvalues of $\mathbf{A}$, respectively.

The rest of this chapter will be a tour of how to deal with and understand the behavior of nonnormal matrices. In basically all cases these ideas can be generalized to infinite-dimensional linear operators as long as they are closed and bounded.

2.2. Introduction to pseudospectra

Let $\mathbf{A} \in \mathbb{C}^{N\times N}$, $\mathbf{I}$ be the identity, and $z \in \mathbb{C}$, and $\Lambda(\mathbf{A})$ be the eigenvalues of $\mathbf{A}$. The **resolvent** is the operator-valued function

$$\mathcal{R}(z; \mathbf{A}) := (z\mathbf{I} - \mathbf{A})^{-1}$$

is analytic and has point singularities precisely at $z \in \Lambda(\mathbf{A})$. We therefore adopt the convention that the $|\,(z\mathbf{I} - \mathbf{A})^{-1}| = \infty$ for $z \in \Lambda(\mathbf{A})$. (A note: We do sweep some details under the rug, in the case of general operators there may be things in the spectrum of the operator which are not eigenvalues.)

For an arbitrary $\varepsilon > 0$, the $\varepsilon-$**pseudospectra** is defined as the set of values where the resolvent is large

$$\Lambda_\varepsilon(\mathbf{A}) := \{z \in \mathbb{C} : |\,(z\mathbf{I} - \mathbf{A})^{-1}| \;>\; \varepsilon^{-1}\}, \tag{2.5}$$

and therefore the ε-pseudospectrum is an open subset of the complex plane bounded by the ε^{-1}-level curve of the norm of the resolvent. Figure 2.3 illustrates this, but every time there is plot with nested contours it is referring to a three dimensional object. Because of the resolvent's relationship with eigenvalue perturbations, which we will go over shortly, the bands of color are displayed as $\log_{10}(\varepsilon)$.

The usefulness of this way of thinking about the spectrum of a matrix may not be immediately obvious, but let is return to our three example systems in the previous section. Figure 2.4 has the ε-pseudospectra of the matrices for our three matrices in Eq. 2.3. While the three matrices all have the same eigenvalues, the differences in their pseudospectra are visually striking. $\mathbf{A}_3$, the system which showed transient growth for some perturbations, extends into the positive real numbers for

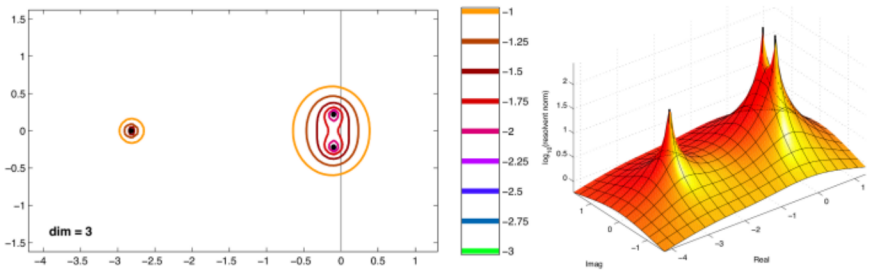

FIGURE 2.3. A view of the ε-pseudospectra (left) which are level sets of the resolvent function (right) for $\varepsilon = 10^{-1}, 10^{-1.25}, 10^{-1.5}, 10^{-1.75}, 10^{-2}$. The peaks are the singularities of the resolvent and correspond to the eigenvalues of the operator.

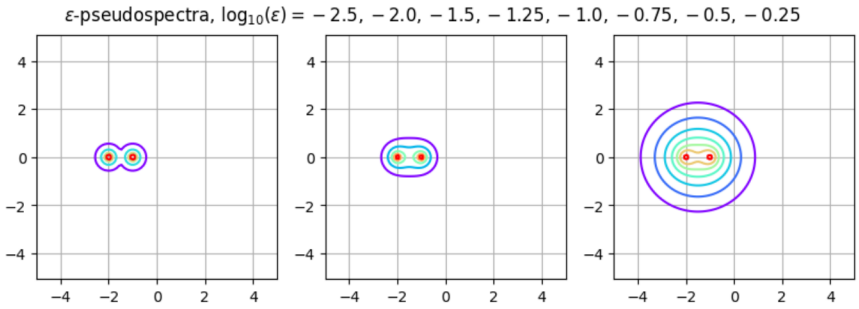

FIGURE 2.4. Back to our first example in Eq. 2.3, a comparison of the pseudospectra for our three systems (left to right) $\mathbf{A}_1$, $\mathbf{A}_2$, and $\mathbf{A}_3$. Transient growth happens when $\Lambda_\varepsilon(\mathbf{A})$ crosses over to the right half of the complex plane.

small perturbations. Formally state this idea, let $\Delta_\varepsilon = \{z \in \mathbb{C} : \ z \ < \varepsilon\}$ be an open ε-ball. It can be shown that if $\mathbf{A}$ is normal then for the 2-norm its ε-pseudospectra is

$$\Lambda_\varepsilon(\mathbf{A}) = \Lambda(\mathbf{A}) + \Delta_\varepsilon$$

and if $\mathbf{A}$ is nonnormal, then

$$\Lambda(\mathbf{A}) + \Delta_\varepsilon \subseteq \Lambda_\varepsilon(\mathbf{A}).$$

Essentially, for a nonnormal system perturbing an eigenvalue by ε can result in a more-than-ε shift of its spectrum. How bad the shift can be is dependent on the condition of the eigenvector matrix, $\kappa(\mathbf{V})$ mentioned in the previous section. This idea is made precise by using the Baur-Fike theorem, details of the proof in **[92]**.

There are several other, equivalent definitions of ε-pseudospectra. The proof of their equivalence can be found in **[92]** for Theorem 2.1 and is a nice example of application of the Hahn-Banach theorem.

THEOREM 2.2.1. *For any matrix $\mathbf{A} \in \mathbb{C}^{N\times N}$ the following definitions of pseudospectra are equivalent:*

- *The set of values where the resolvent is large*

$$\Lambda_\varepsilon(\mathbf{A}) := \{z \in \mathbb{C} : |\,(z\mathbf{I} - \mathbf{A})^{-1}|\ > \varepsilon^{-1}\},$$

- *The set of values that are the eigenvalues of a perturbed matrix $\mathbf{A} + \mathbf{E}, \mathbf{E} \in \mathbb{C}^{N\times N}$*

$$\Lambda_\varepsilon(\mathbf{A}) := \{z \in \mathbb{C} : z \in \Lambda(\mathbf{A} + \mathbf{E}),\ \textit{where } |\,\mathbf{E}| < \varepsilon\} \tag{2.6}$$

- *The set of "pseudoeigenvalues" of $\mathbf{A}$ with corresponding "pseudoeigenvectors." Let $\mathbf{v} \in \mathbb{C}^N, |\,v| = 1$, then*

$$\Lambda_\varepsilon(\mathbf{A}) := \{z \in \mathbb{C} : |\,(z - \mathbf{A})\mathbf{v}|\ < \varepsilon\}$$

- *When $|\,\cdot\,| = |\,\cdot\,|_2$, we can define the ε-pseudospectral set in terms of the smallest singular value of $(z\mathbf{I} - \mathbf{A})$*

$$\Lambda_\varepsilon(\mathbf{A}) := \{z \in \mathbb{C} : \sigma_{\min}(z\mathbf{I} - \mathbf{A}) < \varepsilon\}. \tag{2.7}$$

The last definition is key to efficient computation of 2-norm pseudospectra and provides the foundation for most all of the algorithms required for generating the ε-pseudospectral figures you will see in this document. In conclusion, if you perturb a nonnormal matrix by another matrix of magnitude ε , the eigenvalues of the new matrix may be more than ε away. The pseudoeigenvalues may even be positive for small perturbations, in the next section we will talk about the finite time transient behavior of nonnormal operators. At this point it should be stressed that pseudospectra are norm-dependent creatures: they are defined in terms of the norm of the resolvent and may show

transient growth in one norm and not the other. Ecologists have been aware of the possible weird behavior for some matrices for years now **[68]** and their metrics have historically used the 2-norm, so we will do things in the context of the 2-norm for the sake of comparison.

2.2.1. Real-structured perturbations. Up to now we have focused on complex perturbations of real matrices which gives us information on transient behavior. Another important question in many applications is: "If we measured some of our parameters wrong or perturb the parameters slightly, will our system still be stable?" To answer this question we need information on $\mathbf{A}+\mathbf{E}, \mathbf{E} \in \mathbb{R}^{N\times N}$, i.e. in terms of real perturbations of $\mathbf{A}$.

The **real structured ε-pseudospectra** is defined as the set of values that are the eigenvalues of a perturbed matrix $\mathbf{A}+\mathbf{E}$ where $\mathbf{A}, \mathbf{E} \in \mathbb{R}^{N\times N}$, i.e.

$$\Lambda_\varepsilon^{\mathbb{R}} := \bigcup_{|\,\mathbf{E}|<\varepsilon} \Lambda(\mathbf{A}+\mathbf{E}). \tag{2.8}$$

Now this is easy to state, but harder to calculate since in order to find the closest real matrix of norm ε we need to perform an optimization **[83]**. Let $\sigma_2(.)$ denote the second-largest singular value, then the 2-norm real stability radius

$$\varrho(\mathbf{A}, z) \equiv \left(\inf_{\beta\in(0,1]} \sigma_2\left(\begin{bmatrix} \mathfrak{Re}((z\mathbf{I}-\mathbf{A})^{-1}) & -\beta\mathfrak{Im}((z\mathbf{I}-\mathbf{A})^{-1}) \\ \beta^{-1}\mathfrak{Im}((z\mathbf{I}-\mathbf{A})^{-1}) & \mathfrak{Re}((z\mathbf{I}-\mathbf{A})^{-1}) \end{bmatrix} \right) \right)^{-1}$$

is unimodal (any local minimum is also a global minimum). We use $\varrho(\mathbf{A}, z)$ to make clear the dependence on z, this setup is preferred for computation which we will talk about in the next section. We now define

$$\Lambda_\varepsilon^{\mathbb{R}} := \{z \in \mathbb{C} : \varrho(\mathbf{A}, z) < \varepsilon\}. \tag{2.9}$$

While the real-structured pseudospectra might give us information about how close a system may be to instability, we need complex pseudospectra to give us info about transient behavior of

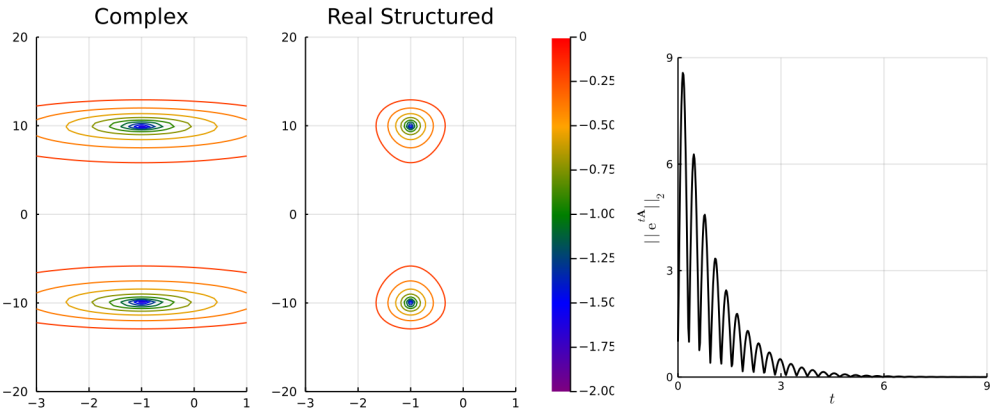

FIGURE 2.5. Real pseudospectra do not determine behavior. For example, here is a comparison of the complex versus real-structured pseudospectra of $M = \begin{bmatrix} -1 & 100 \\ -1 & -1 \end{bmatrix}$. To the right is a plot of the transient trajectory in time, which shows the wildly oscillatory behavior predicted by the complex pseudospectra. This is a log plot, so the orange line represents perturbations of $\varepsilon = 10^{-0.25}$, for example.

$|\, \mathrm{e}^{t\mathbf{A}}|$. To illustrate this point, a comparison of the real-structured versus the standard complex pseudospectra for a small 2x2 matrix a long with the trajectory of $|\, \mathrm{e}^{t\mathbf{A}}|$ can be found in Figure 2.5.

2.3. Distance to instability

One of our motivations for looking at real pseudospectra is answering questions about system stability. Since we will focus on continuous-time systems of ODEs, a matrix representation of such a system is considered stable if all of its eigenvalues lie to the left of the imaginary axis. It is then natural to ask what the smallest magnitude perturbation that results in the pseudospectra to touch the imaginary axis is.

The **distance to instability** or **stability radius** of a matrix $\mathbf{A}$ is defined as

$$\begin{aligned} r_{\mathbb{C}}(\mathbf{A}) &:= \min\{\varepsilon : \text{ boundary of } \Lambda_\varepsilon(\mathbf{A}) \text{ touches } \mathfrak{Re}(z) = 0\} \\ &= \min\{|\, \mathbf{E}| \ : \mathbf{A} + \mathbf{E} \text{ is unstable }, \ \mathbf{E} \in \mathbb{C}^{N\times N}\}. \end{aligned}$$

We have already seen in Figure 2.5 that the complex pseudospectra and real pseudospectra can be quite different. Studying real structured perturbations allows us to identify systems which may be in danger of losing stability despite have eigenvalues far to the left of the imaginary axis or identify

systems which may have wild transient behavior, but are not at risk losing mathematical stability. Let $\sigma_2(.)$ denote the second-largest singular value, then the 2-norm real stability radius

$$r_{\mathbb{R}}(\mathbf{A}) = \left(\sup_{\mathfrak{Re}(z)=0} \inf_{\beta \in (0,1]} \sigma_2 \left(\begin{bmatrix} \mathfrak{Re}((z\mathbf{I}-\mathbf{A})^{-1}) & -\beta\mathfrak{Im}((z\mathbf{I}-\mathbf{A})^{-1}) \\ \beta^{-1}\mathfrak{Im}((z\mathbf{I}-\mathbf{A})^{-1}) & \mathfrak{Re}((z\mathbf{I}-\mathbf{A})^{-1}) \end{bmatrix} \right) \right)^{-1} \tag{2.10}$$

is unimodal (any local minimum is also a global minimum) **[83]**. To put into words, we are finding the smallest ε-magnitude real perturbation matrix that makes the rightmost eigenvalue of $\mathbf{A}$ have zero real part, so we must do a search over the imaginary axis as well as over $\beta \in (0, 1]$.

2.4. Computation of Pseudospectra

2.4.1. Generating the pseudspectral pictures. For complex pseudospectra, the foundation for generating the pseudospectra plots is computing the norm of the resolvent for each z on a mesh (iterating over the real and complex axis in the loop) and then making a contour plot, which can be done for any norm. However, this can get computationally expensive and there are a number of algorithms that use clever ways of calculating the norm of the resolvent depending on the norm **[91]**. In the two norm, it is best to use Equation 5.2 for the calculation on the mesh, and we use an implementation of the slightly more sophisticated and noticeably faster Lanczos iteration with preliminary triangularization **[91]** (and outlined in **[92]**) for generating our pseudopectra figures (e.g. in Figure 2.4). One possible confusion that can happen depending on the algorithm you chose for pseudospectra computation is the value outputted from an algorithm may either be the value of the resolvent norm (ε^{-1}) in Equation 2.5 or the value of ε as a perturbation magnitude such as in Equation 5.2. All figures in this dissertation has the contour plots in terms of displaying the pseudospectra as $\log_{10}(\varepsilon)$. This means for naive looping over a mesh of z and brute force calculation of the resolvent norm or for our implementation of Lanczos iteration we have to invert each returned value of the mesh point to get things in terms of ε, but algorithms using Eq. 5.2 will return ε without needing any modification.

Real-structured pseudospectra computation requires an optimization search over $\gamma \in (0, 1]$ which requires a singular value decomposition for every test value in the optimization and at every grid point z. Because all the grid point calculations are independent of each other, this is at least an "embarrassingly parallel" problem and we recommend running the calculation over each mesh point

over multiple cores. One thing to keep in mind is that value at each grid point has the possibility of being an underestimate (Let's say we didn't find the true infimum then the value we found was an overestimate which means when we invert it we get an underestimate for the value of ε).

What about more specific structures? What if we want to perturb a Leslie matrix at only nonzero entries? For extremely specific structured perturbations one can use Equation 5.1 and choose random $\mathbf{E}$ for each so that $|\mathbf{E}| < \varepsilon$ for a selection of ε and of structure as specific as you need and then scatter plot the eigenvalues in the complex plane for a bunch of perturbations. For reference, §50 of **[92]** has some examples of such plots.

2.4.2. Computation of the distance to instability. We did not end up using the complex distance to instability, but numerical calculation of the complex distance to instability is usually done by bisection **[14, 33]**. As with the real-structured pseudospectra computation discussed in the previous section (Section 2.4), finding the real distance to instability ($r_{\mathbb{R}}$) requires performing an optimization. However, unlike the straight computation on a grid for displaying the real pseudospectra of we have the additional complication of a min-max problem with no guarantees on the shape or convexity of the function for the optimization over the imaginary axis. There are some things that make the optimization easier, because we have real-valued matrices we can leverage the symmetry in the eigenvalues restrict our search to the either the positive or negative half of the imaginary axis. Since we are dealing with finite operators, the vertical locations of the eigenvalues provide reasonable starting points for the search with a big caveat: We are not guaranteed the nearest real unstable matrix will be located at the complex part of the rightmost eigenvalues. This was proven in a famous counterexample constructed by Demmel in 1987, where the crux of the argument comes down to the fact that $\Lambda_\varepsilon(\mathbf{A})$ is not guaranteed to be convex **[25]**. For the search over the imaginary axis we did a naive random search, selecting points from a combination of a truncated normal distribution about zero and a truncated normal distribution around the imaginary part of the rightmost eigenvalue. We tuned the search so that we would have high precision on the finding the infimum, so that when we did an unsophisticated random search our estimates for the real distance to instability will in general be an overestimate (i.e. Let's say the our guess for the inner optimization of Equation 2.10 is correct, then doing a bad job at the search over the imaginary axis will give an underestimate of the supremum so that when we take the inverse we get an overestimate).

All algorithms in this dissertation were coded in the Julia programming language, we used BlackBoxOptim.jl for the optimization steps in our real-structured pseudospectra and make generous use of the built-in Julia "Distributed" package to do the mesh calculations over multiple cores.

2.5. Understanding transient dynamics

2.5.1. Bounds in ecology literature: Reactivity. The awareness of the possibility of transient amplification of perturbations after small perturbations due to nonnormality has been around since at least 1997 in the ecology literature **[68]**. The *reactivity* **[68]**, or the numerical abscissa $\omega(\mathbf{A})$ is defined as the maximum initial growth rate of $|\,\mathrm{e}^{t\mathbf{A}}|$ away from equilibrium. It is calculated as the maximum real part of the field of values of $\mathbf{A}$ (or the spectral abscissa of the Hermitian part of $\mathbf{A}$). We frame the problem in terms of optimization since later we will modify the problem to look at the optimization on a constrained space.

One way to characterize the transient response of a perturbation is to think about the maximum possible rate of change, $\omega(\mathbf{A})$ right after perturbation $\mathbf{x}$

$$\max_{|\,\mathbf{x}|\neq 0}\left|\frac{1}{|\,\mathbf{x}|}\frac{\mathrm{d}|\,\mathbf{x}|}{\mathrm{d}t}\right]_{t=0} = \lim_{t\to 0^+} t^{-1}\log|\,\mathrm{e}^{t\mathbf{A}}| = \omega(\mathbf{A})$$

Framing the numerical abscissa as a initial rate of change was the approach used in **[68]** and a derivation in terms of expanding out that derivative can be found therein. However, since $\frac{\mathrm{d}\mathbf{x}}{\mathrm{d}t}$ is defined in terms of matrix multiplication by the Jacobian $\mathbf{A}$ we can also think of the maximal initial growth $\omega(\mathbf{A})$ in terms of the optimization problem looking for the maximum real value of the transformation

$$F(\mathbf{A}) := \left\{\frac{\mathbf{x}^*\mathbf{A}\mathbf{x}}{\mathbf{x}^*\mathbf{x}} : \mathbf{x}\in\mathbb{C}^n\right\}$$

which is the definition of the field of values for matrix $\mathbf{A}$. The field of values has many nice properties which are discussed in detail in **[47]**, but one in particular is that $F(\mathbf{A})$ is defined for complex inputs and can give complex outputs, but if you want to only consider the real-valued outputs $\mathfrak{Re}(F(\mathbf{A}))$ then we have the relationship

$$\mathfrak{Re}(F(\mathbf{A})) = F(H(\mathbf{A})) = F\left(\frac{1}{2}(\mathbf{A}+\mathbf{A}^*)\right)$$

where $H(A)$ is the Hermitian part of $\mathbf{A}$. Note that after we sub in for $F\left(\frac{1}{2}(\mathbf{A}+\mathbf{A}^*)\right)$ into the original definition we get the exact same optimization problem of Neubert and Caswell in **[68]**, a Rayleigh quotient that we want to maximize over input vectors $\mathbf{x}$

$$\begin{aligned}\omega(\mathbf{A}) &= \max_{|\,\mathbf{x}|\neq 0} \frac{\mathbf{x}^T H(\mathbf{A})\mathbf{x}}{\mathbf{x}^T\mathbf{x}} \\ &= \max_{\lambda_i} \Lambda\left(\frac{1}{2}(\mathbf{A}+\mathbf{A}^*)\right) .\end{aligned} \tag{2.11}$$

The solution to this problem, vector $\mathbf{v}_\omega$, is the eigenvector that corresponds to the largest eigenvalue $\lambda_1(H(A))$ which is the maximum value of this ratio over all $\mathbf{x}$ **[47]**. The value $\lambda_1(H(A)) = \omega(\mathbf{A})$ is known as the numerical abscissa in numerical analysis and is the reactivity of Neubert and Caswell **[47, 68]**. The numerical abscissa both determines the behavior of $\lim_{t\to 0^+} t^{-1}\log|\,\mathrm{e}^{t\mathbf{A}}|$ and gives us an upper bound on $|\,\mathrm{e}^{t\mathbf{A}}|$ for all $t \geq 0$

$$|\,\mathrm{e}^{t\mathbf{A}}| \leq \mathrm{e}^{t\omega(\mathbf{A})}.$$

If the numerical abscissa is positive, then it is possible for there to be transient growth immediately following a perturbation of the equilibrium and this can happen despite the eigenvalues predicting eventual asymptotic decay **[68, 92]**. It should be noted that we are only guaranteed this growth for the vector solution of the above problem, $\mathbf{v}_\omega$, and it is possible for other perturbation directions to show no initial growth. For now on we will refer to $\mathbf{v}_\omega$ as the "optimal perturbation" vector, this is the unit vector (or a direction vector) that produces the largest initial transient growth and specifies a perturbation direction. The directional dependence in a system's response to a perturbation has been highlighted before (see: **[4, 68]**), so it is natural to ask what happens to the possibility of transient growth if we add more constraints on the direction of the perturbation vector, which we will address in Chapter 4.

The numerical abscissa is useful as an easily-calculated metric for identifying systems with problematic transients, which we will leverage in later chapters. Its main weaknesses is that it only

tells us something about the $t \to 0$ behavior and its nice relationship to Hermitian real part of $\mathbf{A}$ is only available to us in Hilbert spaces.

The next bound tells us something about the finite-time behavior of $|\,\mathrm{e}^{t\mathbf{A}}|$, specifically a time-independent lower bound on transient amplification.

2.5.2. Bounds in ecology literature: Kreiss bound. The Kreiss constant with respect to the left-half of the complex plane uses the resolvent **[54]** and is defined as

$$\mathcal{K}(\mathbf{A}) := \sup_{\mathfrak{Re}(z)>0} \mathfrak{Re}(z)|\,(z\mathbf{I}-\mathbf{A})^{-1}|\,,$$

which gives us another lower bound on $|\,\mathrm{e}^{t\mathbf{A}}|$

$$\sup_{t\geq 0} |\,\mathrm{e}^{t\mathbf{A}}| \geq \mathcal{K}(\mathbf{A}).$$

If we use the results in **[57]** the Kreiss constant also provides an upper bound

$$\sup_{t\geq 0} |\,\mathrm{e}^{t\mathbf{A}}| \leq \mathrm{e}N\mathcal{K}(\mathbf{A}), \qquad N \text{ dimension of } \mathbf{A}^{N\times N}.$$

The Kreiss bound is useful in understanding transient amplification because it can be used in sensitivity analysis using the Sherman-Woodbury-Morrison equation **[44, 89]**. Numerical implementations to calculate the Kreiss bound are nontrivial to implement **[65]**, and since many ecologists may end up plotting $|\,\mathrm{e}^{t\mathbf{A}}|$ vs time anyway it is far easier to just estimate it from plotting for a single parameter set.

2.5.3. Pseudospectra for transient dynamics. This section will be devoted to the study of $\mathbf{x}(t)$ as it evolves with time. While I will focus on the exponentiation of matrices, this theory readily extends to closed linear operators. Before we talk about lower bounds on $|\,\mathrm{e}^{t\mathbf{A}}|$ we need a few preliminaries. The ε-pseudospectral abscissa $\alpha_\varepsilon(\mathbf{A})$ is define as the largest real part of $\Lambda_\varepsilon(\mathbf{A})$ (Figure 2.6). For a negative-stable matrix $\mathbf{A}$ and $\varepsilon > 0$, if $\alpha_\varepsilon(\mathbf{A}) > \varepsilon$ then the $|\,\mathrm{e}^{t\mathbf{A}}|$ must have transient growth as it evolves with time. This "overlap" of the ε-pseudospectraal abscissa that extended over the expected perturbation magnitude ε gives us another definition of the numerical abscissa $\omega(\mathbf{A})$:

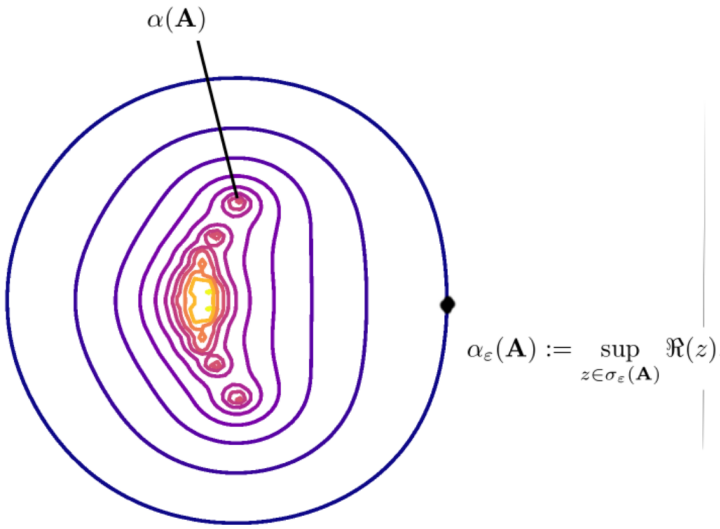

FIGURE 2.6

$$\omega(\mathbf{A}) = \lim_{\varepsilon\to\infty} \alpha_\varepsilon(\mathbf{A}) - \varepsilon.$$

THEOREM 2.5.1. *([92], §15) Let* $\mathbf{A}$ *be a matrix, if* $|(z\mathbf{I}-\mathbf{A})^{-1}| = K/\mathfrak{Re}(z)$ *for some* $z \in \mathbb{C}$ *with* $\mathfrak{Re}(z) > 0$ *and* $K > 1$*, then*

$$\sup_{t/ge0} |\,\mathrm{e}^{t\mathbf{A}}| \geq K.$$

The ε*-pseudospectral abscissa* $\alpha_\varepsilon(\mathbf{A})$ *is finite for each* $\varepsilon > 0$*. Taking the rightmost value of* z *in the complex plane of the level contour* $|(z\mathbf{I}-\mathbf{A})^{-1}|$ *gives us the convenient lower bound*

$$\sup_{t\geq 0} |\,\mathrm{e}^{t\mathbf{A}}| \geq \alpha_\varepsilon(\mathbf{A})/\varepsilon \qquad \forall \varepsilon > 0. \tag{2.12}$$

Now, we have already mentioned the Kreiss constant. If we take the supremum over $\varepsilon > 0$ *of the above we get the second definition of the Kreiss constant*

$$\mathcal{K}(\mathbf{A}) := \sup_{\varepsilon>0} \alpha_\varepsilon(\mathbf{A})/\varepsilon,$$

so that

$$\sup_{t\geq 0} \left| \mathrm{e}^{t\mathbf{A}} \right| \geq \mathcal{K}(\mathbf{A}). \tag{2.13}$$

If $a = \mathfrak{Re}(z)$*, then for any* $\tau > 0$*,*

$$\sup_{0<t\leq\tau} \left| \mathrm{e}^{t\mathbf{A}} \right| \geq \mathrm{e}^{a\tau} \Big/ \left(1 + \frac{\mathrm{e}^{a\tau} - 1}{K}\right). \tag{2.14}$$

Equation 5.6 makes precise the conditions for seeing transient growth for a given perturbation $|\mathbf{E}| = \varepsilon$. when an ε-pseudospectral contour extends into the right half of the complex plane we can expect some perturbations to lead to transient growth (the "reactivity" observed by **[68]**). During this time of transient growth z behaves like an eigenvalue and $\left| \mathrm{e}^{t\mathbf{A}} \right|$ evolves like e^{at}. How long this lasts for depends on the resolvent norm at z. we see from Eq. 5.7 that the larger the resolvent norm is. the larger K is and the longer the time scale that z behaves like an eigenvalue of $\mathbf{A}$. At this point two subtleties should be stressed. Firstly. these bounds depend on the resolvent. which means complex perturbations are involved. Even if we are only concerned with real matrices that act on real vectors we still need the complex perturbation to understand the time evolution behavior. We have already shown an example of where complex perturbations predict the transient behavior. but real perturbations fail to in Figure 2.5. but also in (**[92]**. pg. 457). Secondly. these give bounds in terms of the operator norm. so they represent the worst case response to a perturbation. It could be that a subset of matrix perturbations result in no transient growth. and one way this manifests is that not all vector inputs to $\mathrm{e}^{t\mathbf{A}}$ may result in transient amplification.

2.5.4. An example of a very nonnormal matrix without unruly transients. So far we have spent a lot of time talking about nonnormality and its relation to transients. but is a nonnormal matrix is not doomed to bad behavior. It is quite possible for the eigenvalue sensitivity to be concentrated on the negative side in such a way that the matrix not in danger of having a positive pseudoeigenvalue. Let $\mathbf{A}$ be a 20 X 20 upper triangular matrix of negative ones such that

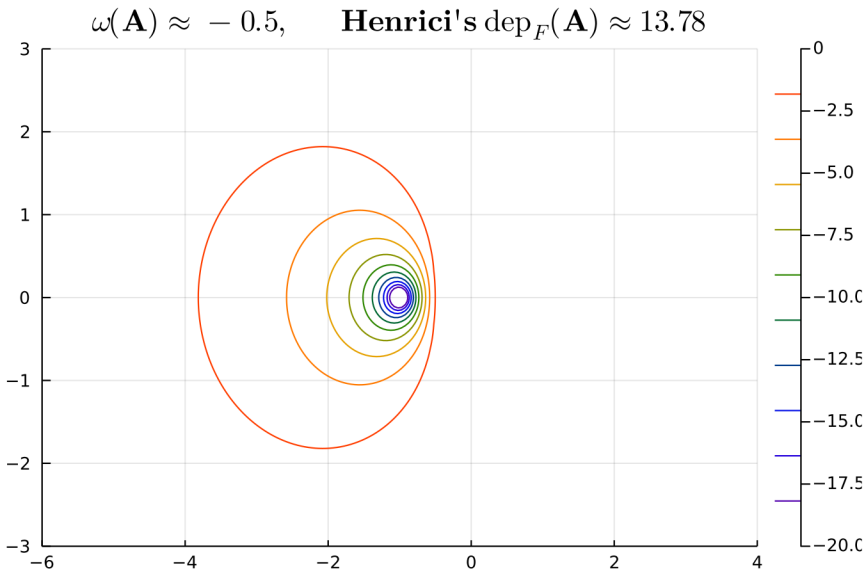

FIGURE 2.7. The complex pseudospectra for a 20 X 20 matrix upper matrix tiled with -1.

$$\mathbf{A} = \begin{bmatrix} -1 & -1 & \dots & -1 \\ 0 & -1 & \ddots & \vdots \\ \vdots & \ddots & \ddots & -1 \\ 0 & \dots & 0 & -1 \end{bmatrix}$$

If this matrix was representative of a dynamical system, we would call this a "recipient-controlled" system (if not a rather extreme case). The calculated numerical abscissa is $\omega(\mathbf{A}) \approx -0.5$ and the Henrici's departure from nonnormality is $\mathrm{dep}_F(\mathbf{A}) \approx 13.78$. While this matrix is quite nonnormal, it does not have a positive numerical abscissa and will not show transient growth for any perturbation direction.

2.6. Pseudospectra in context

We have given a very brief introduction to pseudospectra and the behavior of nonnormal matrices and introduced some illustrative examples of some subtleties to keep in mind. The most important conclusion, that eigenvalues may not give good information about finite-timescales and this has something to do with transient amplification, is one already known to ecologists for quite some time now. However, it is an open question how community structure, perturbation structure, and species

attributes might contribute to stability and transient dynamics [**85**]. Pseudospectral theory gives a starting framework to begin answering ecological questions that is more flexible than looking at simple reactivity (or the numerical abscissa).

We approach the question of how network structure and species attributes may contribute to transient dynamics by looking at what contributes to nonnormality in model systems, which is a necessary requirement for transient dynamics. Normality is a strong condition to meet, so we start by looking at biological constraints that might break the symmetry in species interactions, such as body size ratios and conversion efficiency. However, as we have shown, a system can be highly nonnormal but in a way that does not affect either transient dynamics or stability; these are the rare cases where the eigenvalues do accurately describe behavior and it is unknown to what extent stable ecological systems may meet this requirement.

One important consequence of nonnormality is that there exists linear (or linearized) dynamical systems that will always show transient growth or perturbation amplification for some perturbation directions. Previous ecological research has approached this problem by using the numerical abscissa as a flag for stable systems that may amplify perturbations, but not what types of perturbations may result in transient behavior. We leverage the optimization version of the definition of the numerical abscissa to study how network structure may lead to ecological systems to show transient amplification to removal perturbations, which has implications for management decisions in monitoring an ecosystem after a preserve is opened or closed and multi-species fisheries.

Finally, real-structured pseudospectra may not give us information about transient behavior but they are useful for telling us if a system may be in danger due to small changes in parameters. For ecological communities, it is unknown whether transient growth may be a signal a system that is close to instability. Even for systems which are not in danger of showing transient amplification of some types of perturbations can still be nonnormal, resulting in systems whose transient phase may last longer than expected and whose distance to instability is smaller than what their eigenvalues predict. For the latter, this is a case where just considering sign on numerical abscissa may be misleading when trying to understanding system behavior and it must be supplemented with other methods.

We close with the reminder that pseudospectra are norm-dependent. it is completely possible for a matrix to show transient growth in response to perturbations in one norm and not the other. The 2-norm is often used because existing in a Hilbert space gives us some nice easy-to-calculate metrics to identify systems which might have transient behavior and the algorithms to calculate pseudospectra in the 2-norm are efficient and easy to implement; we too fall into the trap of convenience for much of this dissertation due to the nature of our approach. However, it is hard to interpret the biological meaning of the two norm and for some systems it may be more natural to think about the 1-norm (the total density or abundance across all age classes or species). The benefit of using pseudospectra over some of the previous metrics found in ecological literature is that it is possible to choose whatever norm makes the most sense for the problem.

CHAPTER 3

Generalized Lotka-Volterra equations and their simulation

3.1. The generalized Lotka-Volterra equations

The previous chapter introduced nonnormality, pseudospectra, and provided some background intuition for why what sort of things we might need to check to fully understand the transient dynamics and stability of a system. This chapter introduces the model we will use to explore how structure and biological constraints contribute to the dynamics of small ecological networks in the context of nonnormality.

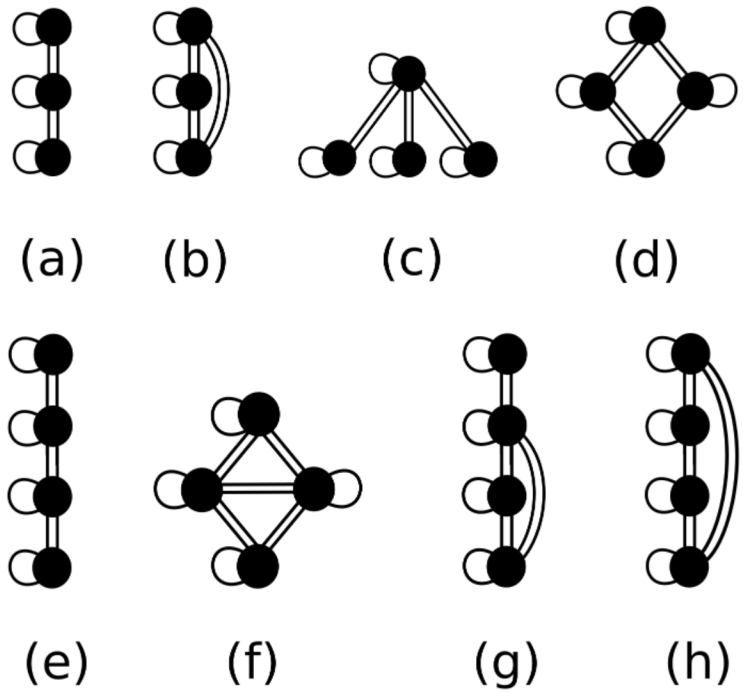

FIGURE 3.1. The eight modules whose dynamics are explored in this paper: (a) three species food chain. (b) three species omnivory. (c) four species generalist predator. (d) four species diamond. (e) four species food chain. (f) four species intraguild predation. (g) four species omnivory, third level omnivore. (h) four species omnivory, fourth level omnivore.

Ecological networks can be extremely large and complex, even a small subset of a community in a simplified food can have many connections over multiple trophic levels in ways where it is hard to tease out which things are most important to contributing to system dynamics [**81**]. A large network may be too complex to study, but only studying pairwise interactions may miss important dynamics such as chaos in the continuous-time case. One common approach to dealing with this complexity is to study small (on the order of 3-4 nodes), repeated subsets of the network structure called *motifs* in network analysis and generally refers to the structure of connections or *modules* in food web theory where the focus is on a weighted, directed network. Modules allow ecologists to bridge pairwise interactions to the dynamics of larger food webs [**87**], and it turns out that in real empirical food webs there are some modules that over-represented relative to synthetic food webs with randomly generated interactions [**8**, **17**].

We chose eight small network module configurations to focus on (Fig. 3.1): Four are common food web modules found in empirical food webs (three species omnivory, four species diamond, and four species intraguild predation) [**8**] and the other four were chosen to explore how trophic level, multiple prey species, and omnivory may influence stability and reactivity of feasible parameter sets. The community dynamics were described by the generalized Lotka-Volterra equations, which are one of the simplest models to explicitly describe the trophodynamics (dynamics of the trophic interactions) of S interacting species in an ecological network and are commonly used in community ecology studies [**30**, **36**, **64**, **104**]:

$$\frac{\mathrm{d}N_i}{\mathrm{d}t} = N_i \left(r_i + \sum_j a_{ij} N_j \right), \qquad i = 1, \ldots, S. \tag{3.1}$$

Here r_j are the intrinsic per-capita growth rates for each species where it is understood that $r_j > 0$ for basal species and $r_j < 0$ is the starvation rates for nonbasal species. The parameters a_{ij} are the per-capita consumptive interaction rates, i.e., if species i is consumed by species j then $a_{ij} < 0$ and $a_{ji} > 0$ [**102**]. We assume a simple linear functional response (Type I) for the predator as well as intraspecific dampening (the $a_{ii}N_i^2$ terms). In order to include asymmetry into predator-prey interactions due to body size ratio, assimilation efficiency or metabolics, which may be important to determining trophic interactions [**12**, **31**, **103**], we introduce an asymmetry parameter, c_s (coupling

symmetry), sensu **[35]** which is defined so that the negative interaction coefficient of the resource on the consumer scales as $c_s = a_{ji}/a_{ij}$. This form of the Lotka-Volterra equations was chosen for its simplicity in explicitly calculating the equilibrium point and Jacobian matrix. Let $[\mathbf{a_{ij}}]$ be the $S \times S$ matrix of coefficients of the interaction parameters a_{ij} and $\mathbf{r}$ be the $S \times 1$ vector of per-capita growth rates, then the equilibrium, $\mathbf{N}^*$, is the $S \times 1$ solution vector to

$$\mathbf{r} + [\mathbf{a_{ij}}]\mathbf{N}^* = 0.$$

So long as $[\mathbf{a_{ij}}]$ is invertible, this system of equations has the unique solution

$$\mathbf{N}^* = -[\mathbf{a_{ij}}]^{-1}\mathbf{r} \tag{3.2}$$

and the Jacobian matrix at this equilibrium is given by

$$A_{ij} = N_i^* a_{ij} \ .$$

The biological meaning and terminology associated with the Jacobian matrix has historically varied in food web ecology **[74]** and at this point it is worthwhile to clarify some nomenclature. In this dissertation the a_{ij} parameters in the original Lotka-Volterra equations will be referred to as the "predator-prey interaction parameters. The Jacobian, $\mathbf{A}$, corresponds to the "Community matrix" of **[74]** where each entry A_{ij} is interpreted as the direct effect of the average species j individual on species i's population growth rate.

3.2. Simulation and parameter set generation

We had two goals in mind when setting up the feasible parameter search: To include the minimal amount of detail in order for realistic-looking systems to emerge and to thoroughly explore the parameter space to generate such systems. For each of the sets of the parameters in Equation 3.1 we calculated the linearization around the guaranteed unique equilibrium by directly solving Equation 3.2. For each module type in Figure 3.1 we drew 100,000,000 parameter sets as outlined in Appendix B.1 and kept those which were considered *feasible*, i.e. the equilibrium contains no species with a negative density ($N_i^* \geq 0$ for all N_i); parameter sets which were not feasible were discarded (similar

to **[104]**). The enforcement of the feasibility requirement is why we go from parameterizing the original Lotka-Volterra equations and finding the Jacobian rather than using the random matrix approach of starting with the Jacobian that is common in community ecology research **[2, 3, 63]**. Another notable detail is that we excluded diagonally dominant matrices since we know they are guaranteed to be stable by the Gershgorin disc theorem **[43]**. The distributions and explanation for each of the parameters can be found in Table 3.1. The quantities calculated and tracked for each parameter set can be found in Table 3.2.

3.3. Results of the parameter set generation

The end result for our choices were that despite not enforcing this in the parameter search, the equilibrium densities of our systems frequently followed a "pyramid" pattern where lower trophic levels had higher equilibrium density levels (Appendix B.2). For the modules where the predators feed on multiple prey at the same trophic level, the predator has the highest consumption of the most abundant prey, but the positive benefit of the prey on the predator are roughly the same for all choices of prey. Except for the two trophic level four species generalist module, finding a feasible parameter set was rare but once a feasible system was found it was highly likely to be stable (Table 3.3). In the average our parameter sets displayed strong-weak consumer-resource pattern where a predator feeding on multiple species has the strongest resulting interaction strength with the most abundant prey (Appendix B.2) and a predator that consumes multiple prey species has only one strong interaction.

It is apparent from our results that number of trophic levels, rather than number of species is more important for finding a stable parameter set with feasible equilibrium. The two-trophic level four species generalist module had orders of magnitude more stable parameter sets found all the other modules with more trophic levels. For the limited number of network structures studied there appears to be the pattern that the number of trophic levels, rather than number of species, seems to correlate with the proportion of reactive parameter sets found. A more detailed analysis with larger food webs would be needed to see if that pattern holds true in the general sense.

TABLE 3.1. A reference table for the parameters and the distributions they were drawn for the generalized Lotka-Volterra equations of eight different module structures.

parameter	description	distribution or value
r_i	growth rate of basal species (+)/starvation rates of nonbasal species (-)	Uniform(0.1, 1)
a_{ij}	per-capita consumption rate of predator on prey	-(Uniform(0.01, 1))
c_s	asymmetry parameter controlling assimilation efficiency/body size ratio	-(Uniform(0.0000001, 1))
a_{ji}	per-capita consumption rate of predator on prey (+)*	$c_s a_{ji}$

* = sign clarifications

TABLE 3.2. Values tracked for each parameter set during the initial parameter set search and in later chapters.

value	description	calculation
$\mathfrak{Re}\left(\max_{\lambda_i}\ \sigma(\mathbf{A})\right)$	maximum real eigenvalue	-
$\omega(\mathbf{A})$	numerical abscissa/reactivity	$\max_{\lambda_i}\ \sigma\left(\frac{1}{2}(\mathbf{A}+\mathbf{A}^*)\right)$
$\mathrm{dep}_F(\mathbf{A})$	Henrici's departure from normality	$\left(\sum_{j=1}^{N}\sigma_j^2 - \sum_{j=1}^{N}\ \lambda_j\ ^2\right)^{1/2}$
Values collected in later chapters		
$\gamma(\mathbf{A})$	structured numerical abscissa for removal perturbations	gradient ascent search on restricted domain
$r_{\mathbb{R}}$	real distance to instability	(see Equation 2.10)
$\lvert\,\mathbf{A}^{-1}\rvert^{-1}$	distance to singularity	-

TABLE 3.3. The proportion breakdown of stable, stable reactive, unstable, and unstable reactive systems for each module (given as %). The raw number of non-negative equilibria out of 100.000.000 sets of parameters for each simple Lotka-Volterra network module is reported in the rightmost column.

Here S = stable, US = unstable, and R = reactive

	positive coexistence			$\geq$ 1 species extinct			
(module)	S	SR	USR	S	SR	USR	**Total #**
generalist (4 species)	35.3553	64.2347	0.0	0.0026	0.4073	0.0001	31,785,650
omnivory (3 species)	11.9691	87.1983	0.1438	0.0002	0.6878	0.0009	4,438,997
chain (3 species)	14.9089	84.6195	0.0	0.0019	0.4698	0.0 *	3,122,030
diamond (4 species)	4.2403	94.9187	0.0	0.0002	0.8407	0.0001	965,307
omnivory (4 sp. 3rd L)	4.4686	94.8607	0.0314	0.0019	0.6361	0.0012	885,023
intraguild predation	3.682	95.446	0.0504	0.0	0.8212	0.0003	868,217
omnivory (4 sp. 4th L)	2.4291	96.6124	0.0	0.0004	0.9581	0.0	759,739
chain (4 species)	4.227	95.1618	0.0	0.0053	0.606	0.0	416,516

* = This entry was reported as zero because there was only 1 system found
NOTE: No systems were found to be purely unstable (and not also reactive), so those columns were omitted

CHAPTER 4

A study on pulse perturbations and the transient behavior of nonnormal systems

4.1. A preface

This next chapter may feel a little odd after the pseudospectra chapter since there is not a pseudospectra in sight. However, it covers an important consequence of nonnormality: The tendency for nonnormal systems to amplify perturbations and the fact that the direction of the perturbation (or in the ecological case, which species you perturb) matters. Up to this point a lot of research has been focused on whether or not a system *can* display weird transients, and not if it *will* for the types of perturbations ecological communities commonly experience. In this chapter we show that reactive, or systems with a positive numerical abscissa, make up a majority of the parameter space for small communities and that this sort of amplification happens more than expected for removal perturbations involving multiple species at once.

4.2. Introduction

How does an ecosystem respond to change? Any attempt to describe the dynamics will need to consider at least 1) The timescale, spatial scale, frequency, and magnitude of the disturbance causing the change; 2) The timescale, spatial scale, and magnitude of the response of the system to the disturbance; 3) Some reference point to compare the above to. Deciding on the reference point is of course the hard part, since it sets the expectations for what gets measured and what counts as a long timescale or a large change for the first two.

Ecological stability is a multidimensional concept that characterizes the ecosystem response to external disturbances. To put in simple terms, a system with high stability mostly stays the same after a disturbance and if it does change, it quickly moves back to where it was before [**26**, **46**, **51**]. Under the idea stability we have the more specific concepts of resistance and resilience. Resistance

describes the magnitude of the measured system response to a disturbance, but does not refer to the timescale of the response in any way (how long it takes to recover); systems that have a large magnitude response to a perturbation are said to not be very resistant [77]. Resilience has been a recent popular topic of discussion [1, 37, 78]; and like other stability measures can mean slightly different things depending on the reference point chosen, what actually gets measured, and which discipline is using the term [26, 38]. For our purposes, we take the meaning of resilience to specifically describes the timescale of recovery as in [5, 77] rather than the more general interpretation involving absorbing changes so that the reference point is maintained [46]. We say a system has high resilience if the recovery time after a disturbance is short [78]. Since we will be using a system of ordinary differential equations to describe an ecological system and its interactions between species, our reference point will be a linearization about an equilibrium.

A common way to study ecological stability is through perturbations, or altering the density of one or more species and seeing how the system responds [11, 51]. Theoretical studies tend to focus on either the short end of the timescale (pulse perturbations) or the long end of the timescale (press perturbations) [51]. In this paper we will be looking at pulse perturbations, where a system is instantaneously perturbed by adding or removing members of a species population [11]. The direction of the pulse perturbation, or how the intensity of the perturbation is distributed over all the species in the system, determines the finite-time system dynamics for the system [4, 68]. There is of course comes the practical issue of what and when to measure, and unfortunately there is frequently a mismatch in the timescales studied by theoreticians and empiricists [26]. The finite-time behavior of a system, which is the timescale empirical data is collected on, can be qualitatively quite different than the asymptotic dynamics predicted by many models [39]. These counterintuitive transient dynamics can arise from many sources [41]; since we will be focusing on linearization about an equilibrium we will be using *reactivity* as a proxy for possible transient behavior, defined as the maximum possible initial amplification following a perturbation calculated over all possible perturbations [68]. Systems which have a positive initial amplification (or reactivity) in response to a pulse perturbation despite being asymptotically stable are said to be reactive. The characteristic growth of reactive systems away from the equilibrium may continue for quite some time before decaying, meaning old metrics of resilience which focus on asymptotic decay may be inappropriate

since they are not representative of the population dynamics on the sort of timescales ecological data is collected on [**40**, **68**]. Additional theoretical stability metrics that account for reactivity have since been introduced, such as intrinsic stochastic invariability and average return rate [**4**, **5**]. All of these seek to improve on the original metric of resilience, *asymptotic resilience*, which historically has been used because it is easily calculated from the eigenvalues of the Jacobian matrix determining the system dynamics.

At this point reactivity is a well documented phenomena that is present in discrete-time [**19**] as well as continuous-time models (in particular all predator-prey models when at least one species has density-independent mortality [**71**]). Reactivity is a necessary condition for developing Turing instabilities in spatial pattern formation for systems modeled by reaction-diffusion equations or the discrete-time analog of integrodifference equations [**69**]. Average reactivity tends to increase with the number of species present and number of donor-controlled links [**20**]. Large elements in the Jacobian matrices governing the system dynamics increases the capacity for a system to be reactive in continuous-time systems and can force reactivity in discrete-time systems if the mean element size is large enough [**85**].

Reactivity is important but it comes with a caveat in that it describes the worst possible behavior, i.e. it is an upper bound. Whether or not odd transient behavior can happen is dependent on the perturbation direction [**4**, **68**, **85**]. Stated in biological terms, the pulse perturbation direction is how the intensity of the perturbation is distributed over all the species in the system. Reactivity is said to be *directionally dependent* because the characteristic perturbation amplification may only happen for some combination of perturbations of species densities and this behavior is independent of the total pulse magnitude. Since reactive systems may initially grow exponentially away from an equilibrium and take a long time to eventually decay back, this brings up the possibility of ecological systems which fail to be resilient and resistant for only some types of perturbation. It is still unknown how specific the conditions need to be for a stable reactive system to display the characteristic transient growth.

Here we leverage the definition reactivity and its roots in the Rayleigh quotient to investigate if pulse perturbations which alter species densities by either leaving them untouched or removing them are amplified. This type of structured perturbation is relevant for studying reactivity in systems after

TABLE 4.1. A reference table for the model used in this chapter. Details on parameter set generation can be found in Chapter 3. We use the generalized Lotka-Volterra equations to describe the dynamics of small network modules of 3-4 species given by $\frac{\mathrm{d}N_i}{\mathrm{d}t} = N_i\left(r_i + \sum_j a_{ij}N_j\right), \qquad i = 1, \ldots, S$ for S interacting species. This was done for the eight different network module structures in Figure 3.1.

parameter	description	calculation
r_i	growth rate of basal species (+)/starvation rates of nonbasal species (-)	-
$\mathbf{r}$	the $S \times 1$ vector of r_i's	
a_{ij}	per-capita consumption rate of predator on prey	-
c_s	asymmetry parameter controlling assimilation efficiency/body size ratio	-
a_{ji}	per-capita consumption rate of predator on prey (+)*	$c_s a_{ji}$
$[\mathbf{a_{ij}}]$	$S \times S$ matrix of interaction parameters	
N_i	density of species i	-
$\mathbf{N}^*$	the $S \times 1$ vector of equilibrium densities	$\mathbf{N}^* = -[\mathbf{a_{ij}}]^{-1}\mathbf{r}$
$\mathbf{A}$	the $S \times S$ Jacobian matrix	$A_{ij} = N_i^* a_{ij}$

* = sign clarifications

catastrophic natural disasters, the trajectory of recovering communities after extractive activities have been discontinued (such as fishing), and to resource pulses (due to some symmetries in the Rayleigh quotient we can flip the sign on the perturbation). We call these *removal* pulse perturbations, and the systems which are reactive for these restricted-structure perturbations Removal Stable Reactive (RSR) systems. Since we would like to understand how community structure might contribute to reactive dynamics, we take the approach of studying simple network modules commonly found in real food webs rather than randomly generated network structures [8].

4.3. Methods

4.3.1. Model Description. We use the model and the parameter sets generated as outlined in Chapter 3. Table 5.2 has a notation summary of the previous chapter for reference.

4.3.2. Optimization to find maximal pulse perturbation. First let us take a brief detour to talk about some properties of the linear systems of ODEs of the form $\frac{\mathrm{d}\mathbf{x}}{\mathrm{d}t} = \mathbf{A}\mathbf{x}$, $\mathbf{x}(0) = \mathbf{x}_0$, where $\mathbf{A}$ is invertible and then we will talk about our specific case. One way to characterize the transient response of a perturbation is to think about the maximum possible rate of change, $\omega(\mathbf{A})$ right after perturbation $\mathbf{x}$

$$\max_{|\,\mathbf{x}|\neq 0}\left|\frac{1}{|\,\mathbf{x}|}\frac{\mathrm{d}|\,\mathbf{x}|}{\mathrm{d}t}\right]_{t=0} = \lim_{t\to 0^+} t^{-1}\log|\,\mathrm{e}^{t\mathbf{A}}| = \omega(\mathbf{A})$$

This was termed "reactivity' in **[68]** and a derivation in terms of expanding out that derivative can be found therein. However, since $\frac{\mathrm{d}\mathbf{x}}{\mathrm{d}t}$ is defined in terms of matrix multiplication by the Jacobian $\mathbf{A}$ we can also think of the maximal initial growth $\omega(\mathbf{A})$ in terms of the optimization problem looking for the maximum real value of the transformation

$$F(\mathbf{A}) := \left\{\frac{\mathbf{x}^*\mathbf{A}\mathbf{x}}{\mathbf{x}^*\mathbf{x}} : \mathbf{x}\in\mathbb{C}^n\right\}$$

which is the definition of the field of values for matrix $\mathbf{A}$. The field of values has many nice properties which are discussed in detail in **[47]**, but one in particular is that $F(\mathbf{A})$ is defined for complex inputs and can give complex outputs, but if you want to only consider the real-valued outputs $\mathfrak{Re}(F(\mathbf{A}))$ then we have the relationship

$$\mathfrak{Re}(F(\mathbf{A})) = F(H(\mathbf{A})) = F\left(\frac{1}{2}(\mathbf{A}+\mathbf{A}^*)\right)$$

where $H(A)$ is the Hermitian part of $\mathbf{A}$. Note that after we sub in for $F\left(\frac{1}{2}(\mathbf{A}+\mathbf{A}^*)\right)$ into the original definition we get the exact same optimization problem of Neubert and Caswell in **[68]**. The Rayleigh quotient that we want to maximize over input vectors $\mathbf{x}$ is

$$\begin{aligned}\omega(\mathbf{A}) &= \max_{|\,\mathbf{x}|\neq 0}\frac{\mathbf{x}^T H(\mathbf{A})\mathbf{x}}{\mathbf{x}^T\mathbf{x}} \\ &= \max_{\lambda_i}\Lambda\left(\frac{1}{2}(\mathbf{A}+\mathbf{A}^*)\right)\ .\end{aligned} \tag{4.1}$$

In the second line we show the solution to this problem, vector $\mathbf{v}_\omega$, is the eigenvector that corresponds to the largest eigenvalue $\lambda_1(H(\mathbf{A}))$ which is the maximum value of this ratio over all $\mathbf{x}$ **[47]**. The value $\lambda_1(H(\mathbf{A})) = \omega(\mathbf{A})$ is known as the numerical abscissa in numerical analysis and is the reactivity of Neubert and Caswell **[47, 68]**. The numerical abscissa both determines the behavior of $\lim_{t\to 0^+} t^{-1}\log|\,\mathrm{e}^{t\mathbf{A}}|$ and gives us an upper bound on $|\,\mathrm{e}^{t\mathbf{A}}|$ for all $t\geq 0$

$$|\,\mathrm{e}^{t\mathbf{A}}| \leq \mathrm{e}^{t\omega(\mathbf{A})}.$$

If the numerical abscissa is positive, then it is possible for there to be transient growth immediately following a perturbation and this can happen despite the eigenvalues predicting eventual asymptotic decay [**68**, **92**]. It should be noted that we are only guaranteed this growth for the vector solution of the above problem, $\mathbf{v}_\omega$, and it is possible for other perturbation directions to show no initial growth. For now on we will refer to $\mathbf{v}_\omega$ as the "optimal perturbation' vector, this is the unit vector (or a direction vector) that produces the largest initial transient growth and specifies a perturbation direction. The directional dependence in a system's response to a perturbation has been highlighted before (see: [**4**, **68**]), so it is natural to ask what happens to the possibility of transient growth if we add more constraints on the direction of the perturbation vector. In optimization terms, this translates to restricting the domain the optimization search is run on.

4.3.2.1. *Modifying the optimization problem for sign-structured inputs.* The last section applies to any linear system, let us return to our particular problem which is a linearization of a system about the equilibrium $\mathbf{N}^*$

$$\frac{\mathrm{d}\mathbf{N}}{\mathrm{d}t} = \mathbf{A}(\mathbf{N} - \mathbf{N}^*) \tag{4.2}$$

to explore how module structure influences the system response to a small pulse perturbation away from the equilibrium $\mathbf{N} = \mathbf{N}^* + \Delta\mathbf{N}$. We are interested in looking at what happens when you restrict the sign structure so that every term in the input vector has the same sign parity. For our particular linearization sign convention above, if we want to think about a removal perturbation where we either leave a species untouched or subtract from the equilibrium population we now have the condition

$$(\Delta\mathbf{N})_i \leq 0, \ \forall i.$$

In our optimization framework above, this is equivalent to adding the constraint $(x_i) \leq 0, \ \forall i$ to our optimization problem in eq. 4.1.

Our optimization problem is quadratic, so for practical purposes it does not matter if we choose our constraint to be $x_i \leq 0, \ \forall i$ or $x_i \geq 0, \ \forall i$ so long as we do not have mixed signs in the vector $\mathbf{x}$, since $\mathbf{x}^T H(\mathbf{A})\mathbf{x} = (-\mathbf{x}^T)H(\mathbf{A})(-\mathbf{x})$. With this constraint on the domain we can no longer use

the property in Equation 4.1, so we use gradient descent method and at each step projected the prospective solution vector v_γ onto the positive real numbers so that negative values in the vector are set to zero. Since positive symmetric matrices will have an all positive solution vector to Equation 4.1, we confirmed the modified gradient descent was working by making the checking that the solutions $\omega(\mathbf{A})$, $\gamma(\mathbf{A})$ and their corresponding vectors v_γ and v_ω matched. One thing to worry about is if the optimization algorithm finds a different or misses a parameter set that has positive numerical abscissa for a removal perturbation. We ran the optimization gradient descent twice and got the exact same number of results for every module except the generalist four species module (which differed by 0.1 %).

At this point we would like to clarify the relationship between our parameters $\omega(\mathbf{A})$ and $\gamma(\mathbf{A})$. Since we are looking at a restricted domain of the same optimization problem in eq. 4.1, $\gamma(\mathbf{A}) \leq \omega(\mathbf{A})$ and $\gamma(\mathbf{A})$ may be negative, meaning that there are no all removal perturbations can result in a positive initial proportional amplification. Both $\omega(\mathbf{A})$ and $\gamma(\mathbf{A})$ describe the system behavior as $t \to 0$, and for linear systems of the form $\frac{\mathrm{d}\mathbf{x}}{\mathrm{d}t} = \mathbf{A}\mathbf{x}$, $\mathbf{x}(0) = \mathbf{x}_0$, where $\mathbf{x}$ represents a population vector then $\omega(\mathbf{A})$ is the maximum possible initial growth rate $\omega(\mathbf{A}) = (\frac{\mathrm{d}}{\mathrm{d}t}|\,\mathrm{e}^{\mathbf{A}}|\,)_{t=0}$. However, since we are interested in perturbations of a system linearized about an equilibrium of the form in Equation 4.2. $\omega(\mathbf{A})$ and $\gamma(\mathbf{A})$ describe by what factor the perturbation $(\mathbf{N} - \mathbf{N}^*)$ is amplified at $t = 0$. As has been brought up in the past, the perturbation that results in the greatest initial amplification my not be the perturbation that results in the largest magnitude "peak' in the amplification envelope (i.e. the trajectory of $|\,\mathrm{e}^{\mathbf{A}}|$ as it evolves with time) **[68]**.

Another point of interest we will look into is resource pulses, which are low-frequency, large-magnitude resource super-abundances that happen over a short time scale **[98]**. In our framework, this would be represented as a positive direction vector of unit length, $\mathbf{v}_r$ with a one in the last index. Similarly to above, we are interested in whether this perturbation is initially amplified which suggests that the system may experience a long transient phase away from the equilibrium before returning. Using Equation 4.1 calculate the growth rate of our specific resource pulse perturbation as

$$\frac{\mathrm{d}|\,\mathbf{v}_r|}{\mathrm{d}t} = \frac{\mathbf{v}_r^T H(\mathbf{A})\mathbf{v}_r}{\mathbf{v}_r^T\mathbf{v}_r},\ \mathbf{v}_r := (1, 0, \ldots, 0)^T.$$

TABLE 4.2. The relative percent positive coexistence equilibria categorized by transient behavior for eight simple Lotka-Volterra network modules. The "expected %' is the proportion of stable reactive parameter sets we should expect to be reactive for strict-removal experiments if the optimal perturbation vectors for SR systems were distributed uniformly in $S-$dimensional space. S being the number of species in the system. This is calculated as $1/2^S$.

(module)	% SRI of S parameter sets	% RSR of SRI	Expected % for RSR of SRI
generalist (4 species)	64.50	12.93	6.25
omnivory (3 species)	87.93	13.29	12.5
chain (3 species)	85.02	9.289	12.5
diamond (4 species)	95.72	20.78	6.25
omnivory (4 sp. 3rd L)	95.50	31.16	6.25
intraguild predation	96.29	31.74	6.25
omnivory (4 sp. 4th L)	97.55	19.94	6.25
chain (4 species)	95.75	15.84	6.25

S = stable systems (which include stable reactive and removal stable reactive)
SRI = stable reactive inclusive (which includes RSR sets)
RSR = removal stable reactive (reactive for species removal pulse perturbations).
Note: I ran the optimization gradient descent twice and got the exact same number of results for every module except the generalist 4 species module (which differed by 0.1 %).

4.4. Results

4.4.1. Initial growth of perturbations. For the remainder of the paper we shall refer to stable reactive systems which are reactive for removal perturbations as RSR (Removal Stable Reactive) systems and those which are not reactive for the optimal removal perturbation simply as SR (Stable Reactive) systems. These two types of system together form a partition of the SRI (Stable Reactive. Inclusive) parameter sets and we will focus on comparing the characteristics of these two subsets of SRI systems. These results reiterate previous finding that eigenvalues are poor predictors of the initial transient behavior of an ecological community. A majority of the generated stable systems we found to also be reactive ($> 85\%$ of the feasible stable systems found for every module except the four species generalist. Table 4.2). The numerical abscissa represents an upper bounder relative to $\gamma(\mathbf{A})$. but it is notable the magnitude of $\gamma(\mathbf{A})$ corresponding to the removal perturbation $\mathbf{v}_\gamma$ for RSR systems was much smaller than the magnitude than the standard numerical abscissa $\omega(\mathbf{A})$. and this was true for all module structures (Table 4.3). Removal stable reactive

TABLE 4.3. A comparison of the average numerical abscissa, $\omega(\mathbf{A})$, and removal numerical abscissa, $\gamma(\mathbf{A})$, for eight different food web module structures. We also include the average rightmost eigenvalue for each dataset (last two columns).

	$\omega(\mathbf{A})$		$\gamma(\mathbf{A})$		$\mathfrak{Re}\left(\max_{\lambda_i}\ \sigma(\mathbf{A})\right)$	
(module)	SR	RSR	SR	RSR	SR	RSR
generalist (4 species)	0.251	0.105	-0.127	0.055	-0.133	-0.046
omnivory (3 species)	0.205	0.402	-0.043	0.067	-0.073	-0.075
chain (3 species)	0.214	0.546	-0.048	0.133	-0.101	-0.166
diamond (4 species)	0.259	0.47	-0.03	0.079	-0.062	-0.054
omnivory (4 sp. 3rd L)	0.263	0.487	-0.031	0.088	-0.07	-0.079
intraguild predation	0.248	0.488	-0.031	0.092	-0.063	-0.063
omnivory (4 sp. 4th L)	0.275	0.284	-0.026	0.043	-0.061	-0.052
chain (4 species)	0.224	0.416	-0.028	0.085	-0.076	-0.091

SR = stable reactive systems (to the exclusion of removal stable reactive systems)
RSR = removal stable reactive (reactive for species removal pulse perturbations).

systems also had a higher average $\omega(\mathbf{A})$ than SR systems, except for the omnivory four species, 4th level omnivore and the generalist four species modules.

4.4.2. Perturbation direction. In order to compare the RSR to the SR parameter sets, we calculate the probability of randomly selecting a vector with all negative entries from $S-$dimensional space as $\frac{1}{2^S}$. This value only depends on the number of species in the system and gives the expected proportion SRI system if the optimal perturbation vectors were uniformly distributed. Systems which can show reactive transient dynamics in response to a removal perturbation happen more likely than expected for the four-species modules, but not the three-species modules (Table 4.2).

We collected the optimal removal vector $\mathbf{v}_\gamma$ and optimal perturbation vector $\mathbf{v}_\omega$ for both the RSR and SR parameter sets. Since we are interested in how structure and removal perturbation direction might differ between the RSR and SR parameter sets, we have histograms of the magnitudes of $\mathbf{v}_\gamma$ in Figures 4.1 - 4.2. The direction of the RSR optimal vectors ($\mathbf{v}_\omega$) that result in the largest initial growth were relatively agnostic to underlying module structure. Unlike the mixed-sign optimal perturbation vector, the optimal removal vector almost never perturbs the basal species, regardless of the network structure (Figure 4.1 - 4.2). Now, just because the optimal perturbation does not involve perturbing the basal species does not exclude a system showing positive initial growth to a resource pulse. However, we tried resource pulse perturbations of the form: just the basal species, just the

second trophic level, and just the basal and second trophic level simultaneously and calculated the Rayleigh quotient of each RSR system at the vector. For our model systems, reactivity to resource pulses are rare and only happens if you perturb multiple trophic levels at once (less than 5% of the RSR systems for each module, except for the four-species food chain and and four-species, 4th level omnivory modules at 6.63% and 7.34% respectively).

One thing the SRS and SR systems shared is the structure of $\mathbf{v}_\gamma$ involves removing the top predator and the species with the smallest equilibrium density on the trophic level below it (Figure 4.1 - 4.2). This only fails for omnivory modules, where it is optimal to perturb the omnivore and its prey directly below it regardless of the trophic level of the omnivore as can be see with the omnivory four-species, 3rd level, module (Figure 4.2). During parameter set generation we noticed that for modules with structural symmetries, like the diamond and four-species generalist, there was an emergent pattern for the top predator to have the highest consumption rate of the most abundant prey. In the case of modules where a predator feeds on multiple prey on the same trophic level (i.e. diamond and generalist modules) the optimal removal perturbation targeted the rarest of the prey species that results in positive growth in response (diamond 97.95% of the datatsets, generalist 100%).

4.4.3. Patterns in perturbation-growth response. So far we have found that perturbations that remove the top predators at multiple trophic levels is the most likely going to result in transient growth (or the slowest decay in the cases of the SR parameter sets). We summarize the sign of the entries of $\mathbf{v}_\omega$ and $\mathbf{v}_\gamma$ for the SR and RSR systems and the corresponding response of the species initial growth or decay $\mathbf{A}\mathbf{v}_\omega$ and $\mathbf{A}\mathbf{v}_\gamma$ in Table 4.4-4.7. Systems which show transient growth to removal perturbations also have a characteristic growth-response sign pattern. With the exception of the four species generalist, perturbation $\mathbf{v}_\gamma$ of SR systems tend to remove the top predator and the result is the consumer one trophic responds with positive growth and the top predator increases back to equilibrium. Because of the way the initial growth is calculated, this suggests that penalty the predator is experiencing due to the simultaneous removal of its prey is greater than the benefit it would gain by the reduction of density-dependent mortality pressure in SRS systems. Stated differently, interaction strength of the positive predator-prey link $A_{i,j}$ is larger relative to the intraspecific dampening, $A_{i,i}$, i.e. the ratio $A_{i,j}/A_{i,i}$ is in general larger in RSR systems than it is in

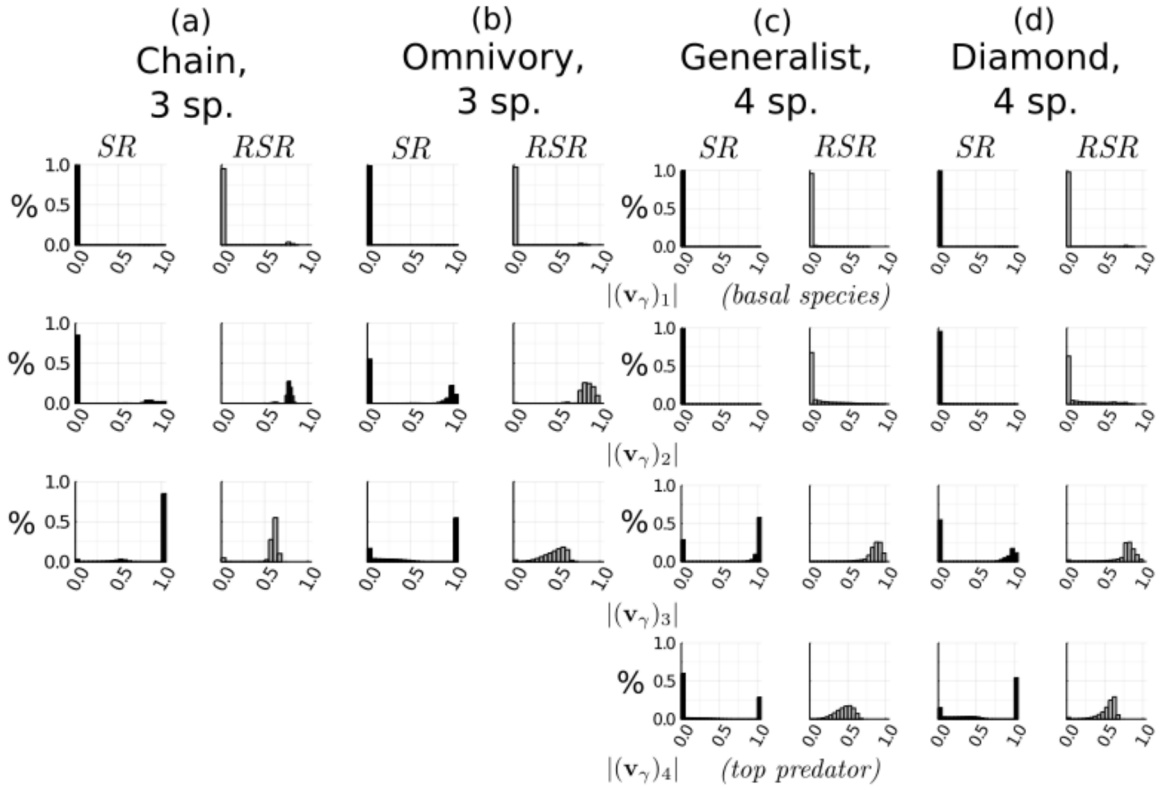

FIGURE 4.1. Distribution of the magnitude at each trophic level for the removal perturbation ($\mathbf{v}_\gamma$) of the SR (Stable Reactive) and RSR parameter (Removal Stable Reactive) sets. Modules with more than one species on the same trophic level (generalist 4 sp. and diamond 4 sp.) were ordered so that higher equilibrium density were assigned a lower index in the $\mathbf{v}_\gamma$ vector. These histograms represent a minimum of 300,000 parameter sets each.

SR systems. This pattern is strongly true in the food chain modules and the dominant pattern in the intraguild predation, diamond, and omnivory modules (Table 4.4-4.7, rows for N_3 and N_4).

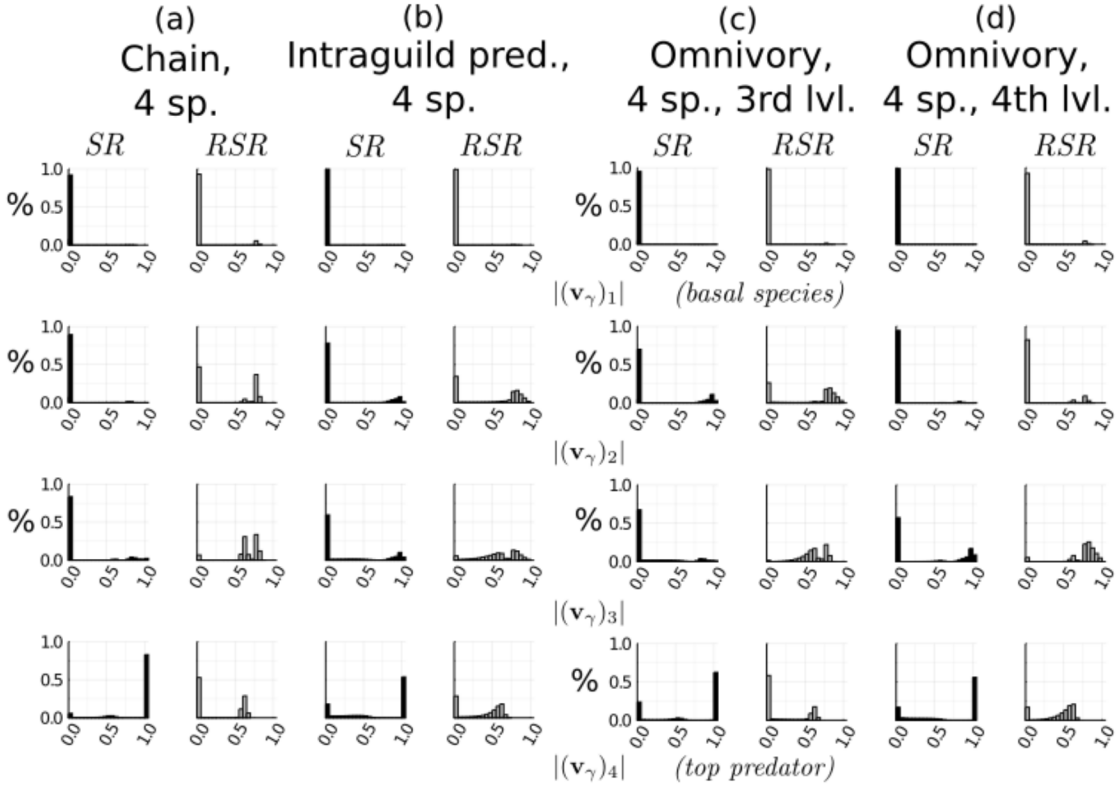

FIGURE 4.2. Distribution of the magnitude at each trophic level for the removal perturbation ($\mathbf{v}_\gamma$) of the SR (Stable Reactive) and RSR (Removal Stable Reactive) parameter sets. These histograms represent a minimum of 300,000 parameter sets each.

4.5. Discussion/Conclusions

This paper addresses how pulse perturbations may be amplified by a system, in particular, how pulses which either only add or only remove species can be initially amplified by the system dynamics. We define the *optimal* perturbation, $\mathbf{v}_\omega$ as the pulse perturbation that results in the largest initial transient growth in the two norm. This type of perturbation can be mixed sign i.e., this would correspond to an experiment where you add members to one species and remove individuals of another in the same perturbation. If the optimization is constrained to find the largest initial growth for a pulse perturbation vector with all negatively-signed entries, we get the the *removal* perturbation, $\mathbf{v}_\gamma$, $(\mathbf{v}_\gamma)_i \leq 0$. One benefit to thinking about removal or additive perturbations is that it removes a level of complexity when considering how network attributes may contribute to the

Chain, 3 sp.

Growth Response Sign		optimal perturbation ($\mathbf{v}_\omega$) sign: +		optimal perturbation ($\mathbf{v}_\omega$) sign: -		removal perturbation ($\mathbf{v}_\gamma$) sign: -		removal perturbation ($\mathbf{v}_\gamma$) sign: **0**	
	+	27.51	11.76	1.39	1.34	0.37	4.82	14.63	95.18
N_1	-	0.42	3.48	70.68	83.42	0.0	0.0	0.0	0.0
	0	0.0	0.0	0.0	0.0	0.0	0.0	85.0	0.0
	+	17.11	3.48	8.71	11.76	14.63	95.18	85.0	0.0
N_2	-	53.99	83.42	20.19	1.34	0.36	4.82	0.01	0.0
	0	0.0	0.0	0.0	0.0	0.0	0.0	0.0	0.0
	+	11.03	83.49	60.07	3.41	85.0	0.0	0.0	0.0
N_3	-	27.42	1.34	1.48	11.76	12.51	95.25	2.48	4.75
	0	0.0	0.0	0.0	0.0	0.0	0.0	0.01	0.0

Omnivory, 3 sp.

Growth Response Sign		optimal perturbation ($\mathbf{v}_\omega$) sign: +		optimal perturbation ($\mathbf{v}_\omega$) sign: -		removal perturbation ($\mathbf{v}_\gamma$) sign: -		removal perturbation ($\mathbf{v}_\gamma$) sign: **0**	
	+	42.99	81.63	2.62	1.87	1.19	2.89	98.81	97.11
N_1	-	0.01	0.45	54.38	16.04	0.0	0.0	0.0	0.0
	0	0.0	0.0	0.0	0.0	0.0	0.0	0.0	0.0
	+	0.02	0.37	39.25	81.71	44.07	97.11	54.74	0.0
N_2	-	45.52	15.88	15.2	2.04	0.87	2.41	0.32	0.48
	0	0.0	0.0	0.0	0.0	0.0	0.0	0.0	0.0
	+	4.23	6.28	20.79	22.84	54.74	0.0	0.0	0.0
N_3	-	61.02	11.74	13.95	59.14	33.07	97.98	12.19	2.02
	0	0.0	0.0	0.0	0.0	0.0	0.0	0.0	0.0

TABLE 4.4. This table explores the trophic-level patterns comparing the sign of the optimal perturbation ($\mathbf{v}_\omega$) and removal perturbation ($\mathbf{v}_\gamma$) to the sign of the initial growth response after the perturbation (calculated as $\mathbf{A}\mathbf{v}_\omega$ and $\mathbf{A}\mathbf{v}_\gamma$, respectively. We partition the reactive stable parameter sets into those that can be reactive for removal perturbations (RSR - Removal Stable Reactive; grey columns) and those which are not reactive for removal perturbations (SR - Stable reactive; white columns). Column-wise represent the sign of the perturbation for the optimal and the removal perturbation and row-wise is the sign of the initial growth response for the different trophic levels starting from N_1 (basal species) to N_n (top predator), e.g. For the three species food chain, 95.25% of the RSR data sets negative growth response to removal of the top predator (N_3).

dynamics. It is easier to think about removing some proportion of the top predator and its prey and following through the dynamics rather than juggling both additions and removals at once, which may additive effects on the dynamics.

We can think of a pulse perturbation in two ways: 1) A sudden change in the systems underlying parameters that would necessitate traveling to a new equilibrium; or 2) A sudden removal or addition of population density. An important example of the first type of pulse perturbation is either opening new marine reserve/closing a fishery. Multispecies fisheries usually removes from the top part of the food chain **[76]** and single species fisheries may, depending on the catch method, perturb multiple

Generalist, 4 sp.

		optimal perturbation ($\mathbf{v}_\omega$) sign				removal perturbation ($\mathbf{v}_\gamma$) sign			
		+		-		-		**0**	
Growth Response Sign		+	2.91	62.04	0.0	6.75	0.0	7.01	42.05	92.99
	N_1	-	0.0	0.26	97.09	30.95	0.0	0.0	0.0	0.0
		0	0.0	0.0	0.0	0.0	0.0	0.0	57.95	0.0
		+	2.51	32.62	0.41	36.17	1.03	42.02	41.06	57.98
	N_2	-	0.58	5.85	96.51	25.37	0.0	0.0	0.0	0.0
		0	0.0	0.0	0.0	0.0	0.0	0.0	57.91	0.0
		+	0.05	0.0	2.86	68.79	71.33	100.0	28.63	0.0
	N_3	-	10.55	31.21	86.53	0.0	0.0	0.0	0.0	0.0
		0	0.0	0.0	0.0	0.0	0.0	0.0	0.03	0.0
		+	0.35	12.32	2.37	8.54	28.63	0.0	0.0	0.0
	N_4	-	96.73	18.89	0.54	60.24	13.42	100.0	57.95	0.0
		0	0.0	0.0	0.0	0.0	0.0	0.0	0.0	0.0

Diamond, 4 sp.

		optimal perturbation ($\mathbf{v}_\omega$) sign				removal perturbation ($\mathbf{v}_\gamma$) sign			
		+		-		-		**0**	
Growth Response Sign		+	68.96	80.65	1.07	1.5	0.53	2.07	45.21	97.93
	N_1	-	0.11	1.07	29.87	16.79	0.0	0.0	0.0	0.0
		0	0.0	0.0	0.0	0.0	0.0	0.0	54.26	0.0
		+	3.88	5.47	51.7	75.87	5.65	41.58	82.35	56.35
	N_2	-	26.64	15.8	17.78	2.86	0.52	2.07	0.0	0.0
		0	0.0	0.0	0.0	0.0	0.0	0.0	11.47	0.0
		+	1.83	1.26	51.58	80.4	45.19	97.93	54.26	0.0
	N_3	-	28.52	16.61	18.07	1.72	0.08	0.39	0.45	1.68
		0	0.0	0.0	0.0	0.0	0.0	0.0	0.02	0.0
		+	2.48	13.8	27.49	3.74	54.27	0.0	0.0	0.0
	N_4	-	57.44	13.44	12.58	69.02	33.71	97.94	12.02	2.06
		0	0.0	0.0	0.0	0.0	0.0	0.0	0.0	0.0

TABLE 4.5. This table explores the trophic-level patterns comparing the sign of the optimal perturbation ($\mathbf{v}_\omega$) and removal perturbation ($\mathbf{v}_\gamma$) to the sign of the initial growth response after the perturbation (calculated as $\mathbf{A}\mathbf{v}_\omega$ and $\mathbf{A}\mathbf{v}_\gamma$, respectively). We partition the reactive stable parameter sets into those that can be reactive for removal perturbations (RSR - Removal Stable Reactive; grey columns) and those which are not reactive for removal perturbations (SR - Stable reactive; white columns). Column-wise represent the sign of the perturbation for the optimal and the removal perturbation and row-wise is the sign of the initial growth response for the different trophic levels starting from N_1 (basal species) to N_n (top predator).

trophic levels due to unintended bycatch **[10, 53]**. During the fished state the target fish populations are kept artificially low with respect to the unfished state, corresponding to a removal perturbation in sign. Once that fishing pressure is released, the system is free to travel back to the unfished equilibrium. Other authors have noted that previously fished populations can experience a long transient period of recovery inside newly placed marine reserves in single species models with multiple age classes **[96]**. Our results that trophic level and food web structure (i.e. whether an omnivore is perturbed rather than a top predator) may also need to be an additional consideration. Similarly

Chain, 4 sp.

Growth Response Sign		optimal perturbation ($\mathbf{v}_\omega$) sign: +		-		removal perturbation ($\mathbf{v}_\gamma$) sign: -		**0**	
	+	31.29	28.48	2.74	8.28	0.35	6.82	2.94	46.27
N_1	-	1.13	5.37	64.83	57.88	0.0	0.0	0.0	0.0
	0	0.0	0.0	0.0	0.0	0.0	0.0	96.71	46.92
	+	25.52	19.0	8.62	6.82	2.94	46.27	13.75	46.92
N_2	-	40.45	44.25	25.41	29.93	0.35	6.82	0.0	0.0
	0	0.0	0.0	0.0	0.0	0.0	0.0	82.95	0.0
	+	17.43	40.85	45.93	22.25	13.77	46.92	82.97	0.0
N_3	-	23.12	30.26	13.52	6.64	2.82	46.34	0.44	6.74
	0	0.0	0.0	0.0	0.0	0.0	0.0	0.0	0.0
	+	5.58	29.57	34.97	41.54	82.97	0.0	0.0	0.0
N_4	-	53.37	8.37	6.08	20.52	11.54	47.32	5.05	45.94
	0	0.0	0.0	0.0	0.0	0.0	0.0	0.44	6.74

Intraguild predation, 4 sp.

Growth Response Sign		optimal perturbation ($\mathbf{v}_\omega$) sign: +		-		removal perturbation ($\mathbf{v}_\gamma$) sign: -		**0**	
	+	80.53	79.09	1.32	0.6	0.21	0.66	46.04	99.34
N_1	-	1.36	3.31	16.78	17.0	0.0	0.0	0.0	0.0
	0	0.0	0.0	0.0	0.0	0.0	0.0	53.74	0.0
	+	8.07	13.54	67.09	72.04	21.73	65.85	78.06	33.49
N_2	-	13.74	12.72	11.1	1.7	0.16	0.58	0.06	0.08
	0	0.0	0.0	0.0	0.0	0.0	0.0	0.0	0.0
	+	5.05	4.15	48.18	54.24	27.21	52.88	56.16	3.57
N_3	-	15.05	10.38	31.72	31.22	14.47	42.32	2.17	1.22
	0	0.0	0.0	0.0	0.0	0.0	0.0	0.0	0.0
	+	3.24	10.07	15.12	5.96	53.74	0.0	0.0	0.0
N_4	-	65.89	29.05	15.75	54.92	30.56	72.63	15.69	27.37
	0	0.0	0.0	0.0	0.0	0.0	0.0	0.0	0.0

TABLE 4.6. This table explores the trophic-level patterns comparing the sign of the optimal perturbation ($\mathbf{v}_\omega$) and removal perturbation ($\mathbf{v}_\gamma$) to the sign of the initial growth response after the perturbation (calculated as $\mathbf{A}\mathbf{v}_\omega$ and $\mathbf{A}\mathbf{v}_\gamma$, respectively). We partition the reactive stable parameter sets into those that can be reactive for removal perturbations (RSR - Removal Stable Reactive; grey columns) and those which are not reactive for removal perturbations (SR - Stable reactive; white columns). Column-wise represent the sign of the perturbation for the optimal and the removal perturbation and row-wise is the sign of the initial growth response for the different trophic levels starting from N_1 (basal species) to N_n (top predator).

to **[96]**. the systems which where most likely to show transients in response to a removal perturbation showed an initial paradoxical decline in response to a removal perturbation (Table 4.4 -4.7) which should be accounted for before a marine reserve is judged to be a failure in the short term.

A common example of an addition pulse perturbation are low trophic level pulses due to climactic or environmentally driven events (eg. extreme flooding, ENSO bringing moisture to normally arid palaces **[82]**), temporal resource accumulation and release (eg. cicadas **[97]**, fruit and seed masting **[52, 75]**), or spatial accumulation and release (eg. storms bringing seaweed to terrestrial

Omnivory, 4 sp., 3rd lvl

Growth Response Sign		optimal perturbation ($\mathbf{v}_\omega$) sign +		optimal perturbation ($\mathbf{v}_\omega$) sign -		removal perturbation ($\mathbf{v}_\gamma$) sign -		removal perturbation ($\mathbf{v}_\gamma$) sign **0**	
N_1	+	50.71	66.99	2.94	3.42	0.34	1.86	37.3	98.14
	-	0.43	0.34	45.92	29.25	0.0	0.0	0.0	0.0
	0	0.0	0.0	0.0	0.0	0.0	0.0	62.36	0.0
N_2	+	2.1	0.28	46.36	65.49	25.48	73.39	11.71	24.75
	-	39.4	22.97	12.13	11.27	0.3	1.71	0.04	0.15
	0	0.0	0.0	0.0	0.0	0.11	0.0	62.36	0.0
N_3	+	11.59	4.47	17.21	22.09	13.32	34.38	62.74	0.0
	-	43.3	30.37	27.9	43.07	20.7	64.09	3.23	1.53
	0	0.0	0.0	0.0	0.0	0.0	0.0	0.0	0.0
N_4	+	10.22	27.7	44.68	7.14	62.75	0.0	0.0	0.0
	-	40.09	48.35	5.02	16.81	14.83	43.73	19.2	54.74
	0	0.0	0.0	0.0	0.0	0.0	0.0	3.22	1.53

Omnivory, 4 sp., 4th lvl

Growth Response Sign		optimal perturbation ($\mathbf{v}_\omega$) sign +		optimal perturbation ($\mathbf{v}_\omega$) sign -		removal perturbation ($\mathbf{v}_\gamma$) sign -		removal perturbation ($\mathbf{v}_\gamma$) sign **0**	
N_1	+	42.42	56.29	1.72	12.27	1.23	8.23	90.09	91.77
	-	0.82	7.88	55.04	23.56	0.0	0.0	0.0	0.0
	0	0.0	0.0	0.0	0.0	0.0	0.0	8.69	0.0
N_2	+	9.48	16.12	26.77	25.84	4.52	12.31	38.54	82.12
	-	45.34	12.14	18.41	45.89	0.88	5.28	0.02	0.28
	0	0.0	0.0	0.0	0.0	0.0	0.0	56.04	0.0
N_3	+	6.55	7.81	21.07	18.74	38.57	82.42	56.04	0.0
	-	36.73	57.89	35.66	15.56	4.16	12.34	1.22	5.24
	0	0.0	0.0	0.0	0.0	0.0	0.0	0.01	0.0
N_4	+	4.52	33.05	39.25	34.73	56.05	0.0	0.0	0.0
	-	54.95	17.5	1.28	14.73	30.43	83.92	13.16	16.08
	0	0.0	0.0	0.0	0.0	0.0	0.0	0.36	0.0

TABLE 4.7. This table explores the trophic-level patterns comparing the sign of the optimal perturbation ($\mathbf{v}_\omega$) and removal perturbation ($\mathbf{v}_\gamma$) to the sign of the initial growth response after the perturbation (calculated as $\mathbf{A}\mathbf{v}_\omega$ and $\mathbf{A}\mathbf{v}_\gamma$, respectively). We partition the reactive stable parameter sets into those that can be reactive for removal perturbations (RSR - Removal Stable Reactive; grey columns) and those which are not reactive for removal perturbations (SR - Stable reactive; white columns). Column-wise represent the sign of the perturbation for the optimal and the removal perturbation and row-wise is the sign of the initial growth response for the different trophic levels starting from N_1 (basal species) to N_n (top predator).

locations **|86|**); see also an excellent review in **|98|**. Our results suggest that resource pulses that perturb up two the bottom two trophic levels is not likely to result in transient growth, despite the systems tested being both classically reactive and reactive for removal perturbations involving the top trophic levels. Stated in terms of stability, this suggests that most systems will be both resistant and resilient to resource pulses.

There are a few necessary simplifications we made in our model that may not accurately represent real systems, one thing our model did not account for was behavioral responses to a

pulses. We modeled closed systems and in practice the immigration of mobile consumers into the system experiencing the resource pulse is important for the consumer numerical response to resource pulses [**99**]. Another important behavioral response is rapid changes in diet. which would represent a network structure rewiring in our model rather than a basic population perturbation [**23**]. Another consideration is pulse duration. we focused on the short end of pulse timescale it is important to note that actual ecological disturbances come in a continuous range of time and spatial scales. frequencies. and magnitudes [**48**, **99**].

In this paper we describe a subclass of systems where doing a removal experiment on the top couple of trophic levels uncovers transient dynamics. This property is mostly network structure-agnostic and implies classical reactivity. The direction of the perturbation matters. just because a system is reactive does not mean it will be reactive for removal perturbations. However. systems that are reactive for removal perturbations happen more frequently than expected. and we confirm that reactive systems make up the majority of the stable parameter sets found. Eigenvalues can be used to describe asymptotic behavior in modeled systems. but they are only good for describing short-term dynamics if a system is normal. which in our case requires the Jacobian matrix to commute with its inverse [**92**]. For the simple predator-prey systems covered by this paper. normality requires the Jacobian of a modeled systems to have a high degree of symmetry (i.e. orthogonal. symmetric. or skew-symmetric) that is not likely to happen given natural constraints on body size. stoichiometry and assimilation efficiency relationships between predators and prey [**12**, **31**, **103**].

CHAPTER 5

Food web structure, nonnormality, and reactivity

In Chapter 2 we discussed nonnormality as necessary but not sufficient condition for transient amplification in systems governed by linear ordinary differential equations or linearizations about an equilibrium. Not all nonnormal systems are doomed to showing wild transients as seen in Section 2.5.4 and not all systems with wild transients are doomed to stability related to parameter sensitivity as shown in Figure 2.5. In this chapter we finally explore the consequences for nonnormality directly for simulated small ecological networks.

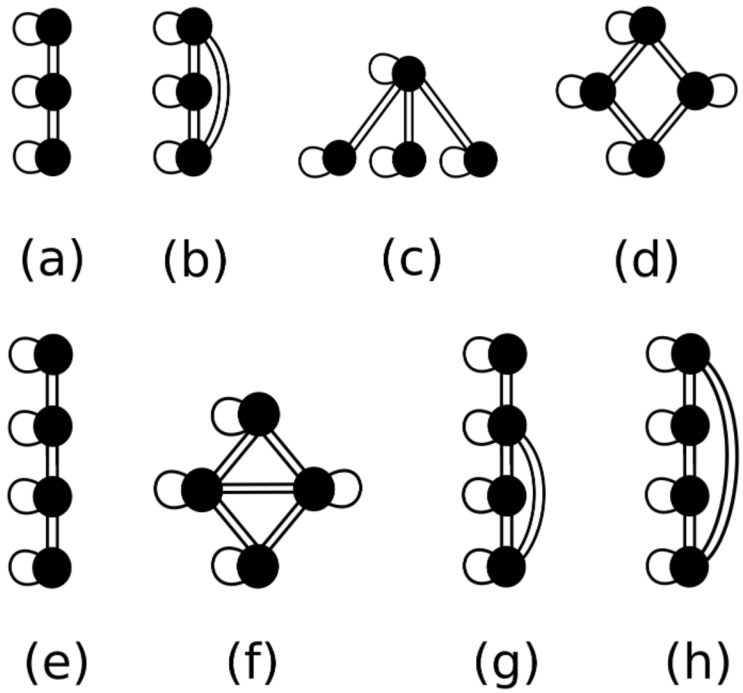

FIGURE 5.1. The eight modules whose dynamics are explored in this paper: (a) three species food chain. (b) three species omnivory. (c) four species generalist predator. (d) four species diamond. (e) four species food chain. (f) four species intraguild predation. (g) four species omnivory, third level omnivore. (h) four species omnivory, fourth level omnivore.

TABLE 5.1. Symbols used in this chapter

$\mathbf{A}$	Generic $n \times n$ matrix
$\mathbf{\Lambda}$	$n \times n$ matrix with the eigenvalues of $\mathbf{A}$ on the diagonal
$\mathbf{V}$	$n \times n$ matrix with the eigenvectors of $\mathbf{A}$ as the columns
$\Lambda(.)$	The set of eigenvalues
$\lambda_i(.)$	generic eigenvalue
$\Lambda_\varepsilon(.)$	The set of ε-pseudospectra
$\Lambda_\varepsilon^{\mathbb{R}}(.)$	The set of real-structured ε-pseudospectra
$\omega(.)$	The numerical abscissa or reactivity of a matrix
$\alpha(.)$	The spectral abscissa. $\alpha(\mathbf{A}) = \max_i \mathfrak{Re}(\lambda_i(\mathbf{A}))$
$\alpha_\varepsilon(.)$	The ε-pseudospectral abscissa
$\mathcal{K}(.)$	The Kriess constant of a matrix
$\kappa(.)$	The condition number of a matrix
$\mathrm{dep}_F(.)$	Henrici's departure from normality of a matrix
$\sigma(.)$	The set of singular values of a matrix

5.1. Introduction

Why do we observe the assemblages of species we do in the wild? What sort of things allow ecological communities resist change? Why are there so many species? Ever since Robert May made the observation in the 1970's that complexity alone does not predict stable ecosystems **[62, 63]** an enormous amount of research and computational effort has been spent to figure out what about the structure and patterns of interacting species do confer stability **[42, 67]**. Frequently, these types of studies have one thing in common, at some point conclusions are drawn based on properties of a set of matrices that represent the Jacobian of a system linearized about an equilibrium **[2, 34, 62, 80, 88]**.

The goal of these studies is generally twofold. First is to discover what details in the structure and interactions do we need to include in order for a system to be *feasible*, i.e. the Jacobian governing the system dynamics has all negative eigenvalues (later this definition was extended to include something about guaranteeing the equilibrium having nonnegative entries). The second goal is to gain some understanding about the *behavior* of the model system in response to perturbations. Ecological systems are constantly subject to perturbations, most metrics of stability are defined in the context of how a system responds to disturbances. We say a system has high resilience if the recovery time after a disturbance is short **[78]**. The rightmost eigenvalue of the Jacobian $\mathbf{A}$ (λ_1), which we will now refer to as the spectral abscissa ($\alpha(\mathbf{A}) = \max \mathfrak{Re}(\lambda_1(\mathbf{A}))$), has historically been used as a metric of resilience, since it represents the asymptotic decay of a perturbation:

$$\lim_{t\to\infty} t^{-1}\log|\,\mathrm{e}^{t\mathbf{A}}|\,=\alpha(\mathbf{A}).$$

Originally this was used in **[79]** in the context of how long it takes for the solution to decay by a factor of 1/e in the time interval (return time $=-1/\max\mathfrak{Re}(\lambda_1(\mathbf{A}))$). Later, Neubert and Caswell introduced the reactivity (otherwise known as the numerical abscissa) as a metric of resilience that at least takes into account possible nonnormal behavior which we have already discussed in detail in previous chapters, but is defined as the maximum possible initial growth after a perturbation of the equilibrium

$$\max_{|\,\mathbf{x}|\neq 0}\left|\frac{1}{|\,\mathbf{x}|}\frac{\mathrm{d}|\,\mathbf{x}|}{\mathrm{d}t}\right]_{t=0}=\lim_{t\to 0^+} t^{-1}\log|\,\mathrm{e}^{t\mathbf{A}}|\,=\omega(\mathbf{A}).$$

The other aspect of stability introduced in Chapter 4 is something called *resistance*, which describes the magnitude of the measured system response to a disturbance; systems that have a large magnitude response to a perturbation are said to not be very resistant **[77]**. The Kreiss constant, which is a lower bound on the maximum possible value $|\,\mathrm{e}^{t\mathbf{A}}|$ takes on it its time evolution, could be considered a metric of resistance (although has yet to be explicitly stated as such in an ecological context) **[89]**.

As we have shown in Chapter 2, pseudospectra are a tool that gives a more nuanced view of system dynamics and stability as well as providing a mathematical understanding of how the two can be connected. This chapter investigates the role of nonnormality plays in the sensitivity of ecological networks to perturbations, and following is a list of new things we can check in the framework of pseudospectra that were unavailable to us before.

First, it is possible for a continuous-time linear dynamical system could be nonnormal and not display sensitivity to perturbations, this represents a system that is both resilient and resistant. For avoiding transient amplification of perturbations to the equilibrium (pulse perturbations), the system is nonnormal in a way that its pseudospectra would overlap into the positive real side, but its eigenvalues are bounded away enough from the imaginary axis so that this does not result in a positive numerical abscissa. This case may still have problems with distance to instability, i.e. press perturbations, that change the underlying system parameters, but would not amplify perturbations

to the equilibrium. Another case would be similar to the example we gave in Figure 2.7, where a system was very nonnormal, but this was concentrated away from the real axis. We approach this question in a general sense by seeing if there was a correlation between reactivity and nonnormality for our parameter sets. To test the specific question about parameter sensitivity for systems which do not show transient growth we compared the real distance to instability to introduced in Section 2.3 to the spectral abscissa for a sample of generalized Lotka-Volterra systems of different network structures that have negative reactivity.

Second there was the possibility that a system could amplify perturbations to its equilibrium, but would be robust to real perturbations of its parameters (a tendency to show transient dynamics, but not be in danger of losing stability in the sense of its rightmost eigenvalue becoming positive e.g. Figure 2.5). This sort of system may amplify perturbations to its equilibrium, so may appear to neither be resistant nor resilient, but small changes to the underlying parameters would not cause the system to lose mathematical stability. The fact that there is no ecological stability jargon related to this sort of behavior **[26]** suggests that this may not have every been considered before. Transient amplification of perturbations without underlying parameter sensitivity is possible when the real stability radius is less than the complex stability radius. We check this indirectly by comparing calculating the real distance to instability to the distance to singularity, which when they are close sandwiches the complex distance to instability.

Finally, there is the question of what contributes to nonnormality of in model food webs, a question that has not yet been fully explored **[85]**. We hypothesize asymmetry in predator-prey interactions may contribute to nonnormality in the respective Jacobians. This sort of asymmetry would be due tobody size ratio, assimilation efficiency or metabolics which may be important to determining trophic interactions **[12, 31, 103]**, which is important because it could represent a source of unavoidable nonnormality. We test this by introducing a parameter that controls the asymmetry in predator-prey interactions and compare it to a metric of nonnormality.

5.2. Methods

It is now time we start checking for the consequences of normality we provided intuition for in Chapter 2. We will repeat the relevant equations and theorems so that they are contained in this

TABLE 5.2. A reference table for the model used in this chapter. Details on parameter set generation can be found in Chapter 3. We use the generalized Lotka-Volterra equations to describe the dynamics of eight small network modules of 3-4 species given by $\frac{\mathrm{d}N_i}{\mathrm{d}t} = N_i\left(r_i + \sum_j a_{ij}N_j\right), \qquad i = 1, \ldots, S$ for S interacting species. This was done for the eight different network module structures in Figure 3.1.

parameter	description	calculation
r_i	growth rate of basal species (+)/starvation rates of nonbasal species (-)	-
$\mathbf{r}$	the $S \times 1$ vector of r_i's	
a_{ij}	per-capita consumption rate of predator on prey	-
c_s	asymmetry parameter controlling assimilation efficiency/body size ratio	-
a_{ji}	per-capita consumption rate of predator on prey (+)*	$c_s a_{ji}$
$[\mathbf{a_{ij}}]$	$S \times S$ matrix of interaction parameters	
N_i	density of species i	-
$\mathbf{N}^*$	the $S \times 1$ vector of equilibrium densities	$\mathbf{N}^* = -[\mathbf{a_{ij}}]^{-1}\mathbf{r}$
$\mathbf{A}$	the $S \times S$ Jacobian matrix	$A_{ij} = N_i^* a_{ij}$

* = sign clarifications

chapter, but for the intuition please refer back to the relevant chapter-section pointers given in the text.

5.2.1. Model Description. We use the model and the parameter sets generated for eight difference small network modules (Figure 5.1) as outlined in Chapter 3. Table 5.2 has a notation summary of the model for reference.

In Chapter 4 we found that for small ecological systems governed by the generalized Lotka-Volterra equations, systems with a positive numerical abscissa or "reactivity" can be further partitioned into systems which are reactive for removal perturbations (Removal Stable Reactive, or RSR) and systems which are not (Stable Reactive or SR). These two subgroups together make up what we call the Stable Reactive Inclusive (SRI) parameter sets. We will continue with this partitioning for aspects of this chapter to study the stability properties of small ecological communities since these three types of systems show distinct transient dynamics, but for the purposes of judging stability the separation may be superficial.

5.2.2. Measuring nonnormality. Reactivity has had an important place in theoretical ecology for a while, it is an easy to calculate metric that determines whether a system can amplify

perturbations. However, transient amplification of perturbations it is only one symptom of nonnormality and it is possible for a system to not be reactive and still be closer to dynamical instability than expected. To explore this possibility, for all parameter sets we generated we calculated Henrici's departure from normality

$$\mathrm{dep}_F(\mathbf{A}) = |\,\mathbf{R}|\,_F^2 = \sqrt{|\,\mathbf{A}|\,_F^2 - |\,\mathbf{\Lambda}|\,_F^2} = \Big(\sum_{j=1}^{N} \sigma_j^2 - \sum_{j=1}^{N} \lambda_j{}^2 \Big)$$

where $\{\Lambda_j\}$ and $\{\lambda_j\}$ are the singular and eigenvalues of $\mathbf{A}$, respectively (See Section 2.1.1). Henrici's departure from normality is not the only scalar metric of nonnormality, it would also be reasonable to use the condition number of the matrix of eigenvectors introduced as Equation 2.4 in Section 2.1 but that happens to be discontinuous with respect to the matrix entries **[92]**. We are also interested what biological aspects lead to nonnormality in the Jacobian associated with the dynamics of model ecological communities. One plausible factor that breaks the symmetry in species interactions is such as body size ratios between a consumer and its resource and conversion efficiency **[12, 31, 103]** which in our model is represented by a coupling symmetry parameter c_s (Table 5.2).

5.2.3. Real distance to instability. Thus far we have been concerned with the influence of nonnormality on transient dynamics, now we will consider the influence of nonnormality on dynamical stability. In Chapter 3 we considered the generalized Lotka-Volterra equations (Table 5.2) where the linearization of this nonlinear systems of equations takes the form

$$\mathbf{x}(t) = \mathrm{e}^{t\mathbf{A}}\mathbf{x}_0, \ \mathbf{x}(0) = \mathbf{x}_0$$

and $\mathbf{A}$ is the $S \times S$ Jacobian matrix calculated as in (Table 5.2, where S is the number of species in the network; bottom row). With our model setup, each entry of the Jacobian matrix, A_{ij}, is interpreted as the direct effect of the average species individual, j, on species i's population growth rate **[74]**. What if we measured some of the parameters incorrectly when we set up the model? If some of the parameters change slightly, do we expect to have the same asymptotic dynamics, i.e. is the system still stable? These sort of questions can be framed as perturbations of the Jacobian matrix $\mathbf{A}$. Suppose we have a matrix $\mathbf{E}$ summarizing all the possible small ($|\,\mathbf{E}| < \varepsilon$) changes to $\mathbf{A}$

so that the perturbed system can be written $\mathbf{A}+\mathbf{E}$. The combination of spectra associated all such perturbed matrices, $\Lambda(\mathbf{A}+\mathbf{E})$ for given $\varepsilon, |\,\mathbf{E}| < \varepsilon, \mathbf{E} \in \mathbb{C}^{S\times S}$ is the ε-pseudospectra of $\mathbf{A}$, $\Lambda_\varepsilon(\mathbf{A})$. As covered in Chapter 2, this is equivalent to the pseudoeigenvalue and resolvent-norm definitions of pseudospectra (Theorem 5.2.1) which we will restate here for convenience:

THEOREM 5.2.1. *For any matrix $\mathbf{A} \in \mathbb{C}^{N\times N}$ the following definitions of pseudospectra are equivalent:*

- *The set of values where the resolvent is large*

$$\Lambda_\varepsilon(\mathbf{A}) := \{z \in \mathbb{C} : |\,(z\mathbf{I}-\mathbf{A})^{-1}| \;>\; \varepsilon^{-1}\},$$

- *The set of values that are the eigenvalues of a perturbed matrix $\mathbf{A}+\mathbf{E}, \mathbf{E} \in \mathbb{C}^{N\times N}$*

$$\Lambda_\varepsilon(\mathbf{A}) := \{z \in \mathbb{C} : z \in \Lambda(\mathbf{A}+\mathbf{E}),\ \textit{where } |\,\mathbf{E}| < \varepsilon\} \tag{5.1}$$

- *The set of "pseudoeigenvalues" of $\mathbf{A}$ with corresponding "pseudoeigenvectors." Let $\mathbf{v} \in \mathbb{C}^N, |\,v| = 1$, then*

$$\Lambda_\varepsilon(\mathbf{A}) := \{z \in \mathbb{C} : |\,(z-\mathbf{A})\mathbf{v}| \;< \varepsilon\}$$

- *When $|\,\cdot\,| = |\,\cdot\,|_2$, we can define the ε-pseudospectral set in terms of the smallest singular value of $(z\mathbf{I}-\mathbf{A})$*

$$\Lambda_\varepsilon(\mathbf{A}) := \{z \in \mathbb{C} : \sigma_{\min}(z\mathbf{I}-\mathbf{A}) < \varepsilon\}. \tag{5.2}$$

Now for our particular problem of parameter sensitivity, we are only interested in real-structured perturbations of $\mathbf{A}$ so that $\mathbf{A}+\mathbf{E}, \mathbf{E} \in \mathbb{R}^{N\times N}$ and we are in particular interested in how close $\mathbf{A}$ is to instability for small real perturbations of its parameters. There is one important assumption buried in this setup, this distance to instability as written below is limited to the real numbers, but locations of the entries in our perturbation matrix $\mathbf{E}$ is not constrained. Therefore, for the purposes

of a biological interpretation, the perturbations include what happens if we guessed the network topology of the species interactions wrong.

Calculation of the real distance to instability is an optimization problem [**83**]. Let $\sigma_2(.)$ denote the second-largest singular value, then the 2-norm real stability radius

$$r_{\mathbb{R}}(\mathbf{A}) = \left(\sup_{\mathfrak{Re}(z)=0} \inf_{\beta \in (0,1]} \sigma_2 \left(\begin{vmatrix} \mathfrak{Re}((z\mathbf{I}-\mathbf{A})^{-1}) & -\beta \mathfrak{Im}((z\mathbf{I}-\mathbf{A})^{-1}) \\ \beta^{-1}\mathfrak{Im}((z\mathbf{I}-\mathbf{A})^{-1}) & \mathfrak{Re}((z\mathbf{I}-\mathbf{A})^{-1}) \end{vmatrix} \right) \right)^{-1} \tag{5.3}$$

is unimodal (any local minimum is also a global minimum) [**83**]. To put into words, we are finding the smallest ε-magnitude real perturbation matrix that makes the rightmost eigenvalue of $\mathbf{A}$ have zero real part, so we must do a search over the imaginary axis as well as over $\beta \in (0, 1]$. For more details, this is Equation 2.10 in Section 2.3 .

We implemented Equation 2.10 in the Julia programming language, and the code can be found in Appendix D.

5.2.4. Distance to instability, distance to singularity, and press perturbations. A related problem to distance to instability with ecologically significant interpretations is distance to singularity. The *distance to singularity* of $\mathbf{A}$ is defined as the

$$\varepsilon_{\text{singular}} := \min\{\varepsilon := |\,\mathbf{E}|\, : \mathbf{A} + \mathbf{E} \text{ is singular}\}.$$

The straightforward pseudospectral interpretation is for which ε does the boundary of $\Lambda_\varepsilon(\mathbf{A})$ pass through the origin, i.e. in terms of the resolvent definition of pseudospectra we have

$$|\,(z\mathbf{I}-\mathbf{A})^{-1}|\, = |\,(0\mathbf{I}-\mathbf{A})^{-1}|\, = |\,\mathbf{A}^{-1}|\, = \varepsilon^{-1}$$

so $|\,\mathbf{E}|\, = |\,\mathbf{A}^{-1}|\,^{-1}$ or the smallest singular value of $\mathbf{A}$ or $\sigma_{\min}(\mathbf{A})$ in the 2-norm. While the distance to instability tells us something about whether a system is in danger of developing a positive eigenvalue, the distance to singularity is most useful as a proxy for ill-conditioning. If $|\,\mathbf{A}^{-1}|$ is large, then $\mathbf{A}^{-1}$ will have some large entries and anything depending on this inverse will be expected to amplify errors.

To give a clear example of the difference between the distance to instability and distance to singularity consider the two normal matrices $\mathbf{B_1}$ and $\mathbf{B_2}$

$$\mathbf{B_1} = \begin{bmatrix} (-0.01 + 1i) & 0 & 0 \\ 0 & (-0.01 - 1i) & 0 \\ 0 & 0 & -1 \end{bmatrix}, \quad \mathbf{B_2} = \begin{bmatrix} (-0.01 + 0.00001i) & 0 & 0 \\ 0 & (-0.01 - 0.00001i) & 0 \\ 0 & 0 & -1 \end{bmatrix}.$$

We chose diagonal matrices so we are guaranteed the difficulties of nonnormality are not an issue. The matrices $\mathbf{B_1}$ and $\mathbf{B_2}$ have the same real distance (and complex distance) to instability ($r_{\mathbb{R}}(\mathbf{A}) = 0.01$), however, $|\,{\mathbf{B_1}}^{-1}|^{-1} = 1$ and $\mathbf{B_2}$ is much closer to singularity with $|\,{\mathbf{B_2}}^{-1}|^{-1} = 0.01$. Note that distance to singularity has nothing to do with transient behavior in isolation, plotting $|\,\mathrm{e}^{t\mathbf{B_i}}|$ w.r.t. t for both of these matrices results in the exact same curve. Where distance to singularity becomes useful is that it turns out that the negative inverse of the Jacobian, $-\mathbf{A}^{-1}$, has a nice ecological interpretation in its relationship to press perturbations.

A *press perturbation* is sustained alteration of a species density or numbers over time, it represents a chronic change (e.g. the removal of all of a particular species, or the constant addition of a number of individuals to a system); this is very different then the aforementioned pulse perturbations [?]. Mathematically, a press perturbation takes on the form

$$\begin{aligned} \frac{dN_i}{dt} &= f(\mathrm{N}), \qquad i \neq j \\ \frac{dN_j}{dt} &= f(\mathrm{N}) + I_j, \qquad i = j \end{aligned} \tag{5.4}$$

and if we want to determine the change in the equilibrium density of each species $\mathbf{N}_i^*$ with respect to this chronic change in density of species j, I_j, this is

$$\frac{\partial N_i^*}{\partial I_j} = -(\mathbf{A}^{-1})_{ij}$$

which can be interpreted as the net effect of a sustained unit increase in species j's population growth rate on species i's population size (with all species responding) **|11| |102| |74|**. Essentially, the largest entries in the inverse describe which effects on species i are most important and if $\mathbf{A}$ is ill-conditioned these can be quite large.

5.2.5. Nonnormality, reactivity, and eigenvalues. While this chapter is focused on stability, it is impossible to avoid talking about the consequences of nonnormality on transient dynamics and we include this section to help interpret the coming results. First we will consider the influence of shift the spectrum and leaving the eigenvectors untouched. For a given shift of the spectrum, ζ so that we have $(\mathbf{A} - \zeta\mathbf{I})$, we can expect a shift in the reactivity, or numerical abscissa ($\omega(\mathbf{A})$) by the same amount since

$$\omega_\zeta(\mathbf{A}) = \omega_\zeta(H(\mathbf{A} - \zeta\mathbf{I})) = \lambda_1(\tfrac{1}{2}((\mathbf{A} - \zeta\mathbf{I}) + (\mathbf{A} - \zeta\mathbf{I})^*)) = \lambda_1(\tfrac{1}{2}((\mathbf{A} + \mathbf{A}^* - 2\zeta\mathbf{I}))) = \lambda_1(H(\mathbf{A}) - \zeta\mathbf{I})$$

where $\lambda_1(.)$ corresponds to taking the rightmost eigenvalue. and therefore $\omega_\zeta(\mathbf{A}) = \omega_(\mathbf{A}) - \zeta$. So for two $\mathbf{A}$ with the exact same eigenvectors, we expect the $\mathbf{A}$ with rightmost eigenvalue closer to the imaginary axis to have a faster initial growth rate in $|\,\mathrm{e}^{t\mathbf{A}}|$ w.r.t. t and expect the transient trajectory to decay slower since

$$|\,\mathrm{e}^{t\mathbf{A}}| \geq \mathrm{e}^{t\alpha(\mathbf{A})},\ \forall t \geq 0$$

where $\alpha(\mathbf{A})$ is the spectral abscissa (rightmost eigenvalue) of $\mathbf{A}$.

Less trivially proved than the first two examples is that due to (**[92]**, §15), and is a slight modification of Theorem 5.2.2 introduced in Chapter 2.5.3.

THEOREM 5.2.2. *([92], §15) Let $\mathbf{A}$ be a matrix, if $|\,(z\mathbf{I} - \mathbf{A})^{-1}| = K/(\mathfrak{Re}(z) - \zeta)$ for some $z \in \mathbb{C}$ with $\mathfrak{Re}(z) > \zeta$ and $K > 1$, then*

$$\sup_{t\geq 0} |\,\mathrm{e}^{-\zeta t}\mathrm{e}^{t\mathbf{A}}| \geq K.$$

The ε-pseudospectral abscissa $\alpha_\varepsilon(\mathbf{A})$ is finite for each $\varepsilon > 0$. Taking the rightmost value of z in the complex plane of the level contour $|\,(z\mathbf{I} - \mathbf{A})^{-1}|$ gives us the convenient lower bound

$$\sup_{t\geq 0} |\, \mathrm{e}^{-\zeta t}\mathrm{e}^{t\mathbf{A}}| \,\geq (\alpha_\varepsilon(\mathbf{A}) - \zeta)/\varepsilon \qquad \forall \varepsilon > 0. \tag{5.5}$$

Now, we have already mentioned the Kreiss constant. If we take the supremum over $\varepsilon > 0$ of the above we get the second definition of the Kreiss constant

$$\mathcal{K}(\mathbf{A}) := \sup_{\varepsilon>0} (\alpha_\varepsilon(\mathbf{A}) - \zeta)/\varepsilon = \sup_{\mathfrak{Re}(z)>\zeta} (\mathfrak{Re}(z) - \zeta) \left| \, (z\mathbf{I} - \mathbf{A})^{-1} \right|,$$

so that

$$\sup_{t\geq 0} |\, \mathrm{e}^{-\zeta t}\mathrm{e}^{t\mathbf{A}}| \,\geq \mathcal{K}(\mathbf{A}). \tag{5.6}$$

If $a = \mathfrak{Re}(z)$, then for any $\tau > 0$,

$$\sup_{0<t\leq\tau} |\, \mathrm{e}^{-\zeta t}\mathrm{e}^{t\mathbf{A}}| \,\geq \mathrm{e}^{(a-\zeta)\tau} \Big/ \left(1 + \frac{\mathrm{e}^{(a-\zeta)\tau} - 1}{K}\right). \tag{5.7}$$

To sum things up, for two systems with equal eigenvectors but one system with a smaller spectral abscissa, we also expect the lower bound on maximum value attained by $|\, \mathrm{e}^{t\mathbf{A}}|$ to increase, as well as the initial transient growth rate, and take a longer time to decay back to equilibrium.

5.2.6. Data generation. In addition to tracking the numerical abscissa (reactivity), the asymmetry in interaction strengths due to conversion efficiency or body size differences (c_s), and the rightmost eigenvalue mentioned for all parameter sets generated in Chapter 3, we calculated the distance to instability and singularity for a subset of 10,000 parameter sets for the each of the Stable, Stable Reactive, and Removal Stable Reactive datasets of our eight network module structures (for a total of 240,000 parameter sets). Taking a subset of the data for the distance to instability was absolutely necessary due needing to run an optimization for each one. While each matrix associated with the problem was small (8×8 matrices max), we ended up tuning the algorithm so that the optimization for the search for σ_2 of the inner matrix of Equation 5.3 was highly accurate and the

FIGURE 5.2. I asked my friend and optimization confidant Jeff for the best way to go about 30,000 min max problems and his response was 'Can you buy 30,000 computers?' ... Then I said 'Well, actually I need to do that eight times for a total of 240,000 optimizations' and his response was this image. This image is also representative of my cpu after 26 hours of all eight cores at 100% load. We live in a blessed time of computing where multi-core processors are standard and parallelizing your code is trivially easy in Julia.

naive grid search over the imaginary axis was coarser, resulting in the distance to instability being an overestimate (see Section 2.4.2 for more details).

5.3. Results

5.3.1. Coupling asymmetry and nonnormality. The relationship between nonnormality in the Jacobian and asymmetry in predator-prey interaction parameters c_s is somewhat opaque, but there are a couple of patterns. Figure 5.3 shows a histogram for Henrici's departure from normality $\text{dep}_F(\mathbf{A})$ vs the coupling symmetry due to conversion efficiency or body size ratios c_s. The number of trophic levels in the module is related to both how much asymmetry in the predator prey relationship is tolerated (how far left the data extends on the c_s axis, past which the system is either unfeasible or there is one or more species is extinct at equilibrium) and how extreme of the nonnormality can get on the low end of c_s. Plotting the real part of the rightmost eigenvalue, the spectral abscissa $\alpha(\mathbf{A})$, vs c_s in Figure 5.4 suggests that the cutoff behavior of c_s is due to loss of stability (an eigenvalue becomes positive). We divided the data based on reactivity (Stable vs

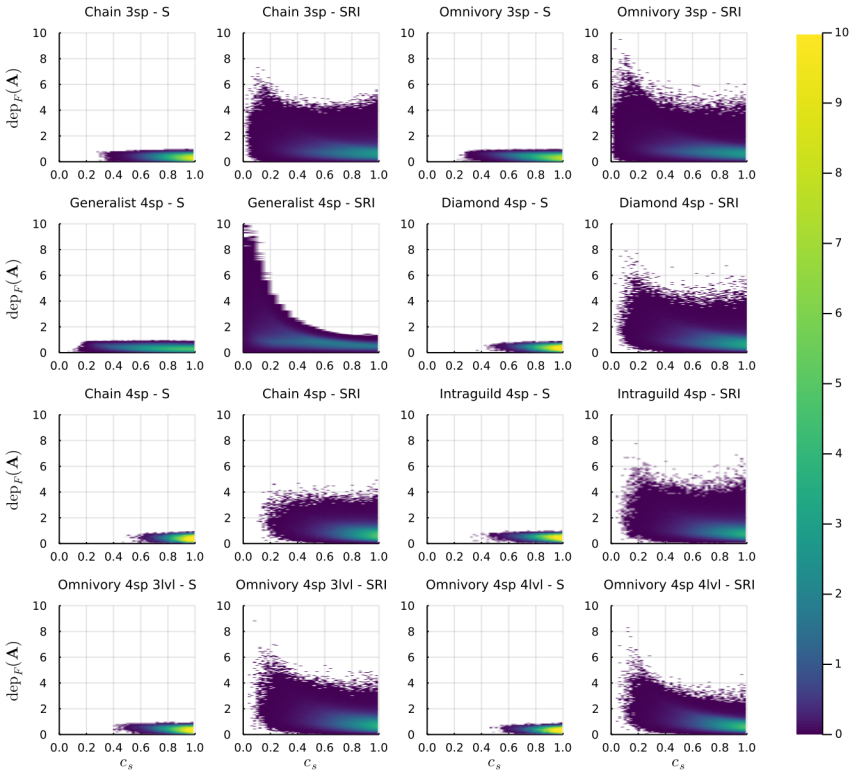

FIGURE 5.3. Histograms showing Henrici's departure from normality $\mathrm{dep}_F(\mathbf{A})$ of the Jacobian vs the coupling symmetry due to conversion efficiency or body size ratios c_s for our dataset of parameterized generalized Lotka-Volterra equations. These histograms show the full parameter sets for all eight network module structures and have been scaled to a probability density function for easier comparison. We split the data down the line for reactive (SRI - Stable Reactive Inclusive; $\omega(\mathbf{A}) > 0$) and nonreactive (S-Stable; $\omega(\mathbf{A}) < 0$). The scale on the histogram was chosen for optimal visual contrast.

Stable Reactive Inclusive). and found that for each module there is a cutoff c_s where anything more asymmetrical results in systems which will amplify some perturbations.

Figures 5.3 and 5.4 suggest a interesting relationship between the eigenvalues and nonnormality in model small communities due to limitations on coupling symmetry c_s, where a smaller $\alpha(\mathbf{A})$ is associated with higher nonnormality. Figure 5.5 plots $\alpha(\mathbf{A})$ vs Henrici's departure from normality, $\mathrm{dep}_F(\mathbf{A})$. While most of the data for each network module sits below $\mathrm{dep}_F(\mathbf{A}) = 2$ the extremes show a relationship between the spectra abscissa and increasing nonnormality. As we show in Chapter 2.5.4, an extremely nonnormal system is not necessarily doomed to a large growth in response to some perturbations, however that does seem to be the case for small network modules governed

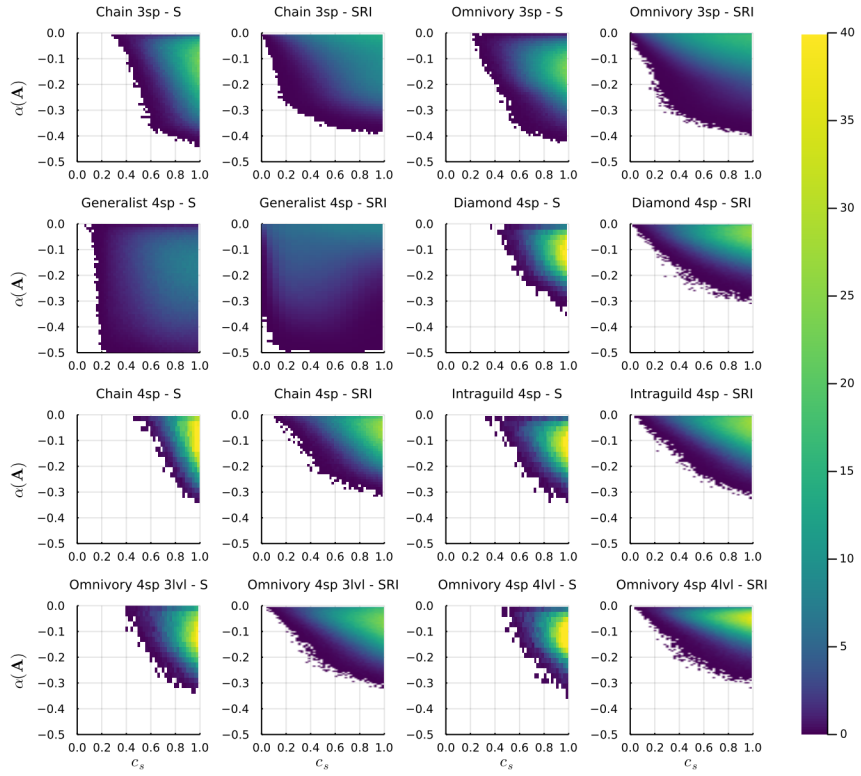

FIGURE 5.4. Histograms showing the spectral abscissa $\alpha(\mathbf{A})$ of the Jacobian vs the coupling symmetry due to conversion efficiency or body size ratios c_s for our dataset of parameterized generalized Lotka-Volterra equations. These histograms show the full parameter sets for all eight network module structures and have been scaled to a probability density function for easier comparison. We split the data down the line for reactive (SRI - Stable Reactive Inclusive; $\omega(\mathbf{A}) > 0$) and nonreactive (S-Stable; $\omega(\mathbf{A}) < 0$). The scale on the heatmap was chosen for optimal visual contrast. The rightmost eigenvalues for the four species generalist extend past the scale shown.

by the generalized Lotka-Volterra equations and the relationship is surprisingly linear (Figure 5.6). Figuring out exactly why $\text{dep}_F(\mathbf{A})$ and $\omega(\mathbf{A})$ have this relationship is buried somewhere in how the eigenvalues of hermitian real part of $\mathbf{A}$, $H(\mathbf{A})$ relates to the singular values of $\mathbf{A}$ for our data set.

5.3.2. Nonnormality and distance to instability. A useful consequence of pseudospectra is that we can relate the spectrum of our matrix of study to the stability of small perturbations of matrix elements, allowing us to answer questions about parameter sensitivity. Figures ?? and ?? show histograms of the ratio, $r_{\mathbb{R}}(\mathbf{A})/\ \alpha(\mathbf{A})$ to get an idea of how well the spectral abscissa would do as an indicator for how close a system is to instability based on perturbations of its parameters. Since for the purposes of stability, the location of spectra in the complex plane also matters, we also

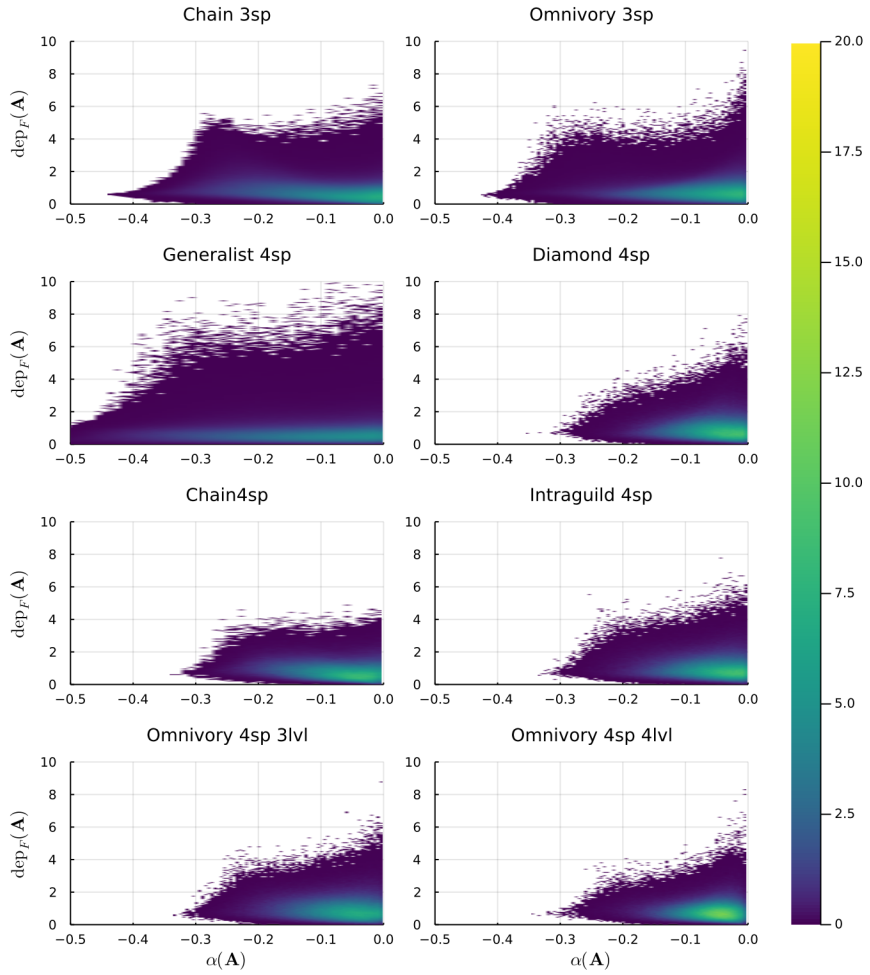

FIGURE 5.5. Histograms showing Henrici's departure from normality $\mathrm{dep}_F(\mathbf{A})$ of the Jacobian vs the real part of the spectral abscissa $\alpha(\mathbf{A})$ for our dataset of parameterized generalized Lotka-Volterra equations. These histograms show the full parameter sets for all eight network module structures and have been scaled to a probability density function for easier comparison. The scale on the heatmap was chosen for optimal visual contrast. The rightmost eigenvalues for the four species generalist extend past the scale shown.

plot a count 2D histogram of the absolute value of the spectral abscissa ($\alpha(\mathbf{A})$ and the real distance to instability ($r_{\mathbb{R}}(\mathbf{A})$) for our eight network modules divided into the three sub categories of different transient behavior: stable (S), stable reactive (SR), and removal stable reactive (RSR) in Figures 5.9 and 5.10. These figures make one well-known bound obvious: The real or complex distance to instability can not be more than the distance of the rightmost eigenvalue to the imaginary axis and this is due to the fundamental problem of a nonnormal system where perturbing an system of a

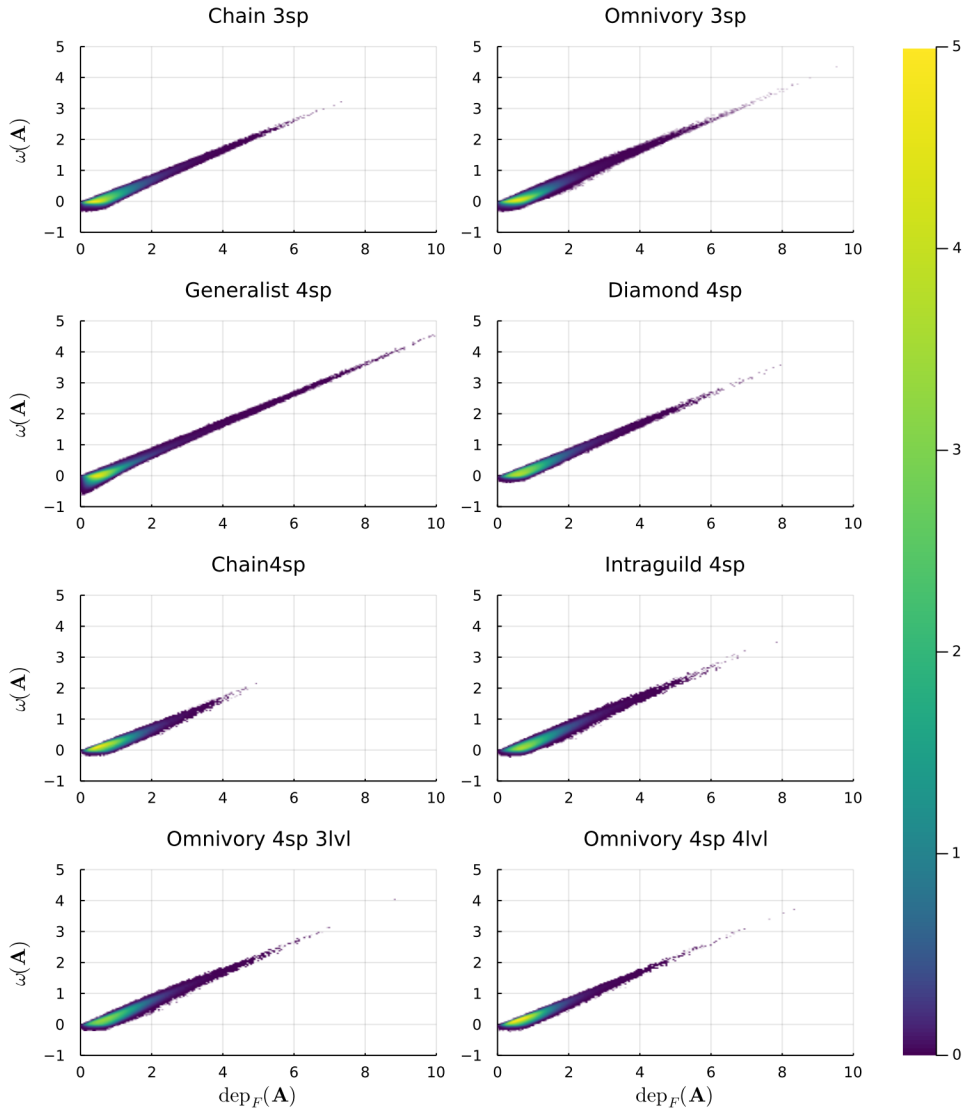

FIGURE 5.6. This figure displays 2D histograms of the numerical abscissa/reactivity $\omega(\mathbf{A})$ vs Henrici's departure from normality $\mathrm{dep}_F(\mathbf{A})$ of the Jacobian, $\omega(\mathbf{A})$. The results are scaled to a discrete probability distribution function to show where the density of points are and we display the marginal histograms to show where the data are accumulating.

matrix of magnitude ε results in a more-ε-shift in the spectrum. Stated formally in set notation, we give this theorem as it appears in **[92]**.

THEOREM 5.3.1. *Take Δ_ε to be the open ε-ball*

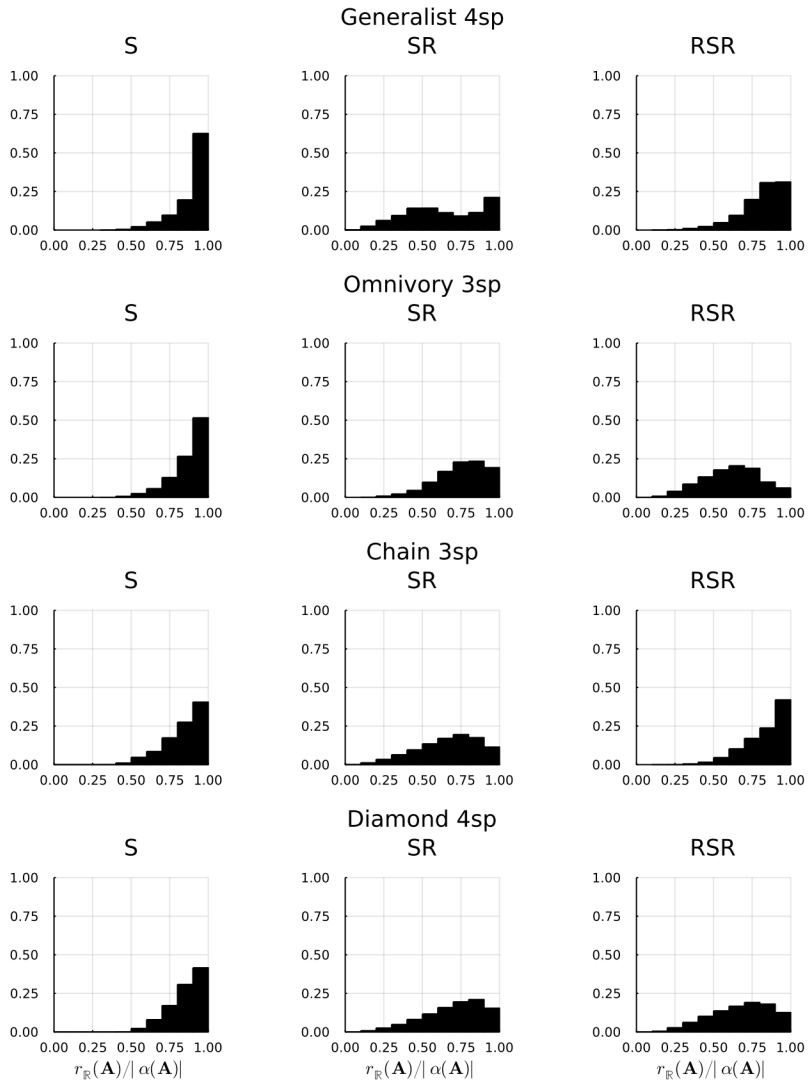

FIGURE 5.7. This figures shows the ratio $r_{\mathbb{R}}(\mathbf{A})/\,\alpha(\mathbf{A})\,|$ between the real distance to instability, $r_{\mathbb{R}}$ and the spectral abscissa $\alpha\mathbf{A}$ for several module structures. The histograms are scaled to a probability density function so that the total area of the bins is 1. All of these parameter sets are of the same size. each histogram represents a subset of 10,000 points.

$$\Delta_\varepsilon = \{z \in \mathbb{C} : \ z \ < \varepsilon\}$$

then for any $\mathbf{A} \in \mathbb{C}^{S\times S}$ *we have*

$$\Lambda_\varepsilon(\mathbf{A}) \supseteq \Lambda(\mathbf{A}) + \Delta_\varepsilon, \ \forall \varepsilon > 0$$

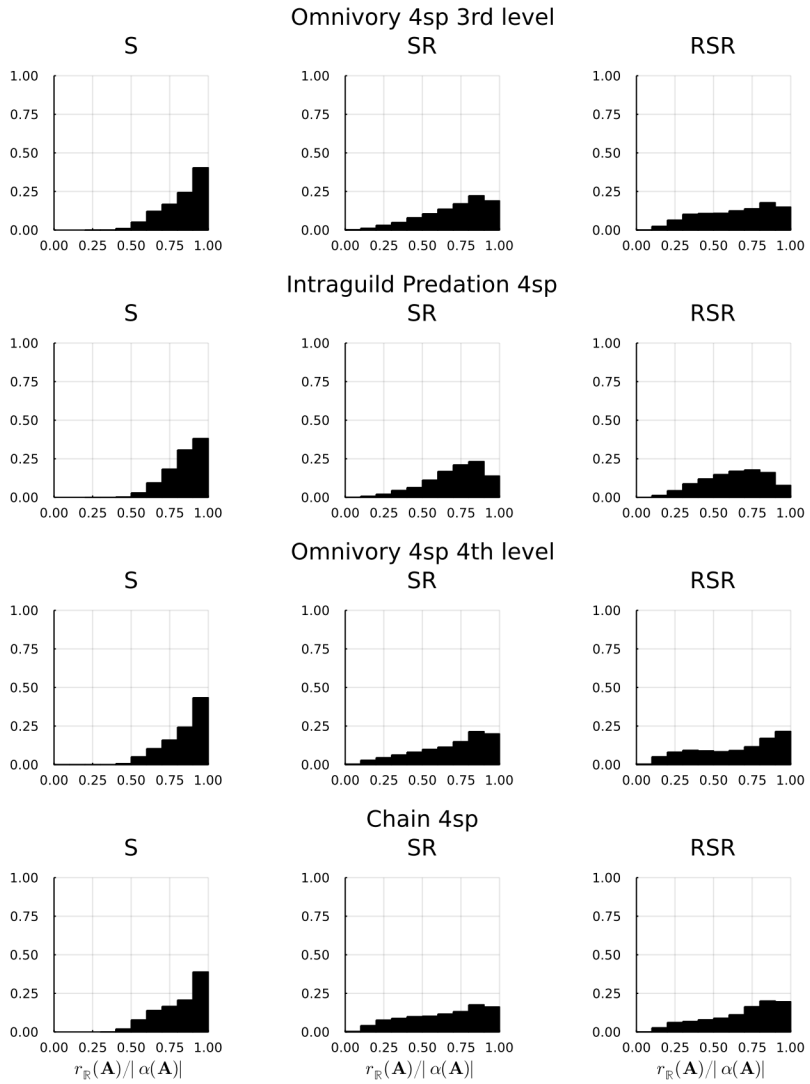

FIGURE 5.8. This figures shows the ratio $r_{\mathbb{R}}(\mathbf{A})/\,\alpha(\mathbf{A})\,$, between the real distance to instability, $r_{\mathbb{R}}$ and the spectral abscissa $\alpha\mathbf{A}$ for several module structures. The histograms are scaled to a probability density function so that the total area of the bins is 1. All of these parameter sets are of the same size. each histogram represents a subset of 10,000 points.

and if $\mathbf{A}$ *is normal and* $|\,.\,| = |\,.\,|_2$*, then*

$$\Lambda_\varepsilon(\mathbf{A}) = \Lambda(\mathbf{A}) + \Delta_\varepsilon,\ \forall \varepsilon > 0.$$

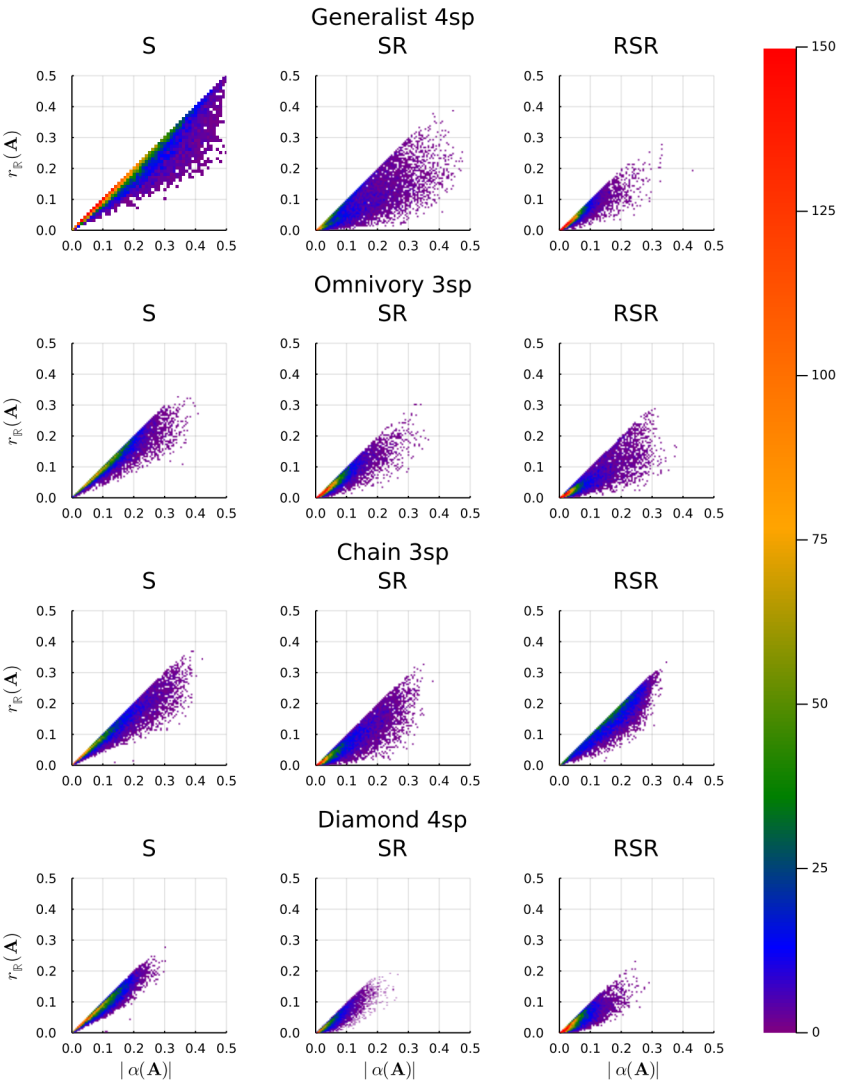

FIGURE 5.9. This figure gives a frequency 2D histogram the real distance to instability ($r_{\mathbb{R}}(\mathbf{A})$) vs the absolute value of the spectral abscissa $\alpha(\mathbf{A})$ for several module structures. For nearly normal systems, these points should be near the $y = x$ line, however, it is clear that even stable, nonreactive systems can be closer to instability than their spectrum suggests. All of these parameter sets are of the same size, each histogram represents a subset of 10,000 points.

So in our case, if we have the smallest ε such that $\Lambda_\varepsilon(\mathbf{A})$ touches the imaginary axis then the rightmost eigenvalue(s) (the spectral abscissa, $\alpha(\mathbf{A})$) is more-than-ε away from the imaginary axis thus $r_{\mathbb{R}}(\mathbf{A}) \leq \alpha(\mathbf{A})$.

The most striking about Figures 5.9 and 5.10 is that even for the stable, non-reactive modules the eigenvalues can still fail to give a good estimate for the real distance to instability, with the

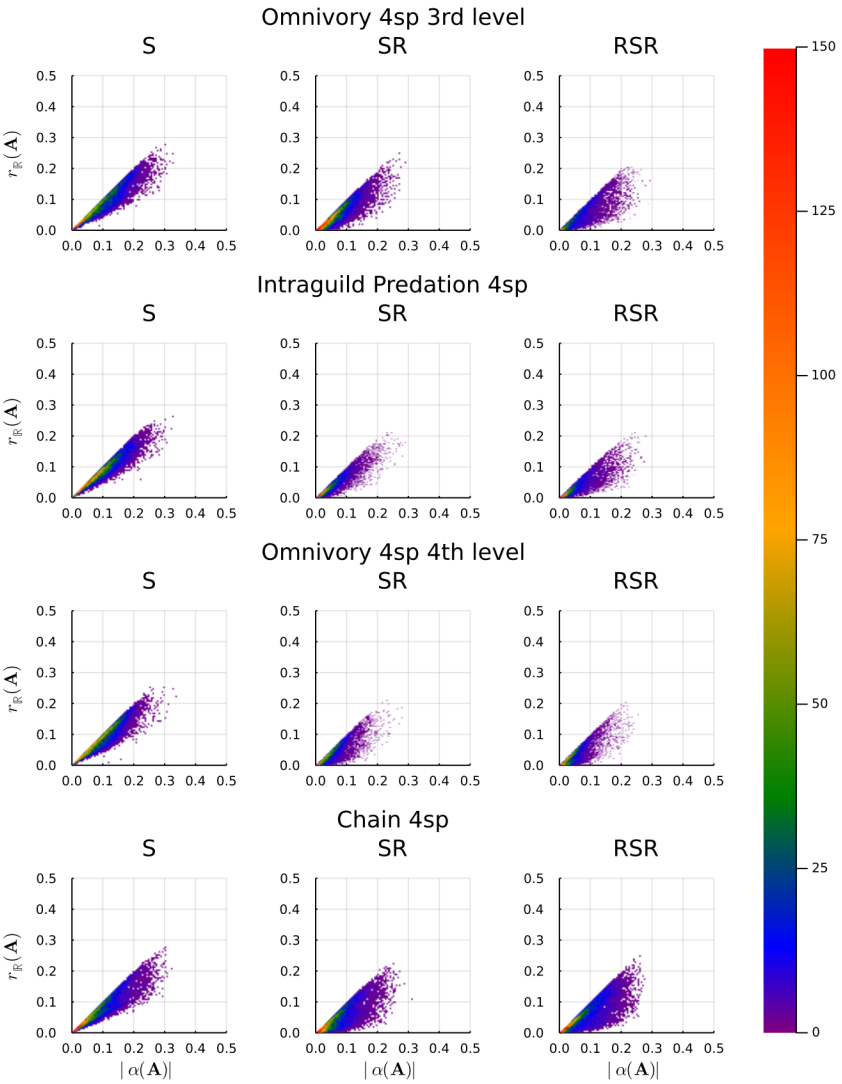

FIGURE 5.10. This figure gives a frequency 2D histogram the real distance to instability ($r_{\mathbb{R}}(\mathbf{A})$) vs the absolute value of the spectral abscissa $\alpha(\mathbf{A})$ for several module structures. For nearly normal systems, these points should be near the $y = x$ line, however, it is clear that even stable, nonreactive systems can be closer to instability than their spectrum suggests. All of these parameter sets are of the same size, each histogram represents a subset of 10,000 points.

exception for the parameter sets that were already close to instability. It is likely that for the parameter sets close to instability, they end up with a positive numerical abscissa and get categorized as stable reactive since all of the parameter sets found have at least some (if not small) amount of nonnormality. However, there is a remarkable similarity between the possible locations the real distance to instability vs spectral abscissa in the upper end of the spectral abscissa for our

data showing distinctly different types of transient dynamics (S, SR, and RSR). This means it is possible to find two systems which have the same spectral distance to instability and same level of sensitivity to perturbations of the Jacobian, but one is guaranteed to amplify some perturbations to the equilibrium and one is guaranteed to not.

In the previous chapter we found a sub-type of system with positive numerical abscissa which shows transient amplification of removal perturbations (RSR-removal stable reactive) which happens more than one might expect based on geometrical arguments. Unlike the structure of the removal perturbation that can result in transients, comparing the SR and RSR columns of Figures 5.9 and 5.10 does not bring any coherent pattern in the influence of network structure and the stability properties of SR and RSR systems.

One thing that is worth mentioning is that while these plots are representative of their subgroups categorized by their transient dynamics, they are not representative of the data set as a whole. As shown in a previous chapter (Table 4.2), and in the four species food webs overwhelming majority of the parameter sets found have a positive numerical abscissa and 15-30% of those can be categorized as RSR (removal stable reactive). So the middle columns of Figures 5.9, 5.10, 5.11, and 5.12 for the SR parameter sets provide an idea what most of the behavior of the whole data set.

5.3.3. Nonnormality and distance to singularity. We compare the distance to instability, $r_{\mathbb{R}}(\mathbf{A})$, to the distance to singularity, $|\,\mathbf{A}^{-1}|^{-1}$, in Figures 5.11 and 5.12. Similar to our results in Figures 5.9 and 5.10, we expect the distance to singularity to be an upper bound for the distance to instability. This relationship is most easily understood by thinking about where the ε-pseudospectra of $\mathbf{A}$, $\Lambda_\varepsilon(\mathbf{A})$ touches imaginary axis (the distance to instability is the smallest such ε for $\Lambda_\varepsilon(\mathbf{A})$ to exactly touch the origin). This gives us two cases: 1) The location of rightmost point of the $\Lambda_\varepsilon(\mathbf{A})$ is dominated by a real eigenvalue and its associated eigenvectors or a complex pair of eigenvalues that has an imaginary part near zero so that the crossing of $\Lambda_\varepsilon(\mathbf{A})$ and happens exactly at the origin. This is the case where the complex distance to instability and distance to singularity are the exact same (Figure 5.15 shows the pseudospectra for a case like this). 2) The location of rightmost point of the $\Lambda_\varepsilon(\mathbf{A})$ is dominated by a pair of complex eigenvalues and their associated eigenvectors and touches the imaginary axis in two locations for a given ε and curves into the negative part of the real axis - thereby excluding the origin (Figure 5.14 has an example, Figure 2.5 in Chapter 2 has

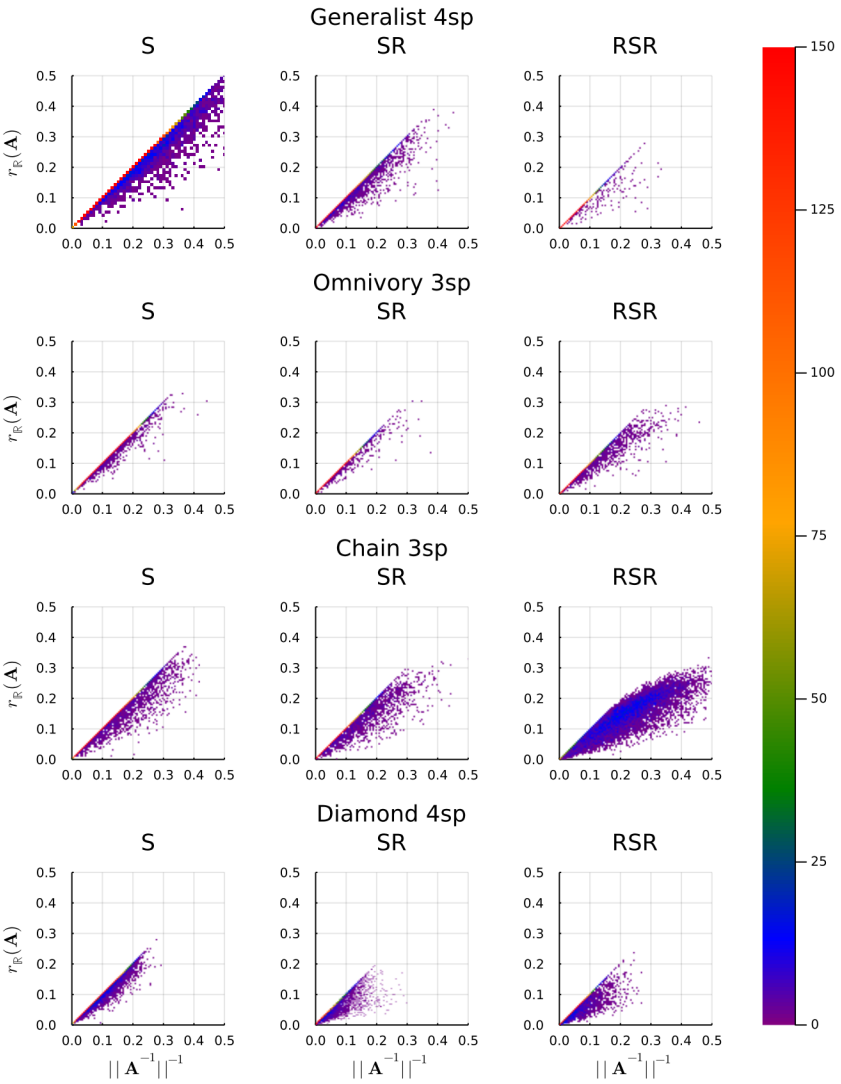

FIGURE 5.11. This figure gives a frequency 2D histogram the real distance to instability ($r_{\mathbb{R}}(\mathbf{A})$) vs the distance to singularity $|\mathbf{A}^{-1}|^{-1}$ for several module structures. For nearly normal systems, these points should be near the $y = x$ line, however, it is clear that even stable, nonreactive systems can be closer to instability than their spectrum suggests. All of these parameter sets are of the same size, each histogram represents a subset of 10,000 points.

an even clearer example). In this case the distance to singularity is greater than the distance to instability since we would have to increase ε to push $\Lambda_\varepsilon(\mathbf{A})$ to the origin.

As mentioned before, the real distance to instability is bounded above by the complex distance to instability, so we have $r_{\mathbb{R}}(\mathbf{A}) \leq r_{\mathbb{C}}(\mathbf{A}) \leq |\mathbf{A}^{-1}|^{-1}$. The clustering of the points along the $y = x$ axis in our results suggests that our real distance to instability is close to the complex distance to

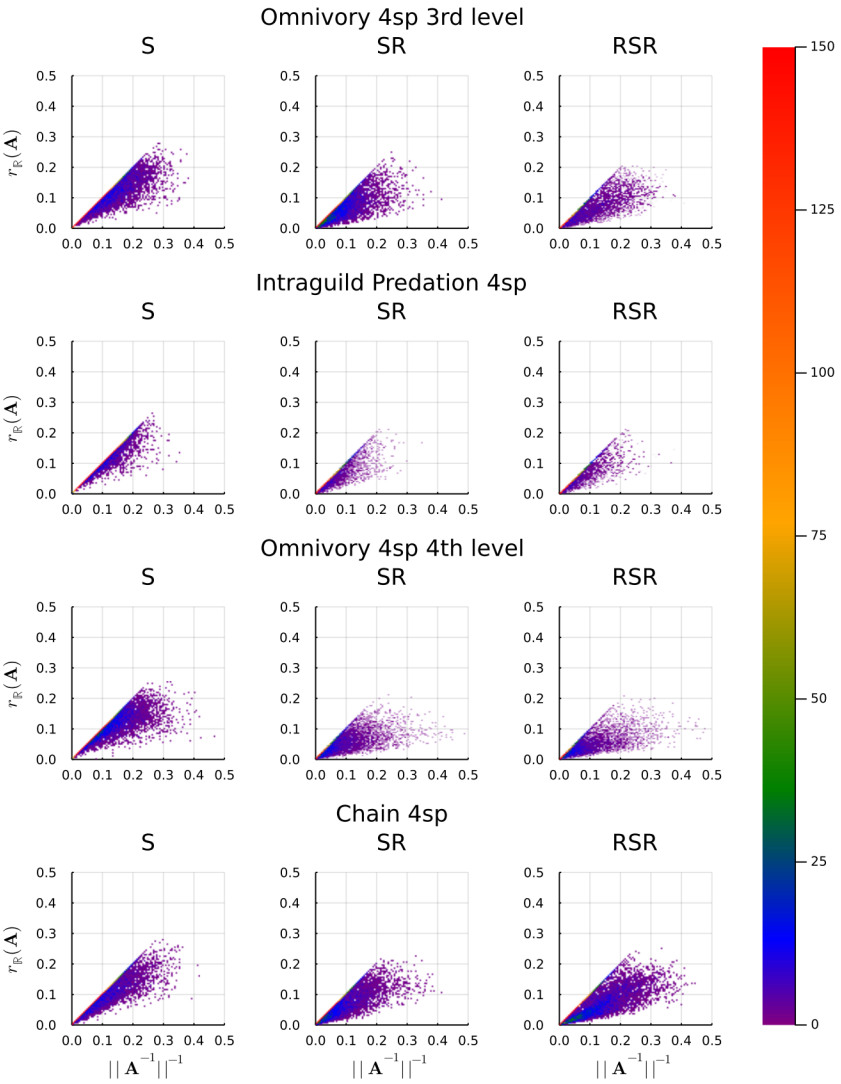

FIGURE 5.12. This figure gives a frequency 2D histogram the real distance to instability ($r_{\mathbb{R}}(\mathbf{A})$) vs the distance to singularity $|\mathbf{A}^{-1}|^{-1}$ for several module structures. For nearly normal systems, these points should be near the $y = x$ line, however, it is clear that even stable, nonreactive systems can be closer to instability than their spectrum suggests. All of these parameter sets are of the same size, each histogram represents a subset of 10,000 points.

instability in many cases. Figure 5.11 shows an interesting situation where for many of the plots we see a line with sparse feathering despite each plot representing an equal amount of points, this is especially true for three species omnivory module. We also found that the in most cases the real distance to instability and the distance to singularity were equal or near equal for most of the cases except for when the distance to instability gets small, which is responsible for the "wedge" pattern

of points. This suggests a general pattern that when system is dangerously near instability, if the rightmost eigenvalues are a complex pair, they have a very small imaginary part.

5.3.4. Measurements of transient dynamics and norm dependence. In this final section we give some examples of the real and complex pseudospectra for a couple of examples and look at the transient trajectory. Pseudospectra are defined in terms of a norm (Equation 2.5) and therefore are a norm-dependent way of describing behavior, a system can show transient amplification of perturbations in one norm and not another. As mentioned in Chapter 2, there is no obviously better choice of norm for the purposes of ecologists studying transient dynamics which other authors have noted in the past **[89]**. Historically, ecologists have used the 2-norm when studying dynamics related to nonnormality (**[5, 7, 19, 68, 70, 71, 85, 88, 95]**), although **[89]** does make use of the 1-norm for both the initial growth and Kreiss bound. Neubert and Caswell utilize the nice relationship between the numerical range as a Rayleigh quotient and the norm of the initial growth of the perturbation to find the maximum initial amplification **[68]** (We cover this relationship in Chapter 4.3.2 when we alter the optimization problem to restrict the domain). The generalization of the calculating the numerical range in other norms does exist (see the Bauer field of values in **[9, 61]**), but it is easier to numerically estimate or ignore it entirely if you are already bothering to calculate the amplification envelope ($|e^{t\mathbf{A}}|$ vs time) for that norm.

We have so far distinction between reactive and nonreactive systems, but one conclusion of the present chapter is that this may be less useful than previously thought due to norm dependence and how nonnormality influences stability of our model systems. We now give some illustrative examples of multidimensional complexity that can go into studying the dynamics of even small, simple ecological systems. For the four species, 3rd level omnivore module we chose three parameter sets to compare the transient dynamics and pseudospectra of: 1) A randomly selected stable, nonreactive system (Figure 5.13); 2) A system where Henrici's departure from normality and reactivity where close to the average values for the pooled dataset (all the feasible parameter sets found for that module were pooled together; Figure 5.14); 3) The most nonnormal parameter set (Figure 5.15).

Figure 5.13 for our stable parameter set displays the type of norm-dependent behavior discussed in previous paragraphs. It is well behaved in the 2-norm and its real distance to instability (2-norm) is close to its spectral distance (nearly the same magnitude as the rightmost eigenvalue). However,

in the one norm we would expect it to amplify perturbations, as seem by the 1-norm amplification envelope (orange). While the reactivity of this example is negative ($\omega(\mathbf{A}) = -0.0301$), it is pretty close to zero. The relationship between induced p-norms of matrices is that they are equivalent but we can not claim that the one norm of the transient trajectory is always greater (or less) than the two norm (Figure 5.15 is a nice counterexample). However, being close to reactivity in the 2-norm may be a good flag to check other norms if it matters for the problem at hand.

Figure 5.14 shows an average and rather tame system: It is not that nonnormal, and while it will amplify perturbations this is only max around a factor of 1.5-2. It is another example where the 1-norm is less well behaved then the two norm, the maximum amplification is larger and the oscillation due to the rightmost eigenvalues being complex happens in a much more lumpy manner than the examples in previous chapters would suggest is possible (and this is the tame example!). In the 1-norm the initial growth is faster and the transient takes slightly longer to decay than the 2-norm trajectory for this example as well.

Our final example is a display of extreme behavior possible when a system is very nonnormal and close to both instability and singularity. The slowness of decay due to being nearly singular is dramatic in this example. while we were able to keep the scales equal on the previous two examples of transient trajectories, we were not able to in Figure 5.15 since it took two orders of magnitude longer to decay than the previous two examples. We also include what happen when you leave the same nonnormality (eigenvectors) but shift the entire spectrum ($\mathbf{A} - 0.1\mathbf{I}$ in our case.) This example hints at one possible way for a system to be resilient (returns to equilibrium quickly) but not resistant (the perturbation is amplified quite a bit). which may happen if system is highly nonnormal but the rightmost eigenvalue is not close to the imaginary axis.

5.4. Discussion

To our knowledge this is the first in-depth look at the consequences for nonnormality beyond categorizing whether a system is reactive ($\omega(\mathbf{A}) > 0$) or not and the first to use pseudospectral methods to study stability. We found that reactivity strongly correlates with a metric of nonnormality in a linear way for small model ecological networks (Figure 5.6) and that even systems which do not show transient amplification of perturbations may be sensitive to changes in their dynamical

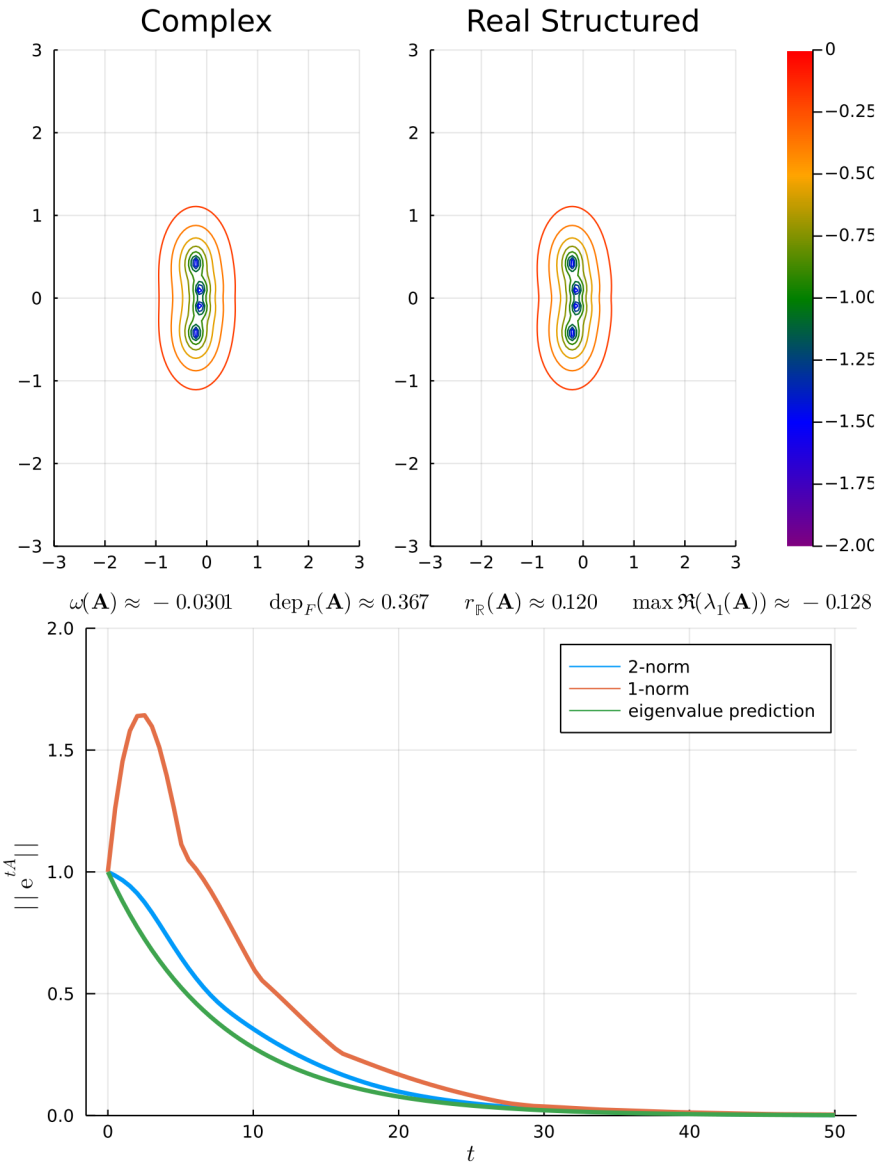

FIGURE 5.13. A "full workup" of a randomly selected parameter set of the four species omnivory, 3rd level ominvore module structure showing the complex pseudspectra, the real-structured pseudospectra, as well as the transient trajectory for the 1-norm, the 2-norm, and the trajectory from the rightmost eigenvalue prediction.

parameters (Figures 5.9 and 5.10). Our results also hint at what symptoms may signal stability loss in ecological systems. It is true for a majority of our parameter sets, the real distance to instability is frequently similar to the distance to singularity and nearly guaranteed on the low end (resulting in the characteristic wedges in Figures 5.11 and 5.12). This could suggest that large magnitude,

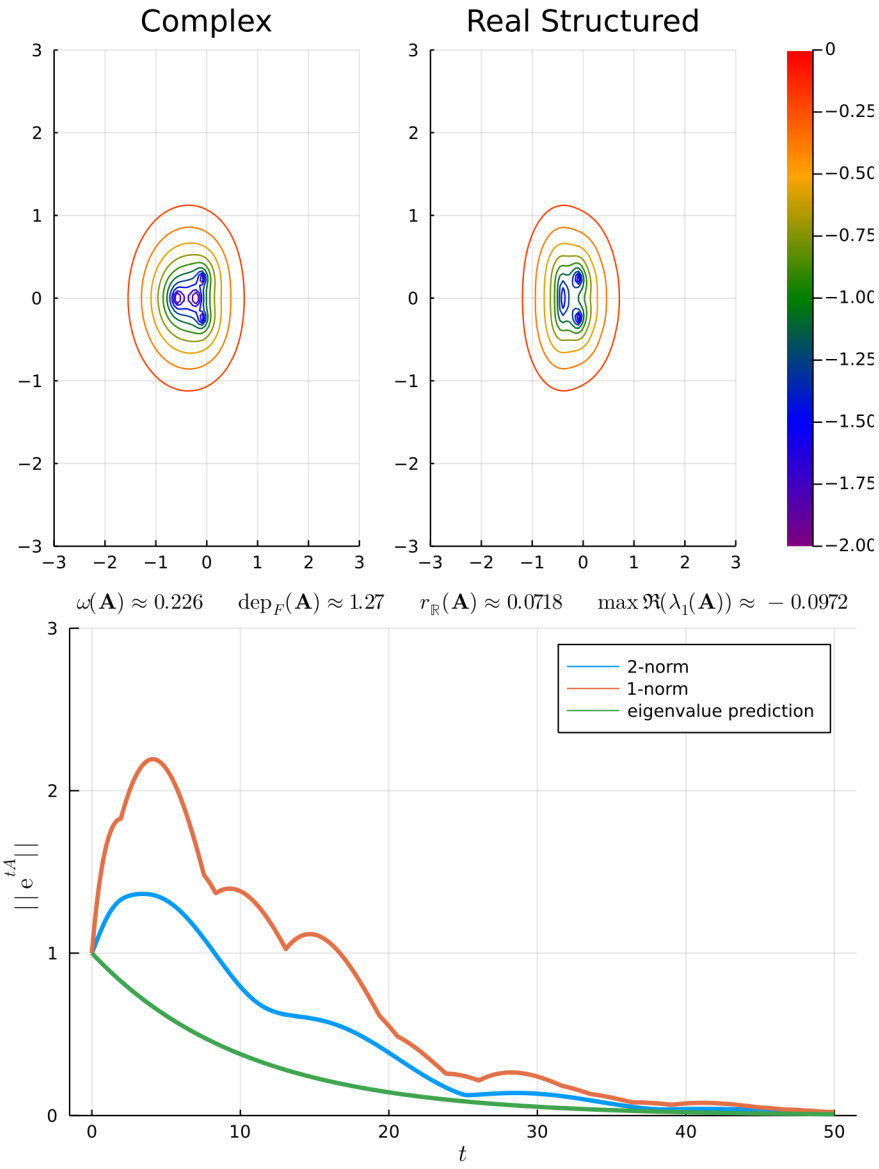

FIGURE 5.14. A "full workup" of an average reactivity and nonnormality parameter set of the four species omnivory. 3rd level ominvore module structure showing the complex pseudspectra, the real-structured pseudospectra, as well as the transient trajectory for the 1-norm, the 2-norm, and the trajectory from the rightmost eigenvalue prediction.

slow decaying transients may characterize nearly unstable systems. The special relationship between press perturbations and the inverse of the Jacobian also suggests that loss of stability may also be associated with large and possibly indirect effects of one species on another [**101**, **102**].

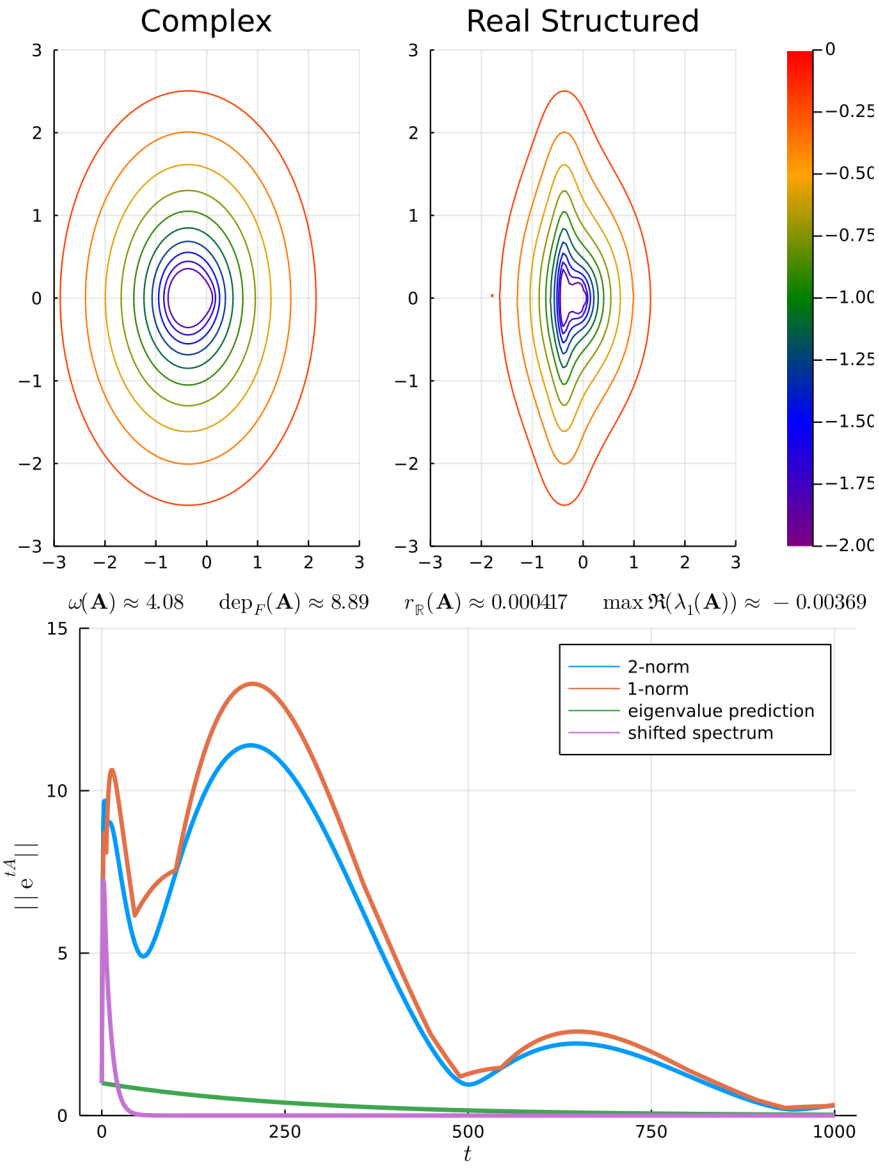

FIGURE 5.15. A "full workup" of system with the highest reactivity and nonnormality in the parameter set of the four species omnivory. 3rd level ominvore module structure showing the complex pseudospectra, the real-structured pseudospectra, as well as the transient trajectory for the 1-norm, the 2-norm, and the trajectory from the rightmost eigenvalue prediction. The Jacobian matrix governing the dynamics is nearly singular

For the first time our results show the existence of systems which have completely different transient behavior in response to perturbations of the equilibrium, but same spectral abscissa and sensitivity to underlying system parameters (same $r_{\mathbb{R}}$, $\alpha(\mathbf{A})$ but different $\omega(\mathbf{A})$). It is hard to say

how important this subclass of systems would be in real ecological communities. As a whole, stable, nonreactive systems were rare and get increasingly rare with increasing trophic levels (see Table 3.3 in Chapter 3). In Figure 5.6 (which shows the full dataset for each module structure rather than a subset of 10,000), the systems with negative numerical abscissa are just barely negative, given the parameter sensitivity it is possible any small change in dynamical parameters that pushes the spectrum to the right could result in a system that can show transient amplification of perturbations. There is also the norm dependence of the numerical abscissa to consider, we show in Figure 5.13 a example system where all perturbation decay in the 2-norm, but can be amplified in the 1-norm.

Unexpectedly, we found that the upper bound on nonnormality increased as the rightmost eigenvalue approaches the imaginary axis for our parameter sets. This suggests that systems near instability could be even less robust to small changes in parameters that result in stability loss than expected. The sandwiching of the real distance to instability to the distance to singularity suggests that the real and complex distance to instability are roughly the same for a majority of our model systems, which excludes the case mentioned in the introduction where perturbations to the equilibrium are amplified, but the system parameters are not sensitive to changes. As can be seen in our plotted examples of real vs complex pseudospectra (Figures 5.13, 5.14, and 5.15), there is a characteristic squishing of the pseudospectra when you consider only real perturbations relative to the complex pseudospectra. In the discussion so far we have talked about the extremes of nonnormality and instability, but there are so many additional nearby questions we did not have time to fully explore about the average systems. Other than the obvious question of why is the relationship between reactivity and nonnormality so linear with nearly the same slope for all of our module structures, the data clearly accumulate in a particular range and demonstrates it is possible to increase nonnormality without increasing reactivity. It could be that for a subset of our feasible systems we do get a sort of accidental optimization to reduce the consequences of nonnormality, and while the first obvious thing to check is the locations of the eigenvalues and it would be interesting to know if there are biological features associated with that (equilibrium population distribution, interaction parameter strengths, etc.).

We had a specific interest in how the coupling asymmetry $c_s = a_{ji}/a_{ij}$ in the predator-prey interaction parameters may contribute to nonnormality because it represents and unavoidable source

of asymmetry in the sense that there will always been inefficiency in the transfer of energy between trophic levels. The relationship between c_s, nonnormality and stability is complicated; c_s seems to determine the bounds on the location the spectrum of a system can live in but the relationship between c_s and nonnormality is not nearly as tidy as we found for reactivity and nonnormality. Regardless of network structure, most of the feasible systems we found were concentrated in a particular range of nonnormality and c_s, but a smaller c_s allowed for more extreme nonnormality and each network structure has a cutoff c_s where all systems are reactive for any smaller values of c_s. The fact that this cutoff c_s is related to the number of trophic levels in the module (the more distance between the top predator and the basal species, the larger the cutoff c_s is) hints at a very old question in ecology: What determines the maximum length of a food chain in a food web?

The observation that maximum food chain length in empirical food webs tends to limit around three to four species was first commented on by Elton in 1927 **[29]** and figuring why that may be has motivated reams of both theoretical and experimental ecological research since then. The two broad hypotheses explaining this pattern is that it my be a problem of dynamics (i.e. systems with longer food chains end up with smaller eigenvalues and therefore have longer return time. **[24, 80]**) and/or a problem of energetics (i.e. since energy transfer between trophic levels is inefficient, only so many levels can be supported **[58, 100]**). Our results suggest it might be a strong mixture of the two, that energy inefficiency represented by c_s may introduce unavoidable nonnormality as well as restrict how negative the rightmost eigenvalue can be for a system that translates into sensitivity to perturbations and the tendency to take a long time to return to equilibrium after a perturbation. The more trophic levels you add, the higher the allowed cutoff for c_s to avoid those aforementioned problems so there is a maximum number of trophic levels a system can support before there is not enough energy transferred to the top level as well as enough sensitivity to perturbations to never be observed on field-experiment timescales. There are some interesting caveats to this around network structure and number of species, for example, the four species diamond module is dynamically distinct from the three species food chain, which is has a subnetwork. Adding a species and the interactions in the diamond relative to the chain resulted in restricting the rightmost eigenvalue closer to the imaginary axis, but also resulted in decreasing the possible discrepancy between the real distance to instability and the spectral distance to instability ($\alpha(\mathbf{A})$) Figure 5.9. Something similar happens with the

four species food chain and adding omnivory links Figure 5.10. We did not design our numerical experiments to test this hypothesis, but looking at the relationship between interaction asymmetry due to energy efficiency, parameter sensitivity and number of sustainable trophic levels for larger food webs looks like a promising avenue of research.

Our goal was to explore the parameter space that small ecological communities could live in, and therefore allowed a range in the distributions the parameters were drawn from to be beyond what may be representative in nature. It is worth noting that for c_s specifically the data accumulates in the range $0.7 < c_s < 1$ for all modules and this is spot on for empirical estimates on the fraction of ingested energy that is lost to feces and urine in carnivores (they report the fraction loss is $\delta = 0.15$ for carnivores, and $\delta = 0.55$ for herbivores **[103]**). This sort of estimate for c_s is works if predator-prey pairs are roughly the same size, but since our equation setup also lumps body size ratio into c_s we expect c_s to be smaller for predator-prey relationships (the per-capita effect of a large predator on smaller prey is larger magnitude than the converse) **[80]**. We hold c_s constant for the entire food web, which may reasonable if we are looking at subgraphs of some larger network, but to have more realistic variation for metabolism and body size relationships we would need to vary it in future studies. It will be interesting to see how including the interaction types we left out as a necessary simplification (e.g. host-parasite interactions **[56, 81]**) and increasing the number of species changes the stability properties of our networks.

We did not demonstrate this here, but it is possible to do more structured perturbations of the Jacobian entries and plot the eigenvalues, which allows checking for specific sensitivities, an example of this can be found in **[92]**. The primary weakness of our approach is that pseudospectra predict worst case behavior, but do not give us anything about specific perturbations that caused this behavior and structured perturbations may be useful for studying a specific model system. The press perturbations of **[11]** and **[102]** may also be a useful supplemental approach. Recall that a press perturbation is a chronic change in in the equilibrium density of a species. it presents a related problem to the type of perturbation pseudospectra represents in that it is related to the system sensitivity. (For clarification: Pseudospectra represent perturbations of the entries of the Jacobian matrix while press perturbations represent a change in the species rate of growth and can be read off the Jacobian's inverse, as seen in Equation 5.4, **[74]**.) Press perturbations were important for

highlighting the importance of indirect effects in ecological communities **[102]** but came with the problem of something called *directional uncertainty*, where the locations and signs of the largest entries in $-\mathbf{A}^{-1}$ are inconsistent for the same food web structure for numerical experiments much like ours that explore a "statistical universe" **[21, 84, 101]**. It has been hypothesized that the degree of aggregation in the early empirical food webs might have been the source of this sensitivity **[81, 101]**, but this sort of parameter sensitivity smells like nonnormality, it would be interesting to see what happens to the directional uncertainty if you exclude systems like the one in Figure 5.15 which is highly unlikely to exist in nature due to being both sensitive to perturbations of all sorts, near instability, and the transients taking too long to decay.

Pseudospectral methods give us a new lens to think about the stability of ecosystems and there are so many old interesting questions than can be studied in a new way. It is general pattern that weak links in food webs are stabilizing in both empirical and model food webs, and this is particularly true for omnivory links **[34, 35, 72]**, so how do strong omnivory links influence a system sensitivity to perturbations? What happens when we increase the number of species? The upper bound on reactivity increases with number of species **[85]** and some of our preliminary explorations suggest that increasing the number of species increases the possibility for nonnormality.

Nonnormality, it so happens, is normal for ecological communities and this requires tools to take that into account. There is also a practical problem: Field experiments generally happen on short time scales (relative to the dynamics of the system), and ecosystems are constantly undergoing perturbations from both biotic and abiotic factors. It is possible the theoretical equilibrium is never observed or even realized in the actual community due to long transient behavior **[32, 39]**. More concerning though is we show that the tendency for long transients is also related to sensitivity to changes in the underlying parameters, which is important considering impacts global climate change may have on food web structure through altering metabolics and body-size relationships **[50, 59, 60]**.

CHAPTER 6

A mechanistic understanding of transient dynamics due to nonnormality

In this dissertation we introduce a lot of new methods and ways of thinking about ecological stability, and in some sense now the real work begins. Pseudospectral methods offer an improved first past filter for finding model ecological systems that may be more sensitive to perturbations than expected, both in sensitivity to underlying parameter changes and to perturbations in equilibrium densities. However, what is missing from the general pseudospectral setup is a notion of what the subspace of perturbations (of the Jacobian elements or the equilibrium) looks like. We address this in a limited way in Chapter 4 when we look at perturbations of a specific sign structure that is relevant to common source of perturbations in nature as well anthropogenic sources, but much more work will be needed to characterize it in full. Natural systems do not sit around politely declining additional perturbations until after the first one decays (if only!), it is critically important to understand how specific (or unspecific) the structure of the perturbations need to be in order to observe the sort of transient dynamics discussed here.

Do natural food webs somehow manage to minimize the effects of perturbations? As could be seen in all of our various histograms in the previous chapter, the locations of our parameter sets do seem to cluster in a particular location in parameter space, especially with regards to nonnormality and reactivity. We also only studied small modules, real food webs are large, complex, and have a variety of interaction types not covered in the present research **[81]**. Why do parasites seem to dominate food web links? Parasites can invert the body-size ratio of the interaction in that parasites are much smaller than their prey and may be another source of asymmetrical links in a food web as well as change the link structure of the food web **[55, 56]**. The next step is to scale up the size of the food webs studied, dig into the biological aspects of why long transients and parameter sensitivity may happen, and figure out what attributes of a food web increase or reduce the likelihood of

perturbation sensitivity. Yodzis in 1989 discusses how the transient trajectory of press perturbed systems moves to a new equilibrium and one cannot help but see the similarities to the present research (**|102|**, Chapter 7). Not only is there the connection to distance to singularity via press perturbations and the inverse of the Jacobian, the sort of experimental dynamics described as a result of a press perturbation hints at a possible mechanism for long transient behavior. Yodzis frames the discrepancy between short term and long term experiments on ant-rodent granivore systems (original source **|22|**) in terms of the indirect effects between plants bearing large seeds and small seeds taking a long time to fully be realized **|102|**. Finding a relationship between the locations and signs of the largest entries in the negative inverse Jacobian,$-\mathbf{A}^{-1}$ and reactivity or the real distance to instability would be the first step in grounding the incredibly abstract idea nonnormality into the more concrete idea of the structure of species interactions. Poorly connected species in empirical food webs tend to have stronger net effects (entries in $-\mathbf{A}^{-1}$ which include indirect effects) than well connected species **|66|**. It would be particularly interesting if large-magnitude indirect effects were associated with longer transients and the time it takes for the transient to decay could be interpreted as taking a while for a perturbation to "walk" the food web and be fully realized.

For the sort of investigation outline in the previous paragraph I would use something other than reactivity as a metric for possible transient growth. As we have shown in the previous chapter, the problem with both the reactivity and eigenvalues as a metric for worst case transient growth and decay is that they represent the very beginning and the very end of the transient phase and fails to differentiate systems which may grow quickly and reach a large maximum amplification, but also decay quickly and systems which take an extremely long time to decay (Figure 5.15 being a prime example of this). Reactivity also does not scale in what I would consider a sane way. $\omega(\mathbf{A}) = 4.08$ in Figure 5.15 and $\omega(\mathbf{A}) = 0.226$ in Figure 5.15, while the timescale of return is al least two orders of magnitude larger for the first system. An easy way around that is to use a different metric for the present of transients that was originally proposed by Neubert and Caswell in 1997 as a metric for return time **|68|**:

$$T_R = \int_0^\infty |\, \mathrm{e}^{t\mathbf{A}}|\ \mathrm{d}t.$$

The practical benefit of this is for the purposes of a computation exploration, we can identify the worst behaving feasible systems using a combination of Henrici's departure from normality, spectral abscissa and numerical abscissa and then numerical integrates to some finite time that fully captures the whole amplification envelope of $|\,\mathrm{e}^{t\mathbf{A}}|$ vs time. We can then calculate T_R for all of the parameter sets and then we have a metric of how bad the system behaves during the finite time and for different norms. This of course comes with the same caveat mentioned in **[68]** that no particular perturbation may exactly match the trajectory of $|\,\mathrm{e}^{t\mathbf{A}}|$, since the operator norm is calculated at every time step; it truly does represent the worst of the worst case behavior.

APPENDIX A

Code for generating pseudospectra

The code for an implementation of Lanczos iteration for efficient computation of pseudospectra. The initial implementation is due to Gabriel Gellner with some minor changes and corrections as well as keeping it up do date with the latest release in Julia.

```
function pslanczos A, x, y; maxiters = 200)
    m = length x)
    m2 = length y)
    @assert m == m2


    sig = C C
    sigmin = zeros m, m)


    N, M = size A)
    #A is a square matrix
    @assert N == M
    T, Z, schureig = schur complex  A) )
    for k = 1 m, j = 1 m
        T1 =  x k) + y j) * 1im) * I - T
        T2 = T1
        sigold = C C
        qold = zeros N, 1)
        beta = C C
        H = zeros maxiters, maxiters)
        q = randn N, 1) + 1im * randn N, 1)
        q = q / norm q)
        for p = 1 maxiters
            v = T1 \  T2 \ q) - beta * qold
            alpha = real dot q, v) )
            v = v - alpha * q
```

```
            beta = norm v[]
            qold = q
            q = v / beta
            # growing the matrix here
            H p + 1, p[] = beta
            H p, p + 1[] = beta
            H p, p[] = alpha
            sig = maximum eigvals H 1 p, 1 p[][]
            if abs sigold / sig - 1[] < 1e-3
                break
            end
            sigold = sig
        end

    #Changed it to 1/sig May 31 so that contours plot the eps

        sigmin [], k[] = 1/sqrt sig[]      end

    return sigmin
end
```

```
# function to be optimized, from Qiu et  al  1995
#       A formula for computation of the real stability radius

function QiuMat A, z, gam[]

    Rz = inv z*I-A[] # The resolvant of A calculated at grid point z
    muR =  real Rz[] -gam*imag Rz[];  1/gam[]*imag Rz[] real Rz[]
    U, sig, Vt = svd muR[]

    return sig 2[] # The objective to minimize on gam in  0,1[]

end
```

```
function RealPseudospectra A, x, y, maxtimeper)

    n = length x)
    m = length y)
    perturbdist = fill NaN, n,m)

    for i in 1 n, j in 1 m

        # Grid point the calculation is happening at in the complex plane
        z = x i) +y j) * 1im



        # Need a basic Julia function to find a global minimum on  0,1),
        #       BlackBoxOptim jl with defaults should work fine

        result = bboptimize gam->QiuMat A, z, gam 1)); SearchRange =  1e-9, 1),
                NumDimensions = 1, TraceMode =  silent, MaxTime = maxtimeper)

        #This will put the value of the eps rather than "resolvant" at each
        #       entry, some large number
        perturbdist j,i) = 1/best_fitness result)
    end

    return perturbdist
end
```

APPENDIX B

Parameter set generation for the generalized Lotka-Volterra equations

B.1. Code for data generation

The function that draws the parameter set based on the distributions described in Table TABLEREF

```
function LVParamDraw foodweb, intradampen,  c_s,
                        distinteraction, distgrowth, basal

n = size foodweb,1
r = zeros n, 1
a_i = zeros n,n

# Draw growth or death rate for non-basal species, the sign is determined by
#the basal vector which has a -1 for nonbasal and a 1 for basal species
for i in 1 n
    r i = basal i *rand distgrowth
end # r vec loop

# Draw the interaction coefficients into an nxn matrix
for i in 1 n, j in 1 n

    if i < j
        interaction = abs rand distinteraction
        a_i i,j = interaction*foodweb i,j
        a_i j,i =  c_s * interaction*foodweb j,i
    elseif i == j

        a_i i,j = intradampen*foodweb i,j # intraspecific dampening term
```

```
        end # if i < _ statement
    end

        return r, a_i_

        end #LVParamDraw function
```

B.2. Average values for the Jacobian matrix and stable equilibrium for each module

For each module we report a matrix with the average values for that entry and a vector the represents the average equilibrium density for each species. We also report the standard deviation (in paratheses) for the mean equilibrium values. The lowest matrix or vector index corresponds to the basal species. In Chapter 4 we identify a subset of Stable Reactive (SR) systems that show transient growth for perturbations that involve only removing some of each species we call Removal Stable Reactive (RSR) systems and report them separately. For modules where there are multiple species on the same trophic level (like the four species generalist and diamond modules) we order them so that the lower index corresponds to larger densities. Without this ordering these modules had the same average densities for things on the same trophic level.

Generalist, four species (SR)

$$\begin{bmatrix} -0.642 & 0.0 & 0.0 & -0.728 \\ 0.0 & -0.405 & 0.0 & -0.54 \\ 0.0 & 0.0 & -0.194 & -0.274 \\ 0.045 & 0.054 & 0.056 & -0.083 \end{bmatrix} \begin{bmatrix} 1.742 & (1.326) \\ 1.059 & (0.602) \\ 0.499 & (0.237) \\ 0.231 & (0.049) \end{bmatrix}$$

Generalist, four species (RSR)

$$\left|\begin{array}{cccc|cc} -0.612 & 0.0 & 0.0 & -0.575 & 1.477 & (1.07) \\ 0.0 & -0.377 & 0.0 & -0.435 & 0.874 & (0.455) \\ 0.0 & 0.0 & -0.178 & -0.222 & 0.401 & (0.17) \\ 0.085 & 0.11 & 0.12 & -0.153 & 0.34 & (0.08) \end{array}\right|$$

Omnivory, three species (SR)

$$\left|\begin{array}{ccc|cc} -0.453 & -0.719 & -0.554 & 1.211 & (0.577) \\ 0.122 & -0.094 & -0.137 & 0.274 & (0.059) \\ 0.073 & 0.07 & -0.077 & 0.217 & (0.049) \end{array}\right|$$

Omnivory, three species (RSR)

$$\left|\begin{array}{ccc|cc} -0.445 & -0.718 & -0.52 & 1.198 & (0.641) \\ 0.123 & -0.095 & -0.127 & 0.261 & (0.056) \\ 0.088 & 0.101 & -0.093 & 0.269 & (0.086) \end{array}\right|$$

Chain, three species (SR)

$$\left|\begin{array}{ccc|cc} -0.446 & -0.952 & 0.0 & 1.878 & (1.547) \\ 0.209 & -0.124 & -0.338 & 0.516 & (0.112) \\ 0.0 & 0.138 & -0.058 & 0.275 & (0.091) \end{array}\right|$$

Chain, three species (RSR)

$$\left|\begin{array}{ccc|cc} -0.447 & -0.943 & 0.0 & 1.837 & (1.676) \\ 0.218 & -0.131 & -0.319 & 0.503 & (0.106) \\ 0.0 & 0.186 & -0.073 & 0.342 & (0.172) \end{array}\right|$$

Diamond, four species (SR)

$$\left|\begin{array}{cccc} -0.407 & -0.721 & -0.708 & 0.0 \\ 0.201 & -0.14 & 0.0 & -0.257 \\ 0.081 & 0.0 & -0.056 & -0.104 \\ 0.0 & 0.074 & 0.064 & -0.05 \end{array}\right| \left|\begin{array}{cc} 1.357 & (0.674) \\ 0.479 & (0.082) \\ 0.196 & (0.023) \\ 0.176 & (0.033) \end{array}\right|$$

Diamond, four species (RSR)

$$\left|\begin{array}{cccc} -0.402 & -0.762 & -0.747 & 0.0 \\ 0.214 & -0.139 & 0.0 & -0.257 \\ 0.076 & 0.0 & -0.052 & -0.097 \\ 0.0 & 0.112 & 0.111 & -0.064 \end{array}\right| \left|\begin{array}{cc} 1.424 & (0.788) \\ 0.491 & (0.087) \\ 0.178 & (0.021) \\ 0.255 & (0.09) \end{array}\right|$$

Omnivory, four species, third level predator (SR)

$$\left|\begin{array}{cccc} -0.373 & -0.846 & -0.622 & 0.0 \\ 0.182 & -0.093 & -0.182 & 0.0 \\ 0.132 & 0.129 & -0.099 & -0.263 \\ 0.0 & 0.0 & 0.121 & -0.052 \end{array}\right| \left|\begin{array}{cc} 1.45 & (0.741) \\ 0.386 & (0.085) \\ 0.382 & (0.064) \\ 0.221 & (0.05) \end{array}\right|$$

Omnivory, four species, third level predator (RSR)

$$\left|\begin{array}{cccc} -0.364 & -0.888 & -0.671 & 0.0 \\ 0.171 & -0.082 & -0.177 & 0.0 \\ 0.157 & 0.179 & -0.103 & -0.292 \\ 0.0 & 0.0 & 0.184 & -0.064 \end{array}\right| \left|\begin{array}{cc} 1.533 & (0.864) \\ 0.356 & (0.094) \\ 0.433 & (0.092) \\ 0.316 & (0.121) \end{array}\right|$$

Intraguild predation (SR)

$$\left|\begin{array}{cccc} -0.432 & -0.83 & -0.587 & 0.0 \\ 0.171 & -0.105 & -0.159 & -0.17 \\ 0.099 & 0.096 & -0.089 & -0.168 \\ 0.0 & 0.068 & 0.078 & -0.053 \end{array}\right| \left|\begin{array}{cc} 1.363 & (0.639) \\ 0.344 & (0.061) \\ 0.288 & (0.053) \\ 0.18 & (0.033) \end{array}\right|$$

Intraguild predation (RSR)

$$\left|\begin{array}{cccc} -0.42 & -0.914 & -0.638 & 0.0 \\ 0.171 & -0.095 & -0.162 & -0.16 \\ 0.113 & 0.127 & -0.089 & -0.188 \\ 0.0 & 0.111 & 0.14 & -0.069 \end{array}\right| \left|\begin{array}{cc} 1.492 & (0.817) \\ 0.333 & (0.07) \\ 0.322 & (0.083) \\ 0.281 & (0.106) \end{array}\right|$$

Omnivory, four species, fourth level predator (SR)

$$\left|\begin{array}{cccc} -0.337 & -0.797 & 0.0 & -0.619 \\ 0.265 & -0.134 & -0.379 & 0.0 \\ 0.0 & 0.14 & -0.056 & -0.13 \\ 0.066 & 0.0 & 0.057 & -0.043 \end{array}\right| \left|\begin{array}{cc} 1.387 & (0.67) \\ 0.563 & (0.094) \\ 0.256 & (0.051) \\ 0.181 & (0.038) \end{array}\right|$$

Omnivory, four species, fourth level predator (RSR)

$$\left|\begin{array}{cccc} -0.323 & -0.763 & 0.0 & -0.593 \\ 0.271 & -0.135 & -0.396 & 0.0 \\ 0.0 & 0.135 & -0.051 & -0.117 \\ 0.08 & 0.0 & 0.077 & -0.049 \end{array}\right| \left|\begin{array}{cc} 1.365 & (0.699) \\ 0.581 & (0.104) \\ 0.238 & (0.062) \\ 0.217 & (0.052) \end{array}\right|$$

Chain, four species (SR)

$$\left|\begin{array}{cccc} -0.37 & -1.012 & 0.0 & 0.0 \\ 0.338 & -0.142 & -0.476 & 0.0 \\ 0.0 & 0.248 & -0.082 & -0.29 \\ 0.0 & 0.0 & 0.1 & -0.034 \end{array}\right| \left|\begin{array}{cc} 1.964 & (1.35) \\ 0.746 & (0.135) \\ 0.451 & (0.105) \\ 0.192 & (0.044) \end{array}\right|$$

Chain, four species (RSR)

$$\left|\begin{array}{cccc} -0.366 & -1.021 & 0.0 & 0.0 \\ 0.346 & -0.142 & -0.487 & 0.0 \\ 0.0 & 0.28 & -0.085 & -0.295 \\ 0.0 & 0.0 & 0.119 & -0.038 \end{array}\right| \left|\begin{array}{cc} 1.981 & (1.474) \\ 0.752 & (0.149) \\ 0.481 & (0.153) \\ 0.222 & (0.062) \end{array}\right|$$

APPENDIX C

Code for iteratively finding the numerical abscissa for removal perturbations

This is basic Gradient Descent/Ascent implementation with one minor twist that makes it work for our particular case: At each step we projected the vector we want to be the maximizer onto the positive real numbers. Everything about the problem is quadratic and the domain is the vectors where all entries are the same sign, so we chose the convention to use positive vectors to make tracking down negative signs easier in the debugging phase.

```
function GradDescentRQ M, xC)

    max_sing_val = maximum svdvals M))
    lip_const = 2*pi*max_sing_val
    step_size = 1/lip_const

    max_iters = 1CCC

    use_accel_step = true

    xC = Pro-ect xC)
    x = xC/norm xC)
    s =  )
    push  s, C)
    gamma = C
    y_prev = zeros size xC))
    f_end = C

    for iter in 1 max_iters
       f, g = GetFunAndGrad M,x)
```

```
        if use_accel_step
            xold = x
            # addition to maximize objective function
            y = Project x + step_size*g;
            x =  1-gamma;*y + gamma*y_prev
            x = x/norm x;
            y_prev = y
            s, gamma = GetAccelStep s;

        else
            # addition to maximize objective function, this function is
            # technically "gradient ascent"
            x = Project x + step_size*g;
            x = x/norm x;
        end

        if mod iter,100; == 0
          println norm x-xold,1;;
        end
        f_end = f
    end
    return x, f_end

end
```

Definition of the Rayleigh quotient funtion and its gradient to pass to the gradient ascent function.

```
function GetFunAndGrad M, x;
    # The function we are trying to maximize is the numerical radius
    #  or sometimes called the field of values; of a matrix M,
    # this function is given by rho = x *M*x / x *x
```

```
    norm_x = norm x)
    Mx = M*x
    rho =  x *Mx) /  norm_x^2)
    f = rho 1,1)
    g =  2/ norm_x^2)) *  Mx - f*x)


    return f, g
end
```

The function to project each step onto the positive reals so we end up with the maximizing vector having all the same sign.

```
# This is where I pro-ect a vector to get all the entries of the same parity,
# max x i),C) for a nonnegative perturbation, min x i),C) for a
# nonpositive perturbation
function Pro-ect x)
    x_p = zeros size x))
    for i in 1 length x)

    # Note that if your initial vector only has negative and zero entries the
    # optimization will return NaNs   For this particular problem, due to it
    # being quadratic in everything the choice of min/max  the choice in domain)
    # doesn t matter since it is not mixed sign

        x_p i) = max x i),C)

    end
    return x_p
end
```

Optional acceleration function.

```
function GetAccelStep s)

    s_next =  1 + sqrt 1 + 4*s end)^2)) / 2
    push  s, s_next)
    gamma =  1-s end-1)) / s end);

    return s, gamma
end
```

APPENDIX D

Code for finding the real distance to instability

This appendix contains the code for our distance to instability calculation runs.

```
#This function calculateds the real-structured distance to instability using the
#propertry from Qiu et  al  1995



function RealStructuredStabRad A, y, maxtimeper #, npts, optimsearch


    m = length y
    perturbdist = fill NaN, 1,m
    #atest = C

    # Calculate the first two points at a higher max time since they are more
    # likely to be the maximizers
    # bboptimize defaults to finding minimums
    z = y 1 * 1im
    result = bboptimize gam->QiuMat A, z, gam 1 ; SearchRange =  1e-9, 1 ,
        NumDimensions = 1, TraceMode =  silent, MaxTime = C C1,
        RandomizeRngSeed = false, RngSeed = 1234
    perturbdist 1  = best_fitness result

    z = y 2 * 1im
    result = bboptimize gam->QiuMat A, z, gam 1 ; SearchRange =  1e-9, 1 ,
        NumDimensions = 1, TraceMode =  silent, MaxTime = C C1,
        RandomizeRngSeed = false, RngSeed = 1234

    perturbdist 2  = best_fitness result
```

```
    # Find the abscissa by calculating over grid points and taking the maximum
    # There is surely a more efficient way of doing this
    for y in 3 m

        # Grid point the calculation is happening at in the complex plane
        z = C +y [] * 1im
        # Need a basic Julia function to find a global minimum on  C,1 ,
        #BlackBoxOptim 1 with defaults should work fine
        # result is going to be some godawful vector, best_candidate result
        #gives the best input and we want best_fitness result  for the value
        #of the optimized fuction
        result = bboptimize gam->QiuMat A, z, gam 1 ; SearchRange =  1e-9, 1 ,
            NumDimensions = 1, TraceMode =  silent, MaxTime = maxtimeper,
            RandomizeRngSeed = false, RngSeed = 1234

        #This will put the value of the "resolvant" at each entry
        perturbdist [] = best_fitness result
    end

    maxperturb, argmax = findmax perturbdist
    return argmax 2 , y argmax 2 , 1/maxperturb


end
```

This function defines the mesh we search over for the calculation of real distance to instability to find the location where the resolvent was minimized. While we are not guaranteed the pseudspectral abscissa will be at the same location on the imagary axis as the rightmost eigenvalue, for our first small set of runs we found it was frequently very close. We took a truncated normal distribution around the imaginary axis location of the rightmost eigenvalue to make a mesh.

```
function RSSRmesh est, npts, bd

    half = Int round npts/2

    if est  = C

        d = TruncatedNormal est, est+C C1, C, 1+est
        ynorm = rand d,half
        y = vcat est, range C, stop =est+bd, length = half, ynorm

    else
        d = TruncatedNormal est, C 1, C, 1+est
        ynorm = rand d,half
        y = vcat est, range C, stop =est+bd, length = half, ynorm



    end

    return y
end
```

The script used to run the real distance to instability calculation is below, we include it to show just how easy it is to parallelize code in Julia. It really is as simple as calling Julia's built in Distributed package and making sure every core loads in the packages. The abbreviations S, SR, NNSR, stand for Stable, Stable Reactive, and NonNegative Stable Reactive which was what we used to call Removal Stable Reactive (RSR) before we decided that it wasn't a meaningful enough name.

```
using Distributed

addprocs 6 #How many cores to use

@everywhere using PseudospectraFoodWebs
```

```
@everywhere using JLD2
@everywhere using FileIO
@everywhere using BlackBoxOptim
@everywhere using SharedArrays
@everywhere using LinearAlgebra
@everywhere using Distributions


datasets =  "generalist4sp" "omnivory3sp" "chain3sp" "diamond" "omnivory4sp3lvl"
            "intraguil" "omnivory4sp4lvl" "chain4sp" ]

samplesize = 10000


maxtimeper = 0 01
npts = 200
bd = 1 # A lame upper bound to search added to the complex eigenvalue
datasetnum = length datasets]
datastart = 3

@time for i in datastart datasetnum

    print datasets i]]
    print "\n"]

    data1 = string directory, "/", datasets i], "_stablereactivedata -ld2"]
    y = -ldopen data1, "a"]
    S_As = y "S_As"]
    SR_As = y "SR_As"]
    NNSR_As = y "NNSR_As"]


    data2 = string directory, "/", datasets i], "_transientscalars2 -ld2"]
    z = -ldopen data2, "a"]
    S_scalars = z "S_scalars"]
    SR_scalars = z "SR_scalars"]
    NNSR_scalars = z "NNSR_scalars"]
```

```
    S_realstab = SharedArray fill NaN, 4, samplesize[]
    SR_realstab = SharedArray fill NaN, 4, samplesize[]
    NNSR_realstab = SharedArray fill NaN, 4, samplesize[]

@sync @distributed for _ in 1 samplesize

        A = S_As  , ,:]
        est = abs S_scalars 5,:,2[]
        Seig = S_scalars 5,:,1[
        y = RSSRmesh est, npts, bd[
        atest, maxpt, realstab = RealStructuredStabRad A, y, maxtimeper[

        S_realstab 1,:[ = realstab
        S_realstab 2,:[ = -realstab/Seig
        S_realstab 3,:[ = atest
        S_realstab 4,:[ = maxpt

        A = SR_As  , ,:]
        est = abs SR_scalars 5,:,2[]
        SReig = SR_scalars 5,:,1[
        y = RSSRmesh est, npts, bd[
        atest, maxpt, realstab = RealStructuredStabRad A, y, maxtimeper[

        SR_realstab 1,:[ = realstab
        SR_realstab 2,:[ = -realstab/SReig
        SR_realstab 3,:[ = atest
        SR_realstab 4,:[ = maxpt

        A = NNSR_As  , ,:]
        est = abs NNSR_scalars 5,:,2[]
        NNSReig = NNSR_scalars 5,:,1[
        y = RSSRmesh est, npts, bd[

        atest, maxpt, realstab = RealStructuredStabRad A, y, maxtimeper[
        NNSR_realstab 1,:[ = realstab
```

```
        NNSR_realstab 2,:) = -realstab/NNSReig
        NNSR_realstab 3,:) = atest
        NNSR_realstab 4,:) = maxpt


        end
        #save the new scalar data structure
    savename = string directory, '/', datasets i), '_realstabilityradius4 :ld2')

    save savename, 'S_realstab', S_realstab, 'SR_realstab', SR_realstab,
            'NNSR_realstab', NNSR_realstab, 'bd', bd, 'npts', npts,
            'maxtimeper', maxtimeper)


    close z)
    close y)
# Reassign the loaded in data so that it gets garbage collected
# The number 3 isn t special, :ust keyboard mashing
    S_As = 3
    SR_As = 3
    NNSR_As = 3
    S_scalars = 3
    SR_scalars = 3
    NNSR_scalars = 3


    GC gc )
end
```

Bibliography

[1] C. R. Allen, D. G. Angeler, B. C. Chaffin, D. Twidwell, and A. Garmestani, *Resilience reconciled*, Nature Sustainability, 2 (2019), pp. 898–900.

[2] S. Allesina and S. Tang, *Stability criteria for complex ecosystems*, Nature, 483 (2012), pp. 205–208.

[3] ———, *The stability–complexity relationship at age 40: A random matrix perspective*, Population Ecology, 57 (2015), pp. 63–75.

[4] J.-F. Arnoldi, A. Bideault, M. Loreau, and B. Haegeman, *How ecosystems recover from pulse perturbations: A theory of short- to long-term responses*, Journal of Theoretical Biology, 436 (2018), pp. 79–92.

[5] J.-F. Arnoldi, M. Loreau, and B. Haegeman, *Resilience, reactivity and variability: A mathematical comparison of ecological stability measures*, Journal of Theoretical Biology, 389 (2016), pp. 47–59.

[6] M. Asllani, R. Lambiotte, and T. Carletti, *Structure and dynamical behaviour of non-normal networks*, arXiv:1803.11542 [nlin], (2018).

[7] G. Barabás and S. Allesina, *Predicting global community properties from uncertain estimates of interaction strengths*, Journal of The Royal Society Interface, 12 (2015), p. 20150218.

[8] J. Bascompte and C. J. Melián, *SIMPLE TROPHIC MODULES FOR COMPLEX FOOD WEBS*, Ecology, 86 (2005), pp. 2868–2873.

[9] F. L. Bauer, *On the field of values subordinate to a norm*, Numerische Mathematik, 4 (1962), pp. 103–113.

[10] J. M. Bellido, M. B. Santos, M. G. Pennino, X. Valeiras, and G. J. Pierce, *Fishery discards and bycatch: Solutions for an ecosystem approach to fisheries management?*, Hydrobiologia, 670 (2011), p. 317.

[11] E. A. Bender, T. J. Case, and M. E. Gilpin, *Perturbation Experiments in Community Ecology: Theory and Practice*, Ecology, 65 (1984), pp. 1–13.

[12] E. L. Berlow, J. A. Dunne, N. D. Martinez, P. B. Stark, R. J. Williams, and U. Brose, *Simple prediction of interaction strengths in complex food webs*, Proceedings of the National Academy of Sciences, 106 (2009), pp. 187–191.

[13] F. Borgioli, D. Hajdu, T. Insperger, G. Stepan, and W. Michiels, *Pseudospectral method for assessing stability robustness for linear time-pericdic delayed dynamical systems*, International Journal for Numerical Methods in Engineering, 121 (2020), pp. 3505–3528.

[14] S. Boyd and V. Balakrishnan, *A regularity result for the singular values of a transfer matrix and a quadratically convergent algorithm for computing its L/sub infinity /-norm*, in Proceedings of the 28th IEEE Conference on Decision and Control,, Dec. 1989, pp. 954–955 vol.2.

[15] J. V. Burke, *Robust stability and a criss-cross algorithm for pseudospectra*, IMA Journal of Numerical Analysis, 23 (2003), pp. 359–375.

[16] J. V. Burke, A. S. Lewis., and M. L. Overton, *Optimization and Pseudospectra, with Applications to Robust Stability*, SIAM Journal on Matrix Analysis and Applications, 25 (2003), pp. 80–104.

[17] J. Camacho, D. Stouffer, and L. Amaral, *Quantitative analysis of the local structure of food webs*, Journal of theoretical biology, 246 (2007), pp. 260–268.

[18] F. Caravelli and P. Staniczenko, *Bounds on transient instability for complex ecosystems*, PLOS ONE, 11 (2016), p. e0157876.

[19] H. Caswell and M. G. Neubert, *Reactivity and transient dynamics of discrete-time ecological systems*, Journal of Difference Equations and Applications, 11 (2005), pp. 295–310.

[20] X. Chen and J. E. Cohen, *Transient dynamics and food-web complexity in the Lotka-Volterra cascade model*, Proceedings of the Royal Society B: Biological Sciences, 268 (2001), pp. 869–877.

[21] J. M. Dambacher, H. W. Li, and P. A. Rossignol, *RELEVANCE OF COMMUNITY STRUCTURE IN ASSESSING INDETERMINACY OF ECOLOGICAL PREDICTIONS*, 83 (2002), p. 21.

[22] D. W. Davidson, R. S. Inouye, and J. H. Brown, *Granivory in a Desert Ecosystem. Experimental Evidence for Indirect Facilitation of Ants by Rodents*, Ecology, 65 (1984), pp. 1780–1786.

[23] A. M. Davis, B. J. Pusey, and R. G. Pearson, *Big floods, big knowledge gap: Food web dynamics in a variable river system*, Ecology of Freshwater Fish, 27 (2018), pp. 898–909.

[24] D. L. DeAngelis, *Energy Flow, Nutrient Cycling, and Ecosystem Resilience*, Ecology, 61 (1980), pp. 764–771.

[25] J. Demmel, *A counterexample for two conjectures about stability*, IEEE Transactions on Automatic Control, 32 (1987), pp. 340–342.

[26] I. Donohue, H. Hillebrand, J. M. Montoya, O. L. Petchey, S. L. Pimm, M. S. Fowler, K. Healy, A. L. Jackson, M. Lurgi, D. McClean, N. E. O'Connor, E. J. O'Gorman, and Q. Yang, *Navigating the complexity of ecological stability*, Ecology Letters, 19 (2016), pp. 1172–1185.

[27] T. A. Driscoll and L. N. Trefethen, *Pseudospectra for the wave equation with an absorbing boundary*, Journal of Computational and Applied Mathematics, 69 (1996), pp. 125–142.

[28] L. Elsner and K. D. Ikramov, *Normal matrices. An update*, Linear Algebra and its Applications, 285 (1998), pp. 291–303.

[29] C. Elton, *Animal Ecology*, Macmillan, New York, NY, 1927.

[30] M. Emmerson and J. M. Yearsley, *Weak interactions, omnivory and emergent food-web properties*, Proceedings of the Royal Society of London. Series B: Biological Sciences, 271 (2004), pp. 397–405.

[31] M. C. Emmerson and D. Raffaelli, *Predator-prey body size, interaction strength and the stability of a real food web*, Journal of Animal Ecology, 73 (2004), pp. 399–409.

[32] T. H. G. Ezard, J. M. Bullock, H. J. Dalgleish, A. Millon, F. Pelletier, A. Ozgul, and D. N. Koons, *Matrix models for a changeable world. The importance of transient dynamics in population management. Transient dynamics and population management*, Journal of Applied Ecology, 47 (2010), pp. 515–523.

[33] M. Freitag and A. Spence, *A Newton-based method for the calculation of the distance to instability*, Linear Algebra and its Applications, 435 (2011), pp. 3189–3205.

[34] G. Gellner and K. McCann, *Reconciling the Omnivory-Stability Debate*, The American Naturalist, 179 (2012), pp. 22–37.

[35] G. Gellner and K. S. McCann, *Consistent role of weak and strong interactions in high- and low-diversity trophic food webs*, Nature Communications, 7 (2016), p. 11180.

[36] T. Gibbs, J. Grilli, T. Rogers, and S. Allesina, *Effect of population abundances on the stability of large random ecosystems*, Physical Review E, 98 (2018), p. 022410.

[37] R. Q. Grafton, L. Doyen, C. Béné, E. Borgomeo, K. Brooks, L. Chu, G. S. Cumming, J. Dixon, S. Dovers, D. Garrick, A. Helfgott, Q. Jiang, P. Katic, T. Kompas, L. R. Little, N. Matthews, C. Ringler, D. Squires, S. I. Steinshamn, S. Villasante, S. Wheeler, J. Williams, and P. R. Wyrwoll, *Realizing resilience for decision-making*, Nature Sustainability, 2 (2019), pp. 907–913.

[38] V. Grimm and C. Wissel, *Babel, or the ecological stability discussions: An inventory and analysis of terminology and a guide for avoiding confusion*, Oecologia, 109 (1997), pp. 323–334.

[39] A. Hastings, *Transients: The key to long-term ecological understanding?*, Trends in Ecology & Evolution, 19 (2004), pp. 39–45.

[40] ———, *Timescales, dynamics, and ecological understanding*, Ecology, 91 (2010), pp. 3471–3480.

[41] A. Hastings, K. C. Abbott, K. Cuddington, T. Francis, G. Gellner, Y.-C. Lai, A. Morozov, S. Petrovskii, K. Scranton, and M. L. Zeeman, *Transient phenomena in ecology*, Science, 361 (2018), p. eaat6412.

[42] A. Hastings, K. S. McCann, and P. C. de Ruiter, *Introduction to the special issue: Theory of food webs*, Theoretical Ecology, 9 (2016), pp. 1–2.

[43] D. Haydon, *Pivotal Assumptions Determining the Relationship between Stability and Complexity: An Analytical Synthesis of the Stability-Complexity Debate*, The American Naturalist, 144 (1994), pp. 14–29.

[44] H. V. Henderson and S. R. Searle, *On Deriving the Inverse of a Sum of Matrices*, SIAM Review, 23 (1981), pp. 53–60.

[45] P. Henrici, *Bounds for iterates, inverses, spectral variation and fields of values of non-normal matrices*, Numerische Mathematik, 4 (1962), pp. 24–40.

[46] C. S. Holling, *Resilience and Stability of Ecological Systems*, Annual Review of Ecology and Systematics, 4 (1973), pp. 1–23.

[47] R. A. Horn and C. R. Johnson, *Topics in Matrix Analysis*, Cambridge University Press, Cambridge, UK, 1991.

[48] A. Jentsch and P. White, *A theory of pulse dynamics and disturbance in ecology*, Ecology, (2019), p. e02734.

[49] C. R. Johnson, E. M. Sa, and H. Wolkowicz, *Normal Matrices*, Ninear Algebra and Its Applications, 87 (1987), pp. 213–225.

[50] T. Kaur and P. S. Dutta, *Persistence and stability of interacting species in response to climate warming: The role of trophic structure*, Theoretical Ecology, 13 (2020), pp. 333–348.

[51] S. Kéfi, V. Domínguez-García, I. Donohue, C. Fontaine, E. Thébault, and V. Dakos, *Advancing our understanding of ecological stability*, Ecology Letters, 22 (2019), pp. 1349–1356.

[52] D. Kelly, *The evolutionary ecology of mast seeding*, Trends in Ecology & Evolution, 9 (1994), pp. 465–470.

[53] L. M. Komoroske and R. L. Lewison, *Addressing fisheries bycatch in a changing world*, Frontiers in Marine Science, 0 (2015).

[54] H.-O. Kreiss, *UBER DIE STABILITATSDEFINITION FUR DIFFEREI ̈ZENGLEICHUNGEN DIE PARTIELLE DIFFERENTIALGLEICHUNGEN APPROXIMIEREN*, BIT, 2 (1962), pp. 153–181.

[55] K. D. Lafferty, S. Allesina, M. Arim, C. J. Briggs, G. De Leo, A. P. Dobson, J. A. Dunne, P. T. J. Johnson, A. M. Kuris, D. J. Marcogliese, N. D. Martinez, J. Memmott, P. A. Marquet, J. P. McLaughlin, E. A. Mordecai, M. Pascual, R. Poulin, and D. W. Thieltges, *Parasites in food webs: The ultimate missing links*, Ecology Letters, 11 (2008), pp. 533–546.

[56] K. D. Lafferty, A. P. Dobson, and A. M. Kuris, *Parasites dominate food web links*, Proceedings of the National Academy of Sciences, 103 (2006), pp. 11211–11216.

[57] R. J. Leveque and L. N. Trefethen, *On the resolvent condition in the Kreiss Matrix Theorem*, BIT, 24 (1984), pp. 584–591.

[58] R. L. Lindeman, *The Trophic-Dynamic Aspect of Ecology*, Ecology, 23 (1942), pp. 399–417.

[59] M. Lindmark, M. Huss, J. Ohlberger, and A. Gårdmark, *Temperature-dependent body size effects determine population responses to climate warming*, Ecology Letters, 21 (2018), pp. 181–189.

[60] M. Lindmark, J. Ohlberger, M. Huss, and A. Gårdmark, *Size-based ecological interactions drive food web responses to climate warming*, Ecology Letters, 22 (2019), pp. 778–786.

[61] G. Lumer, *SEMI-INNER-PRODUCT SPACES*, Transactions of the American Mathematical Society, 100 (1961), pp. 29–43.

[62] R. M. May, *Stability in multispecies community models*, Mathematical Biosciences, 12 (1971), pp. 59–79.

[63] ———, *Will a Large Complex System be Stable?*, Nature, 238 (1972), pp. 413–414.

[64] D. S. Maynard, C. A. Serván, and S. Allesina, *Network spandrels reflect ecological assembly*, Ecology Letters, 21 (2018), pp. 324–334.

[65] T. Mitchell, *Computing the Kreiss Constant of a Matrix*, arXiv:1907.06537 [math], (2019).

[66] J. Montoya, G. Woodward, M. C. Emmerson, and R. V. Solé, *Press perturbations and indirect effects in real food webs*, Ecology, 90 (2009), pp. 2426–2433.

[67] T. Namba, *Multi-faceted approaches toward unravelling complex ecological networks*, Population Ecology, 57 (2015), pp. 3–19.

[68] M. G. Neubert and H. Caswell, *Alternatives to resilience for measuring the responses of ecological systems to perturbations*, 78 (1997), p. 13.

[69] M. G. Neubert, H. Caswell, and J. Murray, *Transient dynamics and pattern formation: Reactivity is necessary for Turing instabilities*, Mathematical Biosciences, 175 (2002), pp. 1–11.

[70] M. G. Neubert, H. Caswell, and A. R. Solow, *Detecting reactivity*, Ecology, 90 (2009), pp. 2683–2688.

[71] M. G. Neubert, T. Klanjscek, and H. Caswell, *Reactivity and transient dynamics of predator–prey and food web models*, Ecological Modelling, 179 (2004), pp. 29–38.

[72] A.-M. Neutel, *Stability in Real Food Webs: Weak Links in Long Loops*, Science, 296 (2002), pp. 1120–1123.

[73] A. Nicol-Harper, C. Dooley, D. Packman, M. Mueller, J. Bijak, D. Hodgson, S. Townley, and T. Ezard, *Inferring transient dynamics of human populations from matrix non-normality*, Population Ecology, 60 (2018), pp. 185–196.

[74] M. Novak, J. D. Yeakel, A. E. Noble, D. F. Doak, M. Emmerson, J. A. Estes, U. Jacob, M. T. Tinker, and J. T. Wootton, *Characterizing Species Interactions to Understand Press Perturbations: What Is the Community Matrix?*, Annual Review of Ecology, Evolution, and Systematics, 47 (2016), pp. 409–432.

[75] R. S. Ostfeld, C. G. Jones, and J. O. Wolff, *Ecological connections in eastern deciduous forests*, (1996), p. 9.

[76] D. Pauly, *Fishing Down Marine Food Webs*, Science, 279 (1998), pp. 860–863.

[77] S. L. Pimm, *The complexity and stability of ecosystems*, Nature, 307 (1984), pp. 321–326.

[78] S. L. Pimm, I. Donohue, J. M. Montoya, and M. Loreau, *Measuring resilience is essential to understand it*, Nature Sustainability, 2 (2019), pp. 895–897.

[79] S. L. Pimm and J. H. Lawton, *Number of trophic levels in ecological communities*, Nature, 268 (1977), pp. 329–331.

[80] ———, *On feeding on more than one trophic level*, Nature, 275 (1978), pp. 542–544.

[81] G. A. Polis, *Complex Trophic Interactions in Deserts: An Empirical Critique of Food-Web Theory*, The American Naturalist, 138 (1991), pp. 123–155.

[82] G. A. Polis, S. D. Hurd, C. T. Jackson, and F. S. Piñero, *El Niño Effects on the Dynamics and Control of Anisland Ecosystem in the Gulf of California*, Ecology, 78 (1997), pp. 1884–1897.

[83] L. Qiu, *A formula for computation of the real stability radius*, (1993).

[84] O. J. Schmitz, *PRESS PERTURBATIONS AND THE PREDICTABILITY OF ECOLOGICAL INTERACTIONS IN A FOOD WEB*, 78 (1997), p. 15.

[85] R. E. Snyder, *What makes ecological systems reactive?*, Theoretical Population Biology, 77 (2010), pp. 243–249.

[86] D. A. Spiller, J. Piovia-Scott, A. N. Wright, L. H. Yang, G. Takimoto, T. W. Schoener, and T. Iwata, *Marine subsidies have multiple effects on coastal food webs*, Ecology, 91 (2010), pp. 1424–1434.

[87] D. B. Stouffer and J. Bascompte, *Understanding food-web persistence from local to global scales*, Ecology Letters, 13 (2010), pp. 154–161.

[88] S. Tang and S. Allesina, *Reactivity and stability of large ecosystems*, Frontiers in Ecology and Evolution, 2 (2014).

[89] S. Townley, D. Carslake, O. Kellie-Smith, D. Mccarthy, and D. Hodgson, *Predicting transient amplification in perturbed ecological systems: Transient dynamics of ecological systems*, Journal of Applied Ecology, 44 (2007), pp. 1243–1251.

[90] L. N. Trefethen, *Pseudospectra of matrices*, in Numerical Analysis, Longman Scientific and Technical, Harlow, Essex, UK, 1991, pp. 234–266.

[91] L. N. Trefethen, *Computation of pseudospectra*, Acta Numerica, 8 (1999), pp. 247–295.

[92] ———, *Spectra and Pseudospectra*, in The Graduate Student's Guide to Numerical Analysis '98, M. Ainsworth, J. Levesley, and M. Marletta, eds., vol. 26, Springer Berlin Heidelberg, Berlin, Heidelberg, 2005, pp. 217–250.

[93] L. N. Trefethen, A. E. Trefethen, S. C. Reddy, and T. A. Driscoll, *Hydrodynamic Stability Without Eigenvalues*, Science, 261 (1993), pp. 578–584.

[94] J. M. Varah, *The computation of bounds for the invariant subspaces of a general matrix operator*, Technical Report CS 66, Computer Science Department, Stanford University, (1967).

[95] A. Verdy and H. Caswell, *Sensitivity Analysis of Reactive Ecological Dynamics*, Bulletin of Mathematical Biology, 70 (2008), pp. 1634–1659.

[96] J. W. White, L. W. Botsford, A. Hastings, M. L. Baskett, D. M. Kaplan, and L. A. Barnett, *Transient responses of fished populations to marine reserve establishment. Transient dynamics in marine reserves*, Conservation Letters, 6 (2013), pp. 180–191.

[97] L. H. Yang, *Periodical Cicadas as Resource Pulses in North American Forests*, Science, 306 (2004), pp. 1565–1567.

[98] L. H. Yang, J. L. Bastow, K. O. Spence, and A. N. Wright, *What Can We Learn from Resource Pulses*, Ecology, 89 (2008), pp. 621–634.

[99] L. H. Yang, K. F. Edwards, J. E. Byrnes, J. L. Bastow, A. N. Wright, and K. O. Spence, *A meta-analysis of resource pulse–consumer interactions*, Ecological Monographs, 80 (2010), pp. 125–151.

[100] P. Yodzis, *Energy flow and the vertical structure of real ecosystems*, Oecologia, 65 (1984), pp. 86–88.

[101] ———, *The Indeterminacy of Ecological Interactions as Perceived Through Perturbation Experiments*, Ecology, 69 (1988), pp. 508–515.

[102] P. Yodzis, *Introduction to Theoretical Ecology*, 1989.

[103] P. Yodzis and S. Innes, *Body Size and Consumer-Resource Dynamics*, The American Naturalist, 139 (1992), pp. 1151–1175.

[104] Q. Zhao, P. J. Van den Brink, C. Carpentier, Y. X. G. Wang, P. Rodríguez-Sánchez, C. Xu, S. Vollbrecht, F. Gillissen, M. Vollebregt, S. Wang, and F. De Laender, *Horizontal and vertical diversity jointly shape food web stability against small and large perturbations*, Ecology Letters, (2019), p. ele.13282.